8.0 Chemical-sedimentary deposits

Chemical sedimentary deposits in Afghanistan include both metallic and industrial mineral types. Metallic deposits are represented by iron deposits (section 8.1) and occurrences and sparse sedimentary manganese deposits (section 8.2). Industrial mineral deposits due to chemical sedimentation include salt and potash (sections 8.3A and B), phosphorite (section 8.4), celestite (section 8.5), barite (section 8.6), sulfur (section 8.7), and gypsum (section 8.8). Deposits related to non chemical-sedimentary processes are discussed in section 7.0. Sedimentary iron deposits are abundant in central parts of Afghanistan and the Haji Gak iron deposit is of world-class size sufficient to support a major mining operation. Additional resources to those already known at Haji Gak and in other locations are likely.

8.1 Sedimentary rock-hosted iron deposits

Contribution by Stephen G. Peters.

Iron deposits hosted in sedimentary rocks in Afghanistan mainly are present within the Proterozoic sedimentary and volcano-sedimentary rock packages. Most are present along the tectonized zone in the center of the country. This includes the large Haji Gak iron ore deposit and nearby occurrences (figs. 8.1-1 and 8.1-2). Additionally, oolitic ironstone iron mineral occurrences also are known in the Devonian and Lower Carboniferous rocks, and some iron-bearing occurrences are also present in the younger Cenozoic sedimentary rocks (Nishiwak, 1970). In addition, vein hematite deposits are present in Proterozoic, Permian and Oligocene rocks but these were not assessed as part of this preliminary study. Other major iron deposits in Afghanistan are spatially related to skarn; mainly around Oligocene intrusive bodies. These skarn occurrences are addressed within the porphyry copper and skarn assessment (see section 5.1). Some workers believe that the Proterozoic-hosted iron deposits are also products of contact metamorphism with the Oligocene intrusive bodies.

8.1.1 Description of sedimentary rock-hosted iron deposit models

The main ore minerals within the sedimentary rock-hosted iron deposits in Afghanistan are magnetite and hematite with lesser martite. The metallogenic age, mineralogy, textures and size of the deposits make them compatible with several model types such as Superior iron deposits, Algoma iron deposits, and iron oxide copper-gold deposits. Sedimentary manganese deposits are a common deposit type with many sedimentary rock-hosted iron deposits through out the world. The U.S. Geological Survey mineral-resource specialists did not have enough information on the Haji Gak iron deposit to determine which (if any) deposit model best described it.

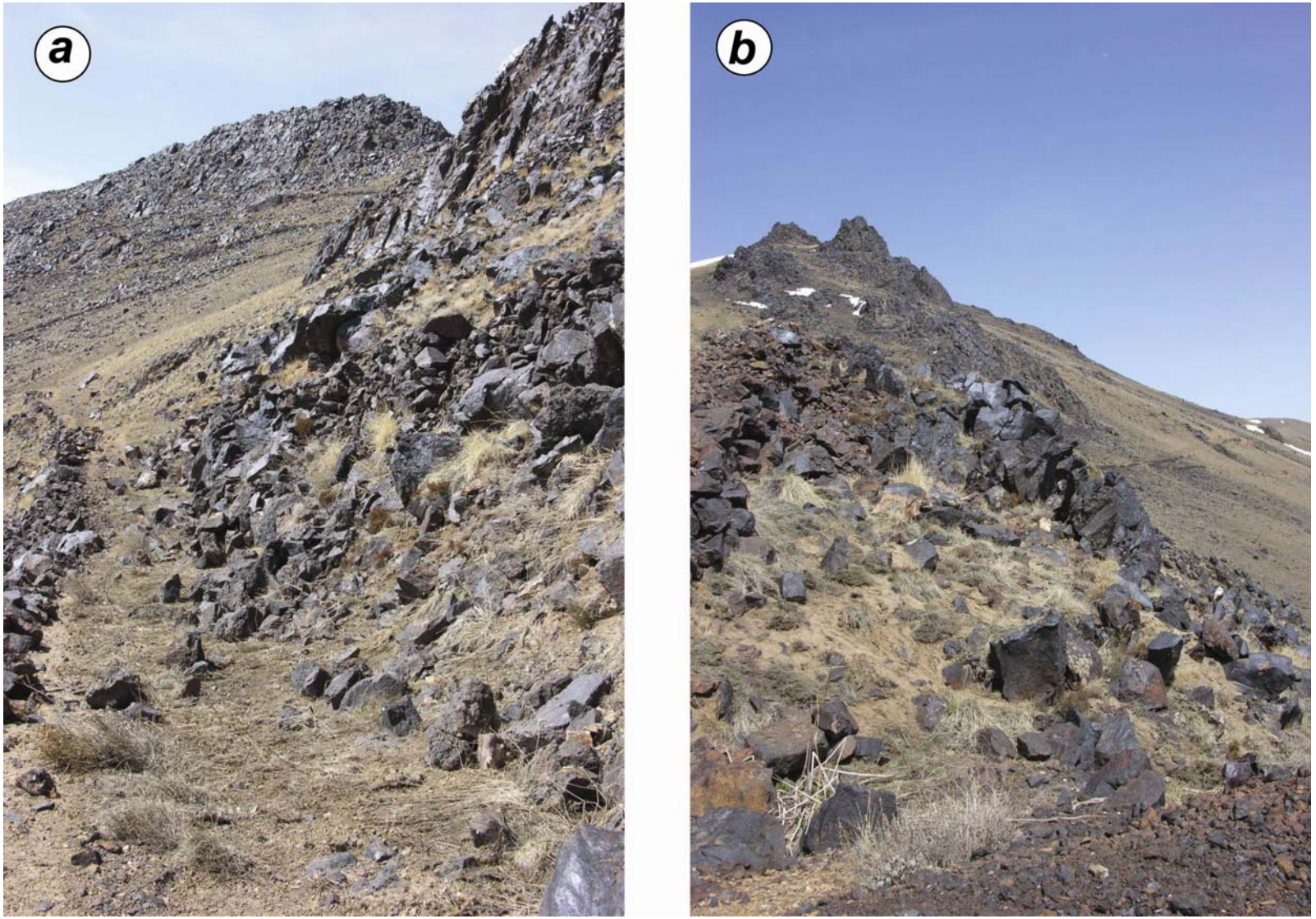

Figure 8.1-1. Photographs of out crops of the Haji Gak sedimentary rock-hosted iron deposit in Bamyan and Wardak Provinces. (a) Pathway along out crops of iron ore. (b) Outcropping layers of iron ore along the crest of the main ridge at Haji Gak. Photographs by Robert Bohannon.

Figure 8.1-2. Photographs of outcrops of the Haji Gak sedimentary rock-hosted iron deposit in Bamyan and Wardak Provinces. (*a*) Photograph with iron deposit at the crest of ridge and foliated schists in the foreground. (*b*) Photography of joint USGS-AGS field reconnaissance team at exploration adit in iron ores of the Haji Gak deposit.

Hereafter, it is cited as being of Haji Gak type. The following descriptions of the various iron deposit models are included to aid classification of Afghanistan's deposits using existing descriptions and will help in classifying future discoveries.

Superior iron deposits. (model 34a, Cannon, 1986a) are the classic banded-iron formations consisting of banded iron-rich sedimentary rock, generally of great lateral extent, typically layered on a centimeter scale with siliceous (chert) beds interlayered with the iron-rich beds. Rock types commonly are interlayered quartzite, shale, and dolomite. Iron formations and host rocks commonly contain sedimentary textures typical of shallow-water deposition in tectonically stable regions. Age range is mostly early Proterozoic (2.0 ± 0.2 by.), but also less commonly Middle and Late Proterozoic. Depositional environment is stable, shallow-water marine, commonly on a stable continental shelf or within an intracratonic basin. Tectonic setting is forelands of Proterozoic orogenic belts. Associated deposit types are sedimentary manganese deposits, which may be present stratigraphically near or be interbedded with the iron formations.

Mineralogy of Superior iron deposits is hematite, magnetite, siderite, and fine-grained quartz. Ores are very fine grained where not metamorphosed. Alteration is generally lacking and only related to ore deposition. The deposits commonly are metamorphosed to varying degrees or are weathered and enriched by supergene processes. No primary controls are usually present. Supergene ores may be localized by irregularities in present or paleo erosion surfaces. Weathering results in conversion of the original iron minerals to Fe-hydroxides and hematite. Silica is partly to totally leached. The end product of weathering is high-grade supergene ore. The deposits generally lie above magnetic anomalies.

Mean tonnages for Superior and Algoma type iron deposits are 170 million metric tons and mean grades are 53 wt. percent iron and 0.031 wt. percent phosphorus (Mosier and singer, 1986).

Algoma iron deposits. (Model 28b, Cannon, 1986b) are also called volcanogenic iron-formation deposits and typically contain beds of banded iron-rich rock usually in volcanic-sedimentary sequences formed in tectonically active oceanic regions. The deposits have similarities to Superior iron deposits and the grade-tonnage model for Algoma iron deposits is included under Superior iron in Cox and Singer (1986). Rock types typically present in the deposits are mafic to felsic submarine volcanic rocks and deep-water clastic and volcaniclastic sediments. These rocks are present as pillowed greenstone, intermediate to felsic tuffs and agglomerate, and poorly sorted clastic sediments. Age of the deposits is mostly Archean. The deposits form in volcano-sedimentary basins, which are equivalent to greenstone belts of Precambrian shields, and generally also form during rapid turbidite sedimentation and thick volcanic accumulations within or adjacent to tectonically active Precambrian shields. Associated deposit types can be Kuroko volcanogenic massive deposits.

Mineralogy consists of magnetite, hematite, and siderite that is interlayered and banded on a centimeter scale with chert. Fine-grained quartz beds are interlayered with iron-rich beds. There is no syngenetic alteration, but the deposits are commonly metamorphosed to varying degrees and weathered. Local ore controls are present within the general volcano-sedimentary setting, but usually are not well established. The development of a sub-basin with low sediment and volcanic input is probably a key factor in ore genesis. Weathering consists of conversion of the iron minerals to Fe-hydroxides and leaching of silica. Intense weathering can form high-grade supergene ores. The deposits generally lie above magnetic anomalies.

Iron oxide copper-gold deposits. (Model 29b, Haynes, 2000) replaces the Olympic Dam copper-uranium-gold (model 29b, Cox, 1986). Iron oxide copper-gold deposits are stratabound breccia and vein-hosted bodies of hematite and/or magnetite with disseminated copper + gold ± Ag ± Pd ± Pt ± Ni ± U ± light rare-earth elements (REE) occurring on broad redox boundaries related to sodic alteration of source rocks

and ore-related potassic and calc-silicate alteration (Haynes, 2000; Hitzman, 2000). An approximate synonym is ironstone copper-gold. Iron oxide copper-gold deposits are similar to sediment-hosted copper deposits in their geochemistry and in the alteration mineralogy of source rocks and host rocks (Haynes, 2000).

Three favorable environments are common: (1) continental margin subduction complexes with local extensional features containing oxidized rocks including subaerial volcanic deposits, conglomerates, red beds, and evaporite deposits; (2) compression, folding, and magmatism of intracratonic basins containing granitic rocks intruding rift-related assemblages; and (3) anorogenic magmatism produced by mantle underplating. The geological environment of iron oxide copper-gold deposits includes A-type or I-type intrusive rocks that belong to the magnetite-series of granitic, syenitic, to gabbroic composition. Oxidized clastic sedimentary rocks and felsic to basaltic subaerial volcanic rocks are the source rocks of ore fluids. Host rocks are volcanic and sedimentary rocks with bedding-parallel permeability, fault zones, and volcanic and tectonic breccias. The deposits are Proterozoic, Mid-Paleozoic, and Mesozoic in age. Associated deposit types include volcanic-hosted magnetite, sediment-hosted copper, and evaporate deposits, which all may occur in the same basinal environments.

Mineralogy in iron oxide copper-gold deposits consists of magnetite and hematite with minor apatite, as well as chalcopyrite and gold and, less commonly, chalcocite and bornite. Pyrite is present in most deposits, as are pyrrhotite, minor uraninite, monazite, platinum-group elements (PGE), molybdenite, sphalerite, galena, bismuthinite, scheelite, arsenopyrite, cobaltite, and nickel-cobalt arsenide minerals. Gangue minerals are quartz, fluorite, scapolite, apatite, calcite, barite and tourmaline. Ore minerals form veins and disseminations in lenticular, elongate iron oxide bodies. Mineralized replacement features may follow bedding and other sedimentary structures. The matrix of breccia pipes and irregular breccia bodies hosts iron oxides and copper minerals. Beds with high pre-ore permeability are the major ore controls. Tectonic or phreatophyric breccias are important controls. Redox fronts control copper deposition.

Alteration is due to oxidized brines that have passed through source-rocks creating albite-rich rocks with Na–scapolite, Mg–chlorite, and Ca–actinolite. The albite zone is depleted in K, Fe, U, REE, S, and most base metals. Iron oxide bodies also exhibit potassic (biotite-K-feldspar) alteration and may contain chlorite, pyroxene, amphibole, epidote, garnet, scapolite, and anhydrite. Potassic alteration commonly cuts or overprints albite alteration. Calcite-dolomite-pyrite veins and disseminations occur outboard of the iron oxide bodies and cut ore-related alteration. Geochemical signature of iron oxide copper-gold deposits is Cu + Au ± Bi ± U ± Ni ± Co ± PGE ± REE.

Tonnages of known iron oxide copper-gold deposits vary widely from very small to 2 billion tons at Olympic Dam, Australia, and 490 million metric tons at La Candelaria, Chile (Haynes, 2000; Hitzman, 2000). The median of 34 deposits is 10 million metric tons. Copper grades range from 0.4 to 5.8 wt. percent. The median of 31 deposits is 1.45 percent. Gold grades may range from 0.2 to 57 grams per metric ton. The median of 25 deposits is 0.8 grams per ton. Silver grades, reported for seven deposits, range from 3 to 19 grams per ton. Cobalt grades from 0.3 to 0.6 weight percent in some deposits.

8.1.2 Description of sedimentary rock-hosted iron tracts

Three separate permissive tracts, sedfe01—Haji Gak Neoproterozoic, sedfe02—Paleoproterozoic, and sedfe03—Mesoproterozoic were delineated in the central parts of Afghanistan. Each of these three ages of Proterozoic rocks, as designated on the geologic maps (Doebrich and Wahl, 2006) contain several iron-bearing mineral occurrences. All of these occurrences are present along the central northeastern-striking central tectonized zone in the country. No tracts were delineated for Phanerozoic sedimentary deposits;

although the U.S. Geological Survey assessment team acknowledges that certain Phanerozoic sedimentary sequences are permissive for oolitic iron deposits.

Permissive tract sedfe01—Haji Gak Neoproterozoic

Deposit types—Superior iron deposits, Algoma iron deposits, iron oxide copper-gold deposits, sedimentary manganese deposits (Cannon and Force, 1986).

Age of mineralization—Proterozoic to Oligocene

Examples of deposit types—Haji Gak deposit, Hazar, Khaish, Chuy, Zerak, and Sausang occurrences on the border between Bamyan and Wardak Provinces.

Exploration history—There is extensive previous exploration in the immediate Haji Gak area for iron deposits. Afghan, Russian, French, and German feasibility studies on the deposit were completed (Afghanistan Geological and Mineral Survey, 1967; DEMAG, 1974; Venot-Pic, 1974). The rest of the tract probably has not had as extensive exploration for iron or manganese deposits. Geochemical stream sediment exploration has taken place throughout the tract. The U.S. Geological Survey assessment team visited the area briefly.

Tract boundary criteria—A permissive tract, sedfe01, for sedimentary-hosted iron deposits of the Haji Gak type was delineated in central Afghanistan to encompass all the Neoproterozoic sedimentary host rocks, which consist of greenschist facies schistose and phyllitic marble, dolomite, sandstone, and metavolcanic rocks (map unit ***Z,scp***) and also spatially Neoproterozoic metavolcanic andesite lava and interlayered sedimentary rocks (map unit ***Z,al***) (fig. 8.1-3). The permissive tract is composed of a number of parts and contains a cluster of deposits, including the Haji Gak iron deposit, along the borders of Bamyan and Wardak Provinces. A favorable tract, sedfe01-f1 was delineated to encompass the geology hosting these deposits (fig. 8.1-4). Additional parts of tract sedfe01 are located in northern Kandahar, Zabul, Uruzgan, Ghazni, and Parwan Provinces (fig. 8.1-3). Tract sedfe01-f1 contains the Haji Gak, Harzar, Khaish, Chuy, and Zerak sedimentary-rock hosted iron deposits (fig. 8.1-6) and a number of vein-hosted iron deposits hosted in the same rocks. Further to the northeast in permissive tract sedfe01 the Dara-i-Neel sedimentary rock-hosted iron deposit is present.

The Haji Gak deposit, in Bamyan Province is the best known iron oxide deposit in Afghanistan, and similar occurrences of this style have been identified along a 600–km-long discontinuous east-west belt. The deposit is greater than 32 km long and contains 16 separate zones, some of which are as much as 5 km in length, 380 m wide and extend 550 m down dip. Seven of these zones have been studied in detail. Iron ore is both primary and oxide (figs. 8.1-5). The primary ore (80 vol. percent of the deposit) is present below 130 m and is composed of magnetite and pyrite, with minor other sulfide minerals including chalcopyrite, and averages 61.3 wt. percent iron. The remaining 20 vol. percent of the ore is oxidized and consists of three hematitic ore types at slightly higher grades. The mineralization is structurally controlled. Previous Russian resource estimates for the entire deposit are 1,700 million metric tons, although the mining reserve estimate for the near surface oxide ore in the most explored area is 85 million metric tons (Momji and Chaikin, 1960; Mirzad, 1961; Kusov, 1963; Kusov and others, 1965a and b; Bouladon and de Lapparent, 1975; Abdullah and others, 1977; http://www.bgs.ac.uk/afghanminerals/femetals.htm).

Total resources for the Haji Gak iron ore deposit are reported by the Ministry of Mines and Industry as industrial reserves (categories A+B+C1) of 110.9 billion metric tons iron ore and an additional possible resource of 2,070 billion metric tons iron ore.

The iron ore occurs in sixteen (16) 20– to 380–m-thick, 60– to 4,800–m-long, 20– to 552–m-wide stratabound ore bodies and additionally in some 1.9– to17–m-thick heaps (in a 100,000 to 859,000 m^2 area) in the following metallurgical ore types and grades:

Ore type	wt. percent iron	Deposit type
Hyderogoetite-polymartite	68.32	Stratabound ore body
Hematite-polymartite	65.68	Stratabound orebody
Carbonate-polymartite	62.83	Stratabound orebody
Hydrogoetite-polymartite	78.98	Heap

Metallurgically deleterious elements in the Haji Gak ores are sulfur in form of sulfate at 0.04 wt. percent and phosphorus at 0.05 wt. percent. Useful elements in the ores are manganese grading 0.19 wt. percent and cobalt and silver combined at between 0.01 and 0.1 wt. percent. Grab samples taken in 2005 by the USGS-AGS Team contained 86 to 395 ppm Ba, up to 44.6 to 11,111 ppm Cu, 1.75 to 124.1 ppm Mo, and several tens of ppm of Pb, Zn, V, and Ni (J. Doebrich, unpublished data, 2006).

The Harzar, Khaish, Chuy, and Zerak sedimentary-rock hosted iron deposits have also been explored and lay adjacent to Haji Gak (fig. 8.1-4). The Harzar iron occurrence lies in Proterozoic greenschist and contains 70–m-wide and about 300–m-long hematite lenses grading up to 62.97 wt. percent iron. The largest of the adjacent iron prospects is the Khaish deposit, also in Bamyan Province, which is hosted in the same Proterozoic rocks as Haji Gak. At Khaish, five smaller prospects have been delineated to date that are 300– to 1,300–m-long and 10– to 20–m-thick and can be traced down dip for 200 m. Speculative resource estimates at Khaish suggest that the deposit may contain up to 117 million metric tons iron ore, but at a lower grade (48.6 wt. percent iron) and 0.1 wt. percent titanium, and 0.019 wt. percent cobalt. The Chuy iron occurrence is 400 m long and 2.5 to 10 m wide, and is composed of a hematite-magnetite stratabound body within quartz-chlorite schist. The Zerak iron occurrence in Baghlan Province lies within a fault zone, and three 90– to 450–m-long 12– to 75–m-wide hematite magnetite zones have been discovered to date. Speculative resources are 20 million metric tons iron ore grading up to 62.5 wt. percent iron. The Dara-i-Neel iron occurrence in the far east part of tract sedfe01 consists of martite float (Kusov and others, 1975a and b; Chmyriov and others, 1973).

A southern part of the sedfe01—Haji Gak Neoproterozoic tract lies to the southwest of the Haji Gak area and contains the Mangasak iron occurrence in Wardak Province and an unnamed stratabound manganese occurrence in northeastern Uruzgan Province (fig. 8.1-6). The Mangasak occurrence lies along the contact between Proterozoic gneiss and schist layers in a 1,200–m-long 50– to 100–m-wide altered carbonated zone containing magnetite as disseminations, nodules, and veinlets (Karapetov and others, 1970). The unnamed manganese occurrence is composed of 1.5 by 7 m lenses within Neoproterozoic cherty marl rocks (Abdullah and others, 1977).

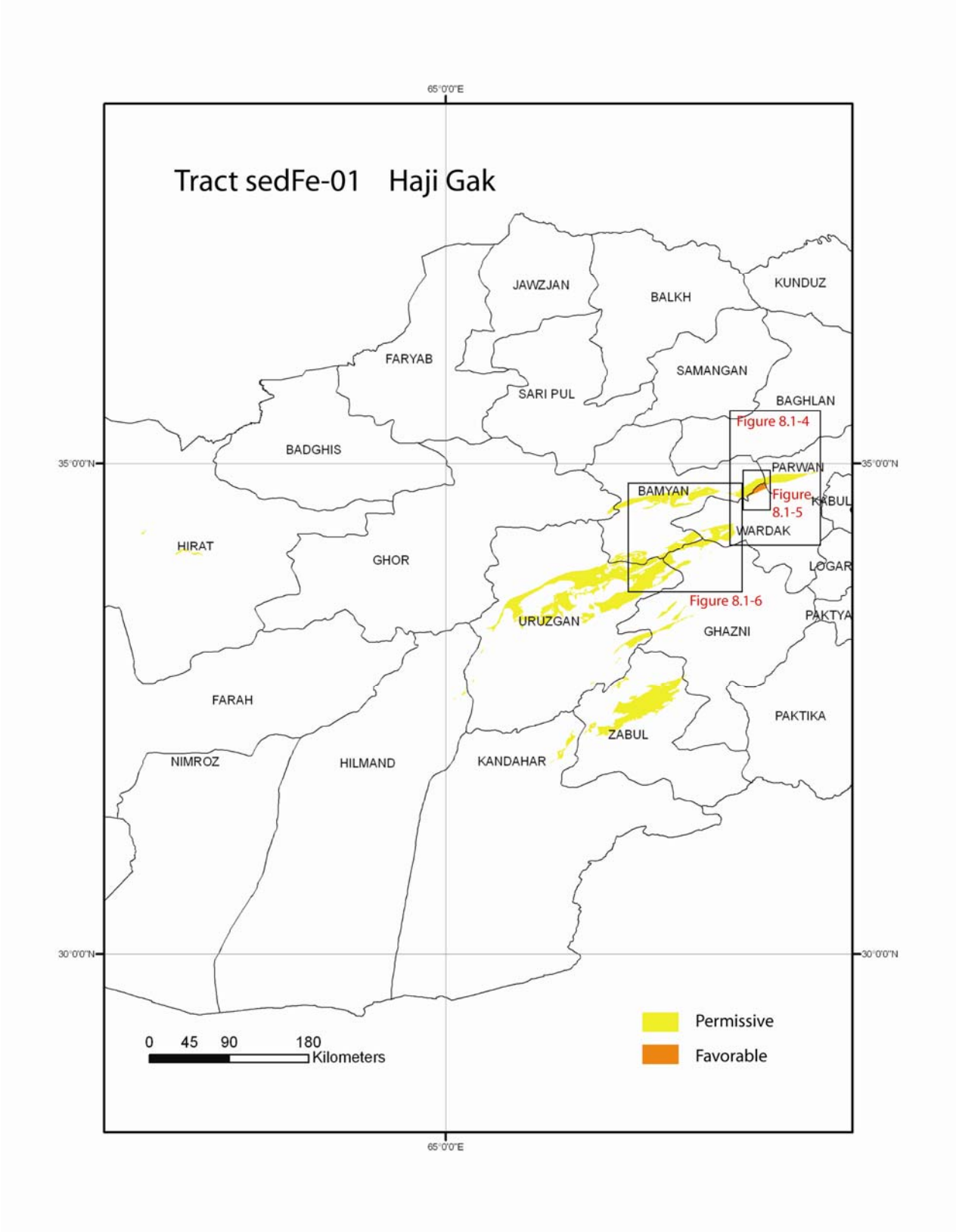

Figure 8.1-3. Map of permissive tract sedfe01—Haji Gak Neoproterozoic for undiscovered sedimentary rock-hosted iron deposits, showing distribution of Neoproterozoic rocks that host the Haji Gak iron deposit (data from Doebrich and Wahl, 2006).

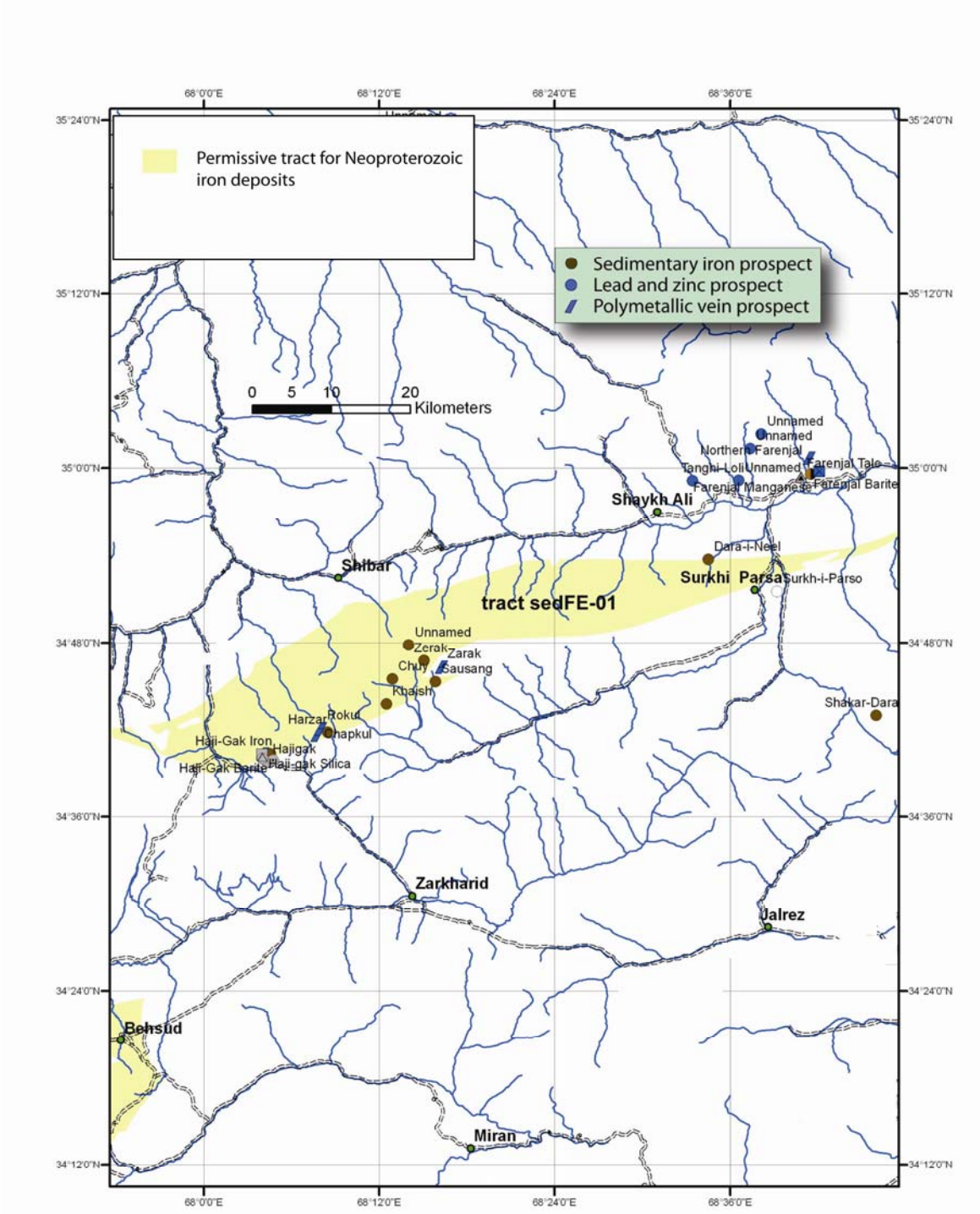

Figure 8.1-4. Map showing parts of permissive tract sedfe01—Haji Gak Neoproterozoic containing the Haji Gak and related deposits

.

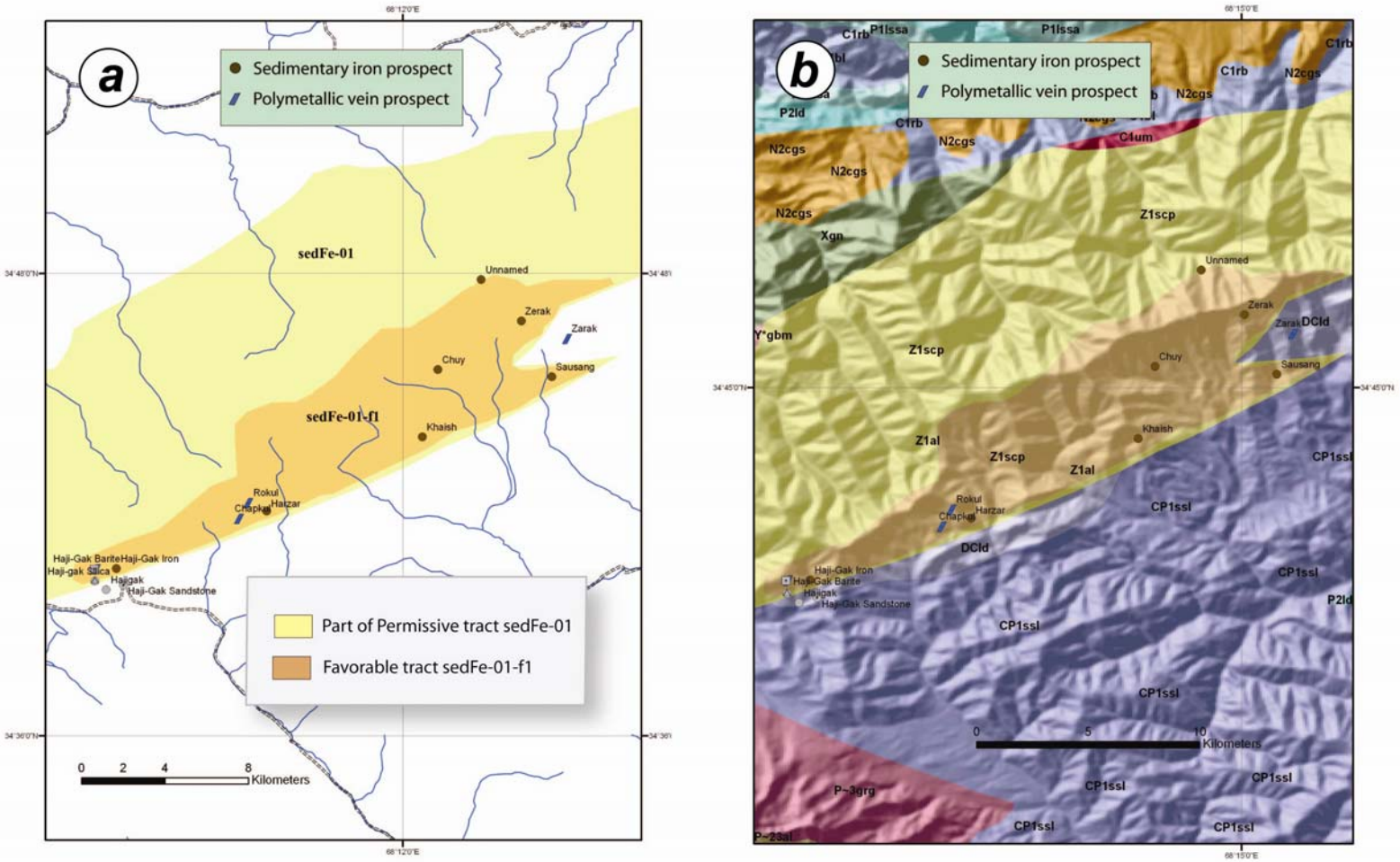

Figure 8.1-5. Maps showing the location of the favorable tract sedfe01-f1 Haji Gak Neoproterozoic within larger permissive tract sedfe01. (*a*) General location of tract sedfe01-f1. (*b*) Geologic units within and surrounding the Haji Gak deposit. Host units within the tract consist of Z_1scp = Neoproterozoic greenschist, marble, dolomite, metavolcanic rocks including phyllite, schist and sandstone, Z_1al = Neoproterozoic marble, dolomite and metavolcanic rocks. Not included in tract: DCld = Late Devonian to Mississippian limestone, dolomite, and schist, and CP_1ssl = Carboniferous to Early Permian sandstone, siltstone, shale, and mafic volcanic rocks.

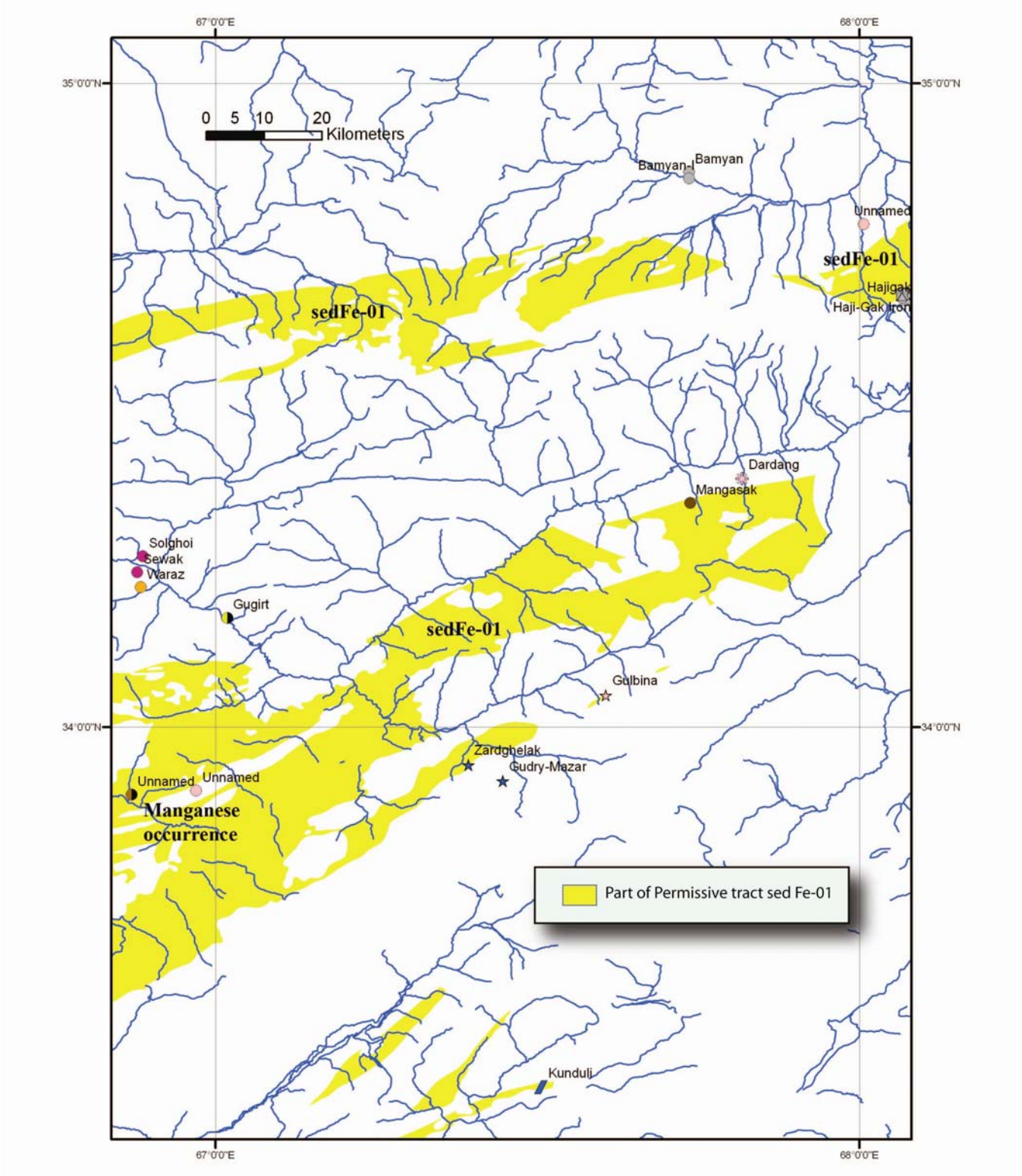

Figure 8.1-6. Map showing southern parts of tract sedfe01 Haji Gak Neoproterozoic which is permissive for undiscovered sedimentary rock-hosted iron deposits. The southern parts of the tract contain the Mangasak iron occurrence and a stratabound unnamed manganese deposit to the southwest. Mineral occurrences symbols from Doebrich and Wahl (2006).

Important data sources—Geologic map, LANDSAT imagery, mineral deposit database (Abdullah and others, 1977; Orris and Bliss, 2002; Doebrich and Wahl, 2006).

Needs to improve assessment—The information most needed is intermediate-scale (1:100,000 and 1:25,000) geologic mapping and geochemical sampling. Local prospects should be visited, resampled, and mapped. These would require site visits.

Optimistic factors—Well-defined deposits are present in the Haji Gak area. There is some indication that additional iron deposits may be present in other parts of the tract.

Pessimistic factors—Except for the Haji Gak area, no significant known occurrences are present within the tract area.

Quantitative estimate—The lack of unique descriptions of the Haji Gak deposit and questions concerning its genesis did not allow unambiguous model selection and the ability to make a quantitative assessment.

Permissive tract sedfe02—Paleoproterozoic

Deposit types—Sedimentary rock-hosted iron deposits: Superior iron deposits, Algoma iron deposits, iron oxide copper-gold deposits, sedimentary manganese deposits (Cannon and Force, 1986)

Age of mineralization—Proterozoic to Oligocene

Examples of deposit types—The tract contains the Nukrakhana, Sumte-Shamir, Jabel-us-Saraj Iron (also called Saraj Iron), Dehe-Kolon, and Hazar iron occurrences in central Parwan Province on the Kapisa Province border, and the Durnama, Panjsher, Nukra-Khana, and Chukri-Naw iron occurrences in east central Parwan Province (figs. 8.1-7 and 8).

Exploration history—There is only limited previous exploration in this part of Afghanistan, although discovery and description of the occurrences in the central and southeastern part of the tract indicate some ground prospecting. The Saraj Iron mineral occurrence contains ancient workings. Geochemical stream sediment exploration has taken place throughout the tract. The U.S. Geological Survey assessment team has not visited the area.

Tract boundary criteria—A permissive tract was delineated to include a number of stratabound iron deposits in Parwan Province and the Paleoproterozoic biotite-amphibolite, garnet-biotite, and garnet-sillimanite-biotite metamorphic rocks, which host them (map unit ***X1gn***). The tract is composed of a number of parts in Baghlan, Parwan, Kapisa, Laghman, north Paktya, Nangarhar, northern Kunar, Nuristan, and central Badakshan Provinces (fig. 8.1-7). The known iron occurrences are composed of pronounced orange to iron-colored color anomalies evident in the LANDSAT imagery (fig. 8.1-8).

A favorable tract, sedfe02-f1, consisting of three parts, was delineated around the known iron mineral occurrences in permissive tract sedfe02 (figs. 8.1-8 and 8.1-9). The favorable tract includes most of the iron-colored LANDSAT anomaly and the Nukrakhana, Saraj Iron (Jabel-us-Saraj Iron), Dehe-Kolon, and Hazar iron occurrences hosted in Paleoproterozoic metamorphic rocks. Nukrakhana occurrences may be the same as the Nukra-Khana occurrence to the east (Khasanov and others, 1967). The Sarj Iron mineral occurrence contains ancient workings and is composed of several large hematite lenses hundred of meters long and 10 to 30 m thick and tabular, ferruginous marble bodies over 1,000 m long and hundreds of meters thick. Speculative resources are 8.2 million metric tons iron (Momji and Chaikin, 1960). The Dehe-Kolon occurrence consists of a 3,000–m-long 10– to 20–m-wide, near horizontal hematite body

(Kafarskiy and others, 1972). The Hazar iron occurrence is hosted in gneiss and marble that are intruded by small diorite plugs, and consist of a hematite-magnetite vein that is 20 m long and 2.0 to 2.5 m wide grading 0.2 wt. percent copper and unknown amounts of iron (Denikaev and others, 1971).

A second favorable tract, sedfe02-f2, was delineated in three parts in permissive tract sedfe02—Paleoproterozoic around the Durnama, Panjsher, Nukra-Khana, and Chukri-Naw iron occurrences in east central Parwan Province (figs. 8.1-9). The occurrences are hosted in marble. A north-south-striking iron-colored color anomaly in LANDSAT imagery under lies beneath the Chukri-Naw and Nukra-Khana iron occurrences and cross cuts the grain of the geology and the trend of the tracts (fig. 8.1-10). The Durnama occurrence consists of several 10– to 60–m-long 1– to 5–m-wide hematite lenses grading 55 to 60 wt. percent iron, 0.2 wt. percent copper, and 0.03 wt. percent zinc (Kafarskiy and others, 1972). The Panjsher iron occurrence is 3,000 to 5,000 m long and 10 to 20 m wide and composed of hematite-bearing rock. Nukra-Khana is composed of several massive hematite, limonite, and siderite lenses, beds, and veins that are between several hundreds to thousands of meters long and 2 to 20 m wide that grade 60 to 65 wt. percent iron (Khasanov and others, 1967). Chukri-Naw occurrence consists of siderite-hematite lenses up to 1,000 m long and between 2 and 15 m wide. Kafarskiy and others (1972) report that German geologists in 1938 took samples here that graded up to 1,223 g/t silver.

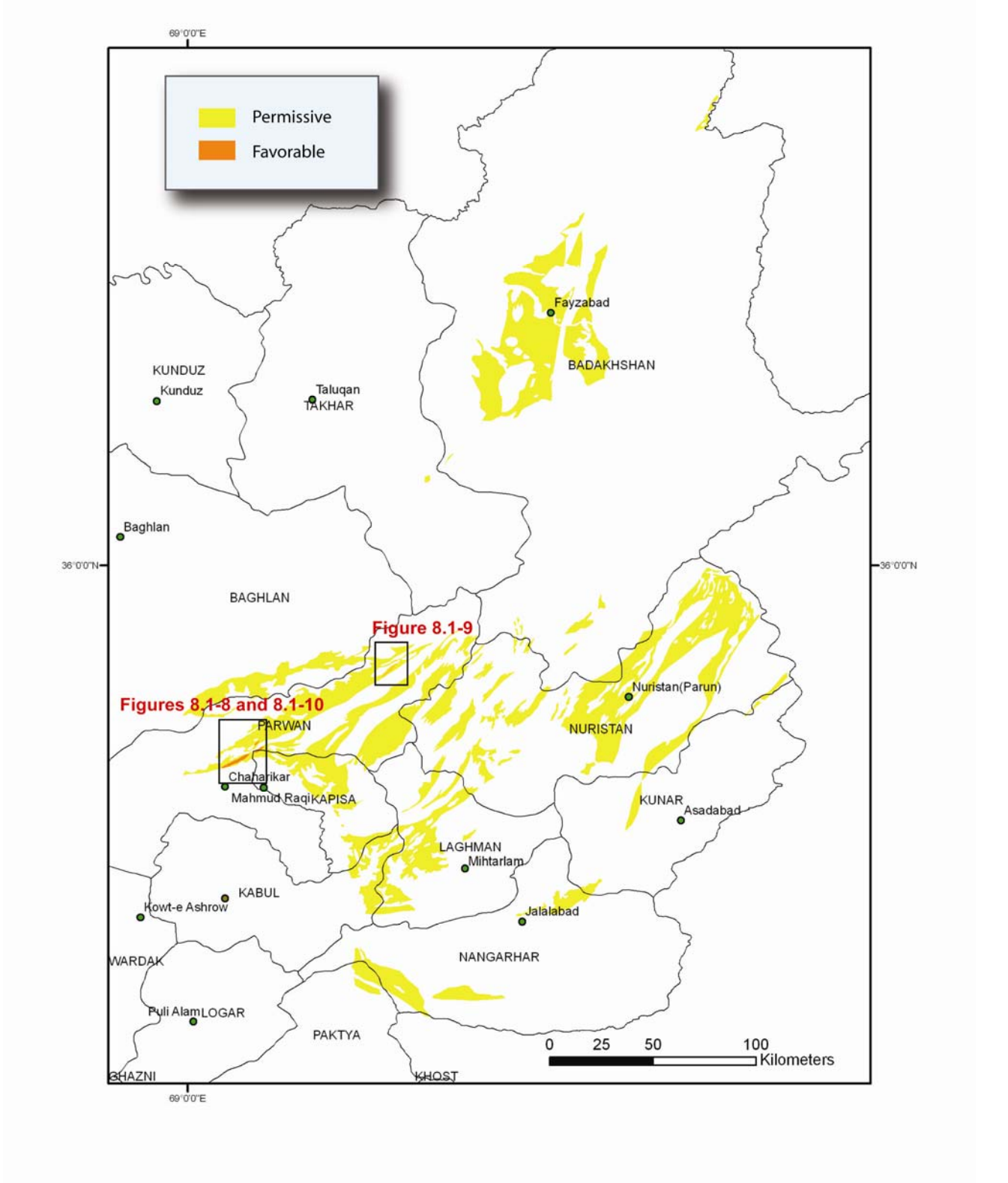

Figure 8.1-7. Map showing location of permissive tract sedfe02—Paleoproterozoic in eastern and northern Afghanistan for undiscovered sedimentary rock-hosted iron deposits

.

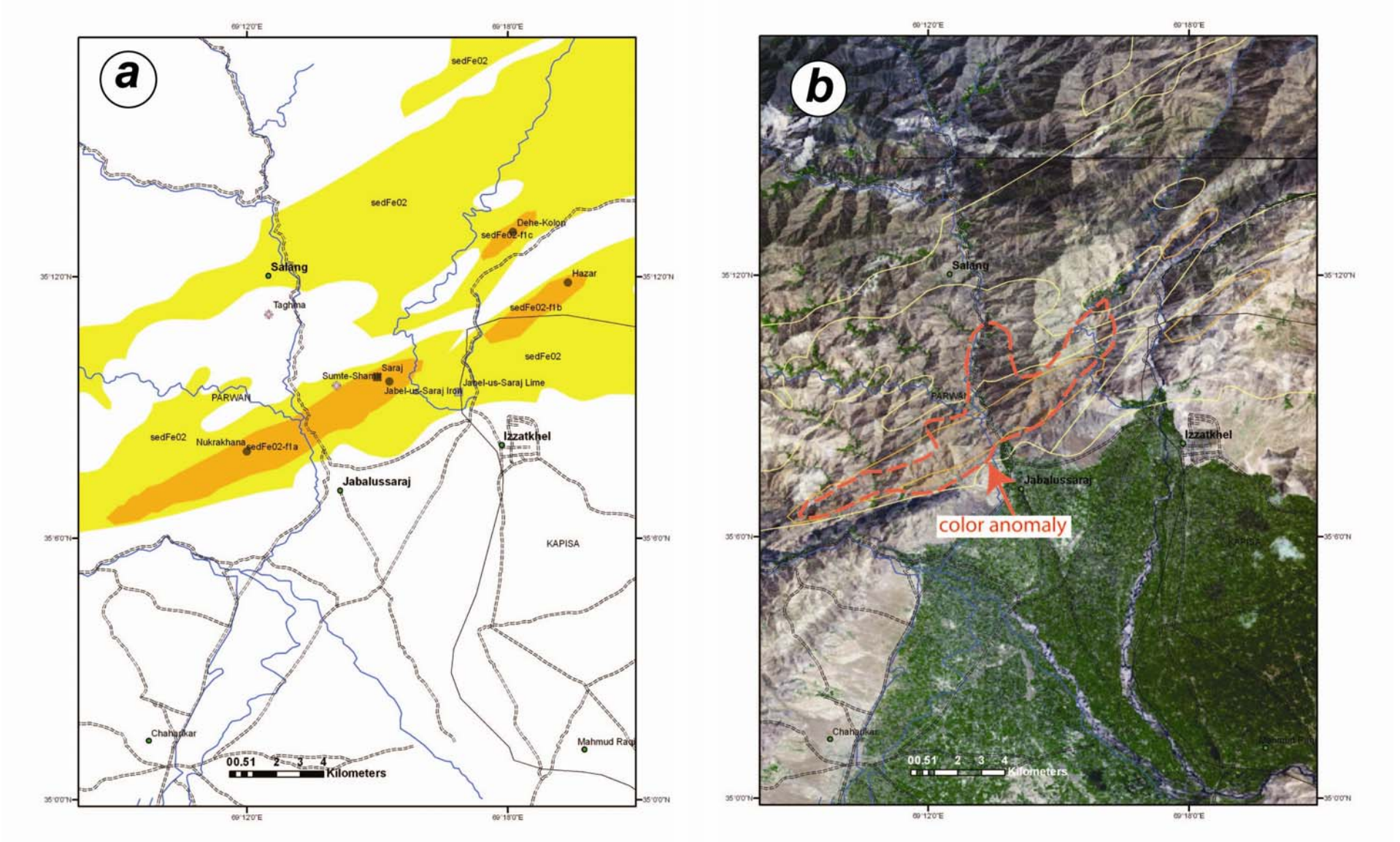

Figure 8.1-8. Maps showing location of the three-part favorable tract sedfe02-f1 in central Parwan Province. (a) Permissive and favorable tracts. (b) LANDSAT image showing view in (a), but also showing the iron-colored anomaly contained within the tract.

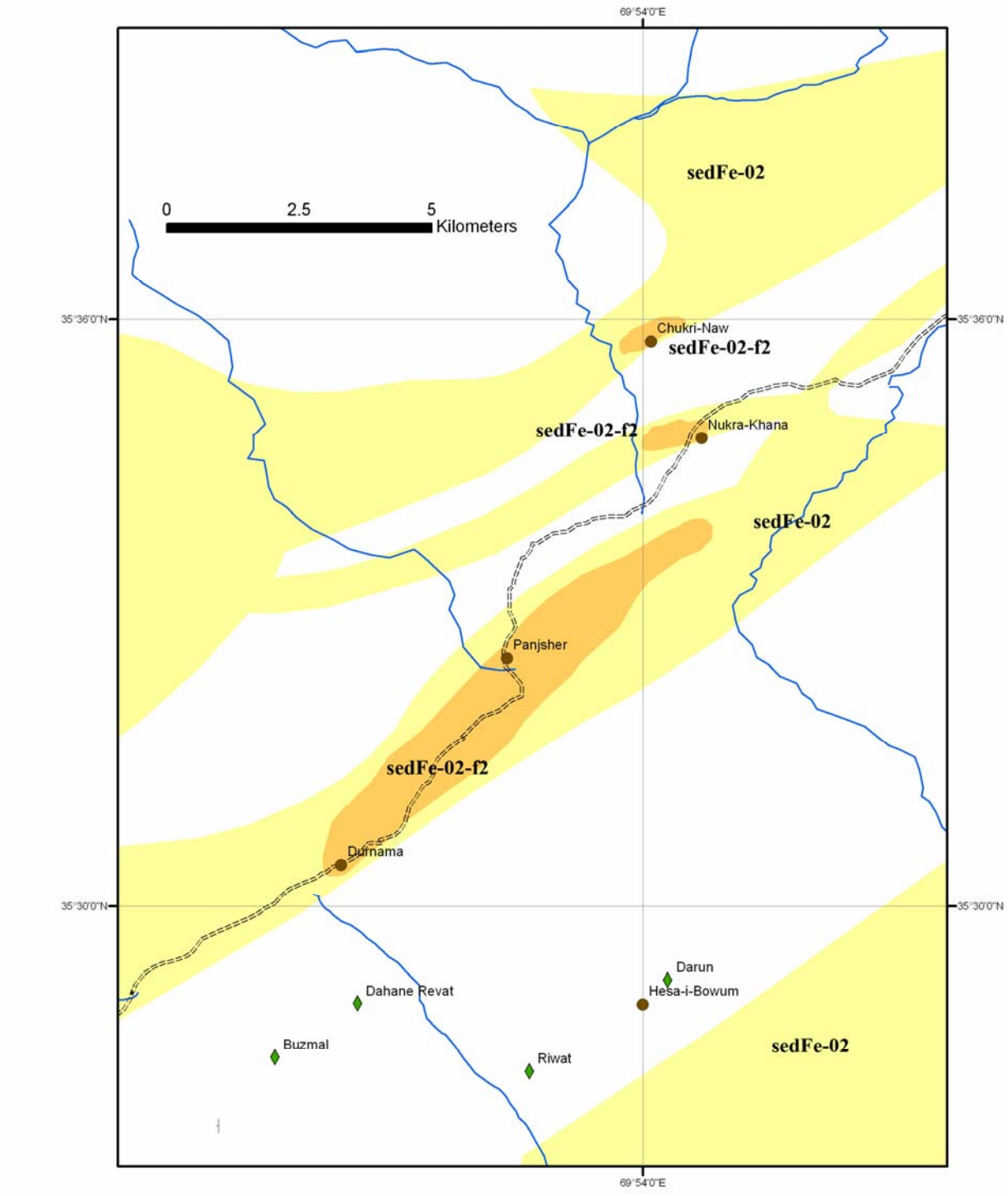

Figure 8.1-9. Map of favorable tract sedfe02-f2 in eastern Parwan Province showing location of known iron mineral occurrences and permissive tract sedFe-02—Paleoproterozoic. A northerly trending color anomaly in Landsat imagery lies between the Nukra-Khana and Chukri-Naw iron occurrences and may also coincide with the reported high silver values (1,223 g/t silver) at Chukri-Naw (Kafarskiy and others (1972).

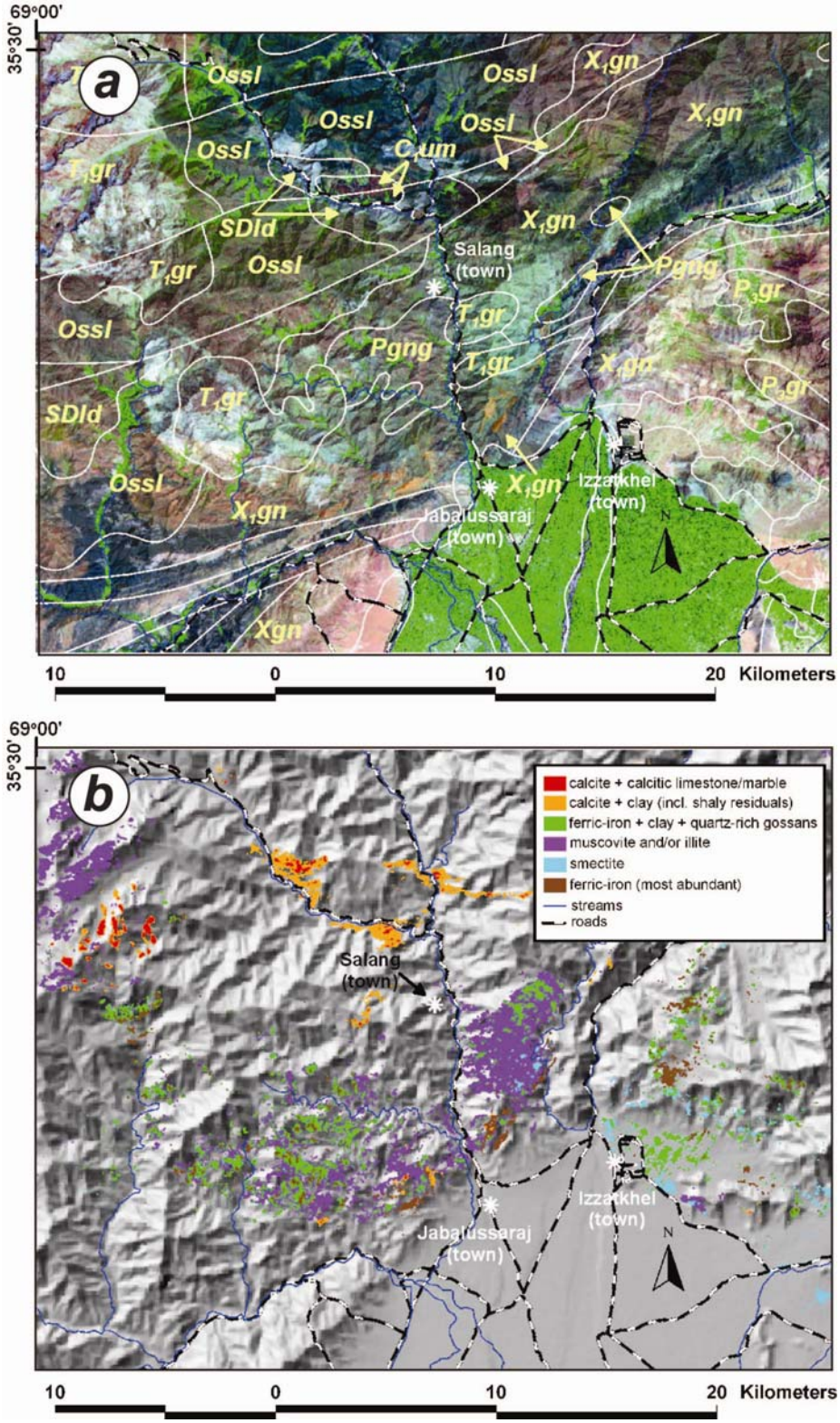

Figure 8.1-10. Maps of ASTER imagery of the area included in favorable tract sedfe02-f1 in central Parwan Province. (*a*) LANDSAT imagery and line geology from Doebrich and Wahl (2006). (*b*) ASTER mapping of calcite, clay ferric iron, muscovite and illite. Analysis by Bernard Hubbard.

***Important data sources*—**Geologic map, LANDSAT imagery, mineral deposit database (Abdullah and others, 1977; Doebrich and Wahl, 2006).

***Needs to improve assessment*—**The information most needed is intermediate-scale (1:100,000 and 1:25,000) geologic mapping and geochemical sampling. Local prospects should be visited, resampled, and mapped in detail. Reconciliation of the geologic map with the LANDSAT color anomalies and location of the high silver values at Chukri-Naw would be important contributions.

***Optimistic factors*—**A number of iron-bearing mineral occurrences, some with extensive strike lengths of over 1 km are present within the central parts of the tract. Assays of samples in these are between 55 and 65 wt. percent iron. Base and precious metals are also present. A number of color anomalies also are present proximal or within the known mineral occurrence clusters.

***Pessimistic factors*—**Most parts of the tracts are void of iron mineral occurrences and the occurrences are restricted to a central tectonized zone.

***Quantitative estimate*—**No mineral assessment was undertaken because the mineral occurrences within the tract were unable to be definitively assigned to a deposit model.

Permissive tract sedfe03—Mesoproterozoic

***Deposit Type*—**Sedimentary rock-hosted iron deposits: Superior iron deposits, Algoma iron deposits, iron oxide copper-gold deposits, sedimentary manganese deposits

***Age of Mineralization*—**Proterozoic to Oligocene

***Examples of Deposit Type*—**The Chasma-i-Reg, Band-i-Sarah occurrences are present in Mesoproterozoic rocks in the west parts of tract sedfe03 within east central Herat Province.

***Exploration history*—**There is only limited previous exploration in this part of Afghanistan, although discovery and description of the occurrences in the central and southeastern part of the tract indicate some ground prospecting. Geochemical stream sediment exploration has taken place throughout the tract. The U.S. Geological Survey team has not visited the area.

Tract boundary criteria*—**Permissive tract sedfe03—Mesoproterozoic was delineated to include the Mesoproterozoic sedimentary and volcanic rocks (map unit ***Ym) composed mainly of greenschist, gneiss, quartzite, marble, and amphibolite. The different parts of the tract lie in Herat, Ghor, north Helmand, and parts of Zabul, Ghanzi, and Wardak Provinces (fig. 8.1-11). The tract includes the Chasma-i-Reg, Band-i-Sarah occurrences located in the far west part of the tract in Herat Province (fig. 8.1-12). The Chasma-i-Reg iron occurrence is hosted in Proterozoic sandstone and limestone and consists of a hematite-bearing 2–km-long and 300–m-wide zone. The Band-i-Sarah iron occurrence lies along a fault zone in Proterozoic limestone and consists of hematite mineralization over an area of 300 by 100 m (Dronov and others, 1972).

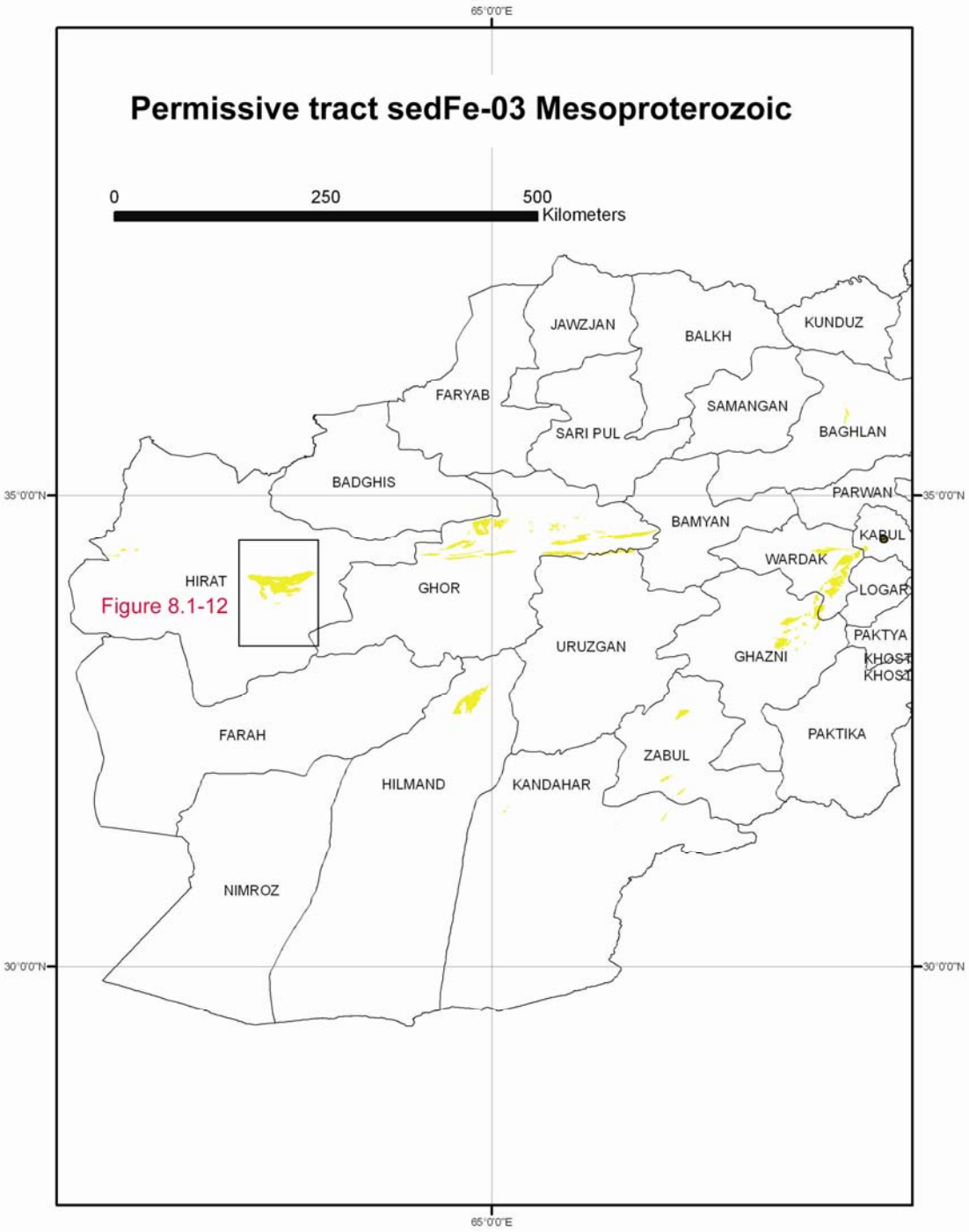

Figure 8.1-11. Map showing the location of permissive tract sedfe03—Mesoproterozoic for undiscovered sedimentary rock-hosted iron deposits.

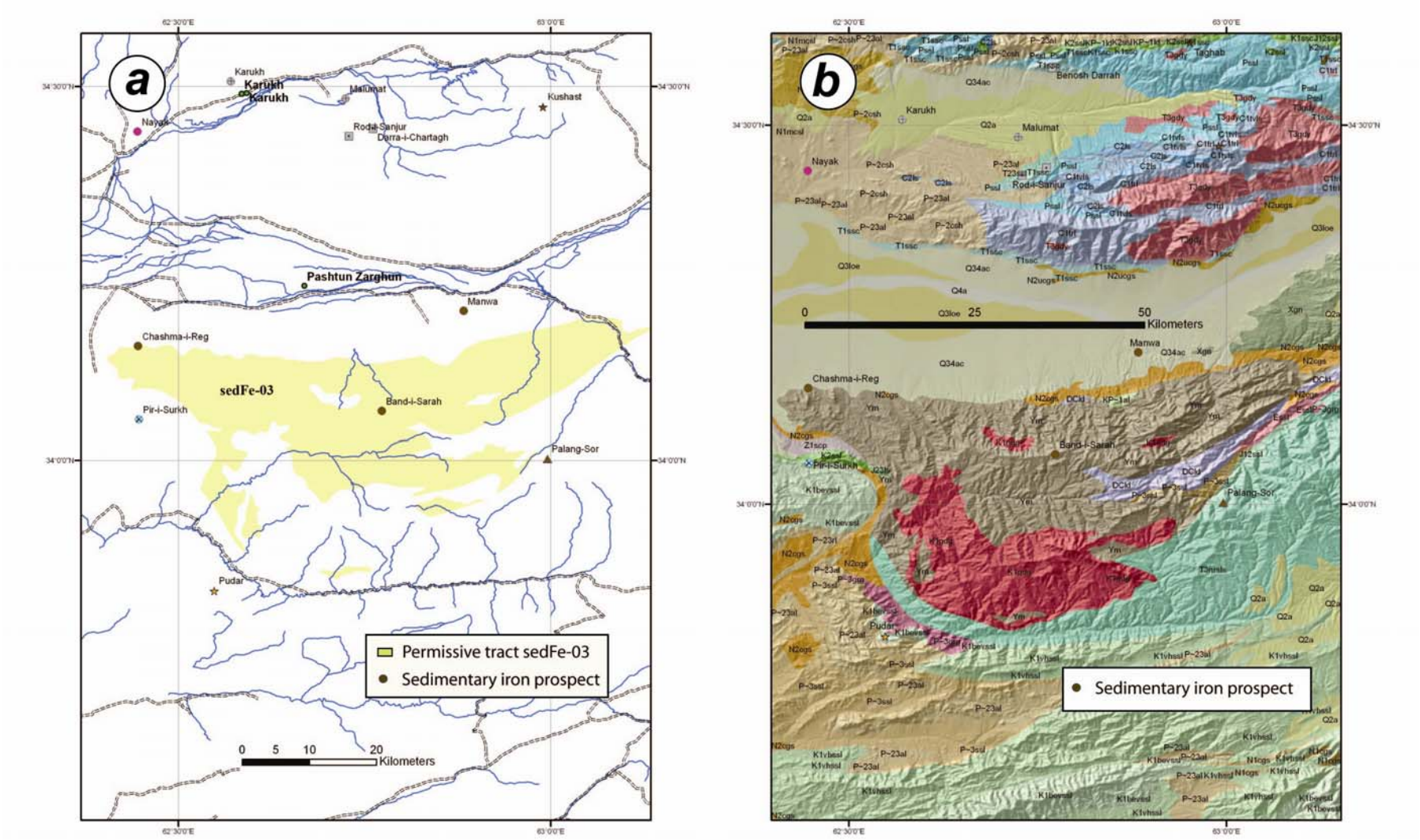

Figure 8.1-12. Maps showing the location of iron mineral occurrences in the western parts of permissive tract sedFe-03 for undiscovered sedimentary rock-hosted iron deposits. (*a*) Location of Chasma-i-Reg and Band-i-Sarah iron mineral occurrences in western Herat Province. (*b*) Geologic map showing approximate area shown in (*a*) also showing distribution of Mesoproterozoic rocks defining this part of the permissive tract. Tract consists of Ym = Mesoproterozoic greenschist, gneiss, quartzite, marble, amphibolite, metavolcanic and sedimentary rocks, and Z_1scp = Neoproterozoic schist and phyllite composed of greenschist derived from slate, sandstone and metacarbonate rocks from Doebrich and Wahl (2006).

***Important data sources*—**Geochemical halo data, geologic map, aeromagnetic map, LANDSAT imagery, mineral deposit database (Doebrich and Wahl, 2006; Sweeney and others, 2006; Abdullah and others, 1977).

***Needs to improve assessment*—**The information most needed is intermediate-scale (1:100,000 and 1:25,000) geologic mapping and geochemical sampling. Local prospects should be visited, resampled, and mapped in detail. Analysis of the airborne geophysics, particularly to the west of the known outcropping Proterozoic rocks in the tract, would be beneficial. These would require site visits.

***Optimistic factors*—**Two mineral occurrences are present in the western parts of the tract in Herat Province. One of these is over 1 km long and several hundreds of meters thick. These magnetic bodies may correlate with large aeromagnetic anomalies to the west.

***Pessimistic factors*—**Few other iron mineral occurrences are present within the tract.

***Quantitative estimate*—**No quantitative mineral assessment was attempted by the USGS Assessment Team because occurrences within the tract and the description of the lithology made it difficult to identify an appropriate descriptive and tonnage grade model for estimation.

References

Abdullah, Sh., Chmyriov, V.M., Stazhilo-Alekseev, K.F., Dronov, V.I., Gannan, P.J., Rossovskiy, L.N., Kafarskiy, A.Kh., and Malyarov, E.P., 1977, Mineral resources of Afghanistan (2nd ed.): Kabul, Afghanistan, Republic of Afghanistan Geological and Mineral Survey, 419 p.

Afghanistan Geological and Mineral Survey, 1967, Geological structure of the Haji Gak iron deposit and its commercial value: Afghanistan Geological and Mineral Survey, Kabul, 13 p.

Bouladon, J., and de Lapparent, A.F., 1975, Le mineral de fer d'Hajigak (Afghanistan); position stratigraphique, cadre geologique et type du gisement, Translated Title: The iron minerals of Hajigak Pass, Afghanistan; stratigraphic position, geological evolution and type of deposit: Mineralium Deposita, v. 10, no. 1, p. 13–25.

Cannon, W.F., 1986a, Descriptive model of Superior Fe, *in* Cox, D.P., and Singer, D.A., eds., Mineral deposit models: U.S. Geological Survey Bulletin 1693, p. 228.

Cannon, W.F., 1986b, Descriptive model of Alogma Fe, *in* Cox, D.P., and Singer, D.A., eds., Mineral deposit models: U.S. Geological Survey Bulletin 1693, p. 198.

Cannon, W.F., and Force, E.R., 1986, Descriptive model of sedimentary Mn, *in* Cox, D.P., and Singer, D.A., eds., Mineral deposit models: U.S. Geological Survey Bulletin 1693, p. 231.

Chmyriov, V.M., Stazhilo–Alekseyev, K.F., Mirzad, S.H., Dronov, V.I., Kazikhani, A.R., Salah, A.S., and Teleshev, G.I., 1973, Mineral resources of Afghanistan, *in* Afghanistan Department of Geological Survey, (1st ed.): Kabul, Geology and Mineral Resources of Afghanistan, p. 44–86.

Cox, D.P., 1986, Descriptive model of Olympic Dam Cu-Au-U, *in* Cox, D.P., and Singer, D.A., eds., Mineral Deposit Models: U.S, Geological Survey Bulletin 1693, p. 200.

Cox, D.P., and Singer, D.A., eds., 1986, Mineral deposit models: U.S. Geological Survey Bulletin 1693, p. 379.

DEMAG (Creusot–Loire enterprises), 1974, Feasibility study for an integrated iron and steel plant in Afghanistan, Duisberg, Germany, April, 1974, unpub. data.

Doebrich, J.L., and Wahl, R.R., 2006, Geologic and mineral resource map of Afghanistan: U.S. Geological Survey Open–File Report 2006–1038, 1 sheet scale 1:850,000. available on line at *http://pubs.usgs.gov/of/2006/1038/*.

Dronov, V.I., Kalimulin, S.M., Kabakov, O.N., Kotchetkov, A.Ya., Zelenskiy, E.A., Chistyakov, A.N., and Svezhentsov, V.P., 1970, The geology and minerals of the western part of Central Afghanistan, Department of Geological and Mineral Survey, Kabul, unpub. data.

Haynes, D.W., 2000, Iron oxide copper-gold deposits—Their position in the ore deposit spectrum and modes of origin, *in* Porter, T.M., ed., Hydrothermal iron oxide copper-gold and related deposits—A global perspective: Australian Mineral Foundation, Adelaide, p. 71–90.

Hitzman, M. W, 2000, Iron oxide-Cu-Au deposits: what, where, when, and why, *in* Porter, T.M., ed., Hydrothermal iron oxide copper-gold and related deposits—A global perspective: Australian Mineral Foundation, Adelaide, p. 9–25.

Kafarskiy, A.Kh., Stazhilo–Alekseev, K.F., Pyzhyanov, I.V., Achilov, G.Sh., Gorelov, A.I., Bezulov, G.M., and Gazanfari, S.M., 1972, The geology and minerals of the Western Hindu Kush and the eastern part of the Bande–Turkestan, Department of Geological and Mineral Survey, Kabul, scale 1:500,000, unpub. data.

Karapetov, S.S., Stazhilo–Alekseev, K.F., and Kotchetkov, A.Ya., 1970, The geology and minerals of the eastern part of Central Afghanistan (A preliminary report by the Helmand crew on the work in 1968–69), Department of Geological and Mineral Survey, Kabul, unpub. data.

Khasanov, R.M., Plotnikov, G.I., Bayazitov, R., Sayapin, V.I., and Trifonov, A., 1967, Report on revised estimation investigations of mineral deposits and occurrences of copper, lead, zinc and gold in 1965–V. I–II, Department of Geological and Mineral Survey, Kabul, unpub. data.

Kusov, I.K., 1963, Geological mapping, prospecting, and exploration on the iron deposit of Hajigak, USSR v/o Technoexport, contract no. 640, 88 p., Kabul, unpub. data.

Kusov, I.K., Smirnov, M.S., and Reshetayak, V.V., 1965a, Report on prospecting and survey at iron occurrences in Central Afghanistan and the Hajigak iron deposit's estimated reserves, Department of Geological and Mineral Survey, Kabul, unpub. data.

Kusov, I.K., Smirnov, M.S., and Reshetayak, V.V., 1965b, Report on the results of prospecting–survey and reconnaissance works for iron ores in Central Afghanistan with reserve calculation on Hajigak deposit for 1963–1964, USSR v/o Technoexport, contract no. 640, 3 volumes with English translation, Kabul, unpub. data.

Mirzad, S.H., 1961, Iron ore deposit of the Hajigak Pass, Appendix to Journal "Jundun", no. 26, Kabul, unpub. data.

Momji, G.S., and Chaikin, S.I., 1960, Iron ores of Afghanistan, (incomplete) Technoexport, Moscow.

Mosier, D.L., and Singer, D.A., 1986, Grade and tonnage model of Superior Fe and Algoma Fe Deposits, *in* Cox, D.P., and Singer, D.A., eds., Mineral deposit models: U.S. Geological Survey Bulletin 1693, p. 228–230.

Nishiwak i, Chikao, 1970, Iron ore deposits of the Middle East, Asia and the Far East, Survey of world iron ore resources, occurrence and appraisal, report of a panel of experts appointed by the Secretary–General, United Nations, New York, p. 102–206.

Orris, G.J., and Bliss, J.D., 2002, Mines and mineral occurrences of Afghanistan: U.S. Geological Survey Open-File Report 02-110, 95 p.

Venot–Pic, 1974, Feasibility study relating to the development of the Hajigak iron ore mine and Shabashak coal mine, Paris, France, unpub. data.

8.2 Bedded Manganese

Contribution by Stephen G. Peters.

Shallow-marine manganese deposits are not well known in Afghanistan, but the deposit type is present in geologic environments similar to stratabound sedimentary iron deposits in Proterozoic rocks. The USGS Assessment Team suggested that this deposit type be included in the permissive tracts for those deposits, because a known occurrence lies in these rocks in Uruzgan Province (Starshinin and others, 1975) and because manganese deposits are known to be with sedimentary iron deposits. An additional tract was also added for Carboniferous-age rocks in the central parts of the country because a manganese occurrence lies in these rocks in Parwan Province (Kazak and others, 1965). Sedimentary manganese deposits are important to consider because the giant Molango orebody in Mexico has reserves of over 200 million metric tons, with identified resources that total approximately 15 billion tons at an average grade of 10 wt. percent Mn.

8.2.1 Description of Sedimentary Mn model

Sedimentary Mn deposits (model 34b; see also Cannon and Force, 1986) are large concentrations of manganese oxide and/or carbonate minerals that may be present in shallow marine transgressive sequences that have nearby temporally equivalent anoxic deep-water facies. The formation of possible shallow-marine manganese deposits within this generally favorable setting is controlled by vagaries of oceanic circulation and upwelling and of local sedimentary environments. Oxide facies beds contain black oolites or pisolites. Bedded carbonate rocks that would likely be identified as dolomite in the field show abundant secondary manganese minerals on weathered faces or joints. Ores may be either manganese oxides, which locally occur as oolites and pisolites and are very distinctive, or as bedded manganese carbonate that is easily mistaken for dolomite. Any “dolomite” that shows unusual amounts of secondary manganese oxides on weathered surfaces or joints should be tested chemically for manganese content. Alteration consists of secondary manganese oxide concentrations. Geochemical signature consists of Mn–anomalous zones defined by detailed chemical stratigraphy that identify significant stratigraphic horizons. Such anomalous horizons may have regional extent and help guide exploration to the most favorable units.

Specific suggestions are that a few well-exposed stratigraphic sections should be assayed for manganese content, on intervals of a meter or two to search for regionally anomalous units. Such units, if found, should receive special attention in field mapping and be examined for secondary manganese minerals and assayed for manganese if such secondary alteration is found. Oxide facies are very distinctive rocks and should be easily recognizable in field mapping if they are not highly modified by weathering. Carbonate facies may be very cryptic and appear to be dolomite on field examination. “Dolomite” within defined favorable intervals should be closely examined for indications of manganese.

8.2.2 Description of sedimentary manganese tracts

Permissive tracts were delineated to include stratabound occurrences of manganese in the Farenjal prospect in Lower Carboniferous rocks (sedMn01). In addition, the three Proterozoic tracts delineated for sedimentary iron (sedFe01, 02, and 03) are also permissive for manganese and an unnamed prospect in Uruzgan Province.

Permissive tract—sedMn01

Deposit types—Bedded Manganese

Age of mineralization—Lower Carboniferous

Examples of deposit type—Farenjal Manganese occurrence in Parwan Province

The Farenjal prospect is hosted in Lower Carboniferous sedimentary rocks about 500 m west of the Farenjal Barite Deposit and consists of manganese outcrops that are 3 m thick and 120 m long. The zone grades 20 to 40 percent pyrolusite, 50 to 70 percent psilomelane, 2 to 3 percent iron oxides and grades from 28 to 30 wt. percent manganese oxide, 0.03 wt. percent cobalt, and 0.01 to 0.30 wt. percent nickel (Kazak and others, 1965).

Exploration history—Very little exploration is recorded for bedded manganese in Afghanistan and within Lower Carboniferous sedimentary rocks.

Tract boundary criteria—The sedMn01 tract was delineated to include lower carboniferous felsic and mafic volcanic rocks, limestone, shale, sandstone and conglomerate in central Afghanistan (map unit ***C1rb***) that host the Farenjal manganese and barite occurrences in Parwan Province.

Important data sources—Geologic map and mineral occurrence data base (Doebrich and Wahl, 2006).

Needs to improve assessment—Additional field investigation needs to take place within the Lower Carboniferous rocks to identify the specific horizon that is most favorable to host this type of mineralization.

Optimistic factors—Additional barite occurrences are hosted in Mississippian rocks to the north of the tract and may be considered to be part of the tract. The presence of barite indicates that mineralizing systems were present on a wider scale than the known occurrence during the formation of Farenjal.

Pessimistic factors—The Farenjal occurrence is small and isolated and may be the result of extensive weathering, rather than primary mineralization.

Quantitative assessment—No quantitative assessment was attempted by the Assessment Team due to the lack of relevant information regarding the known occurrences regarding deposit model classification.

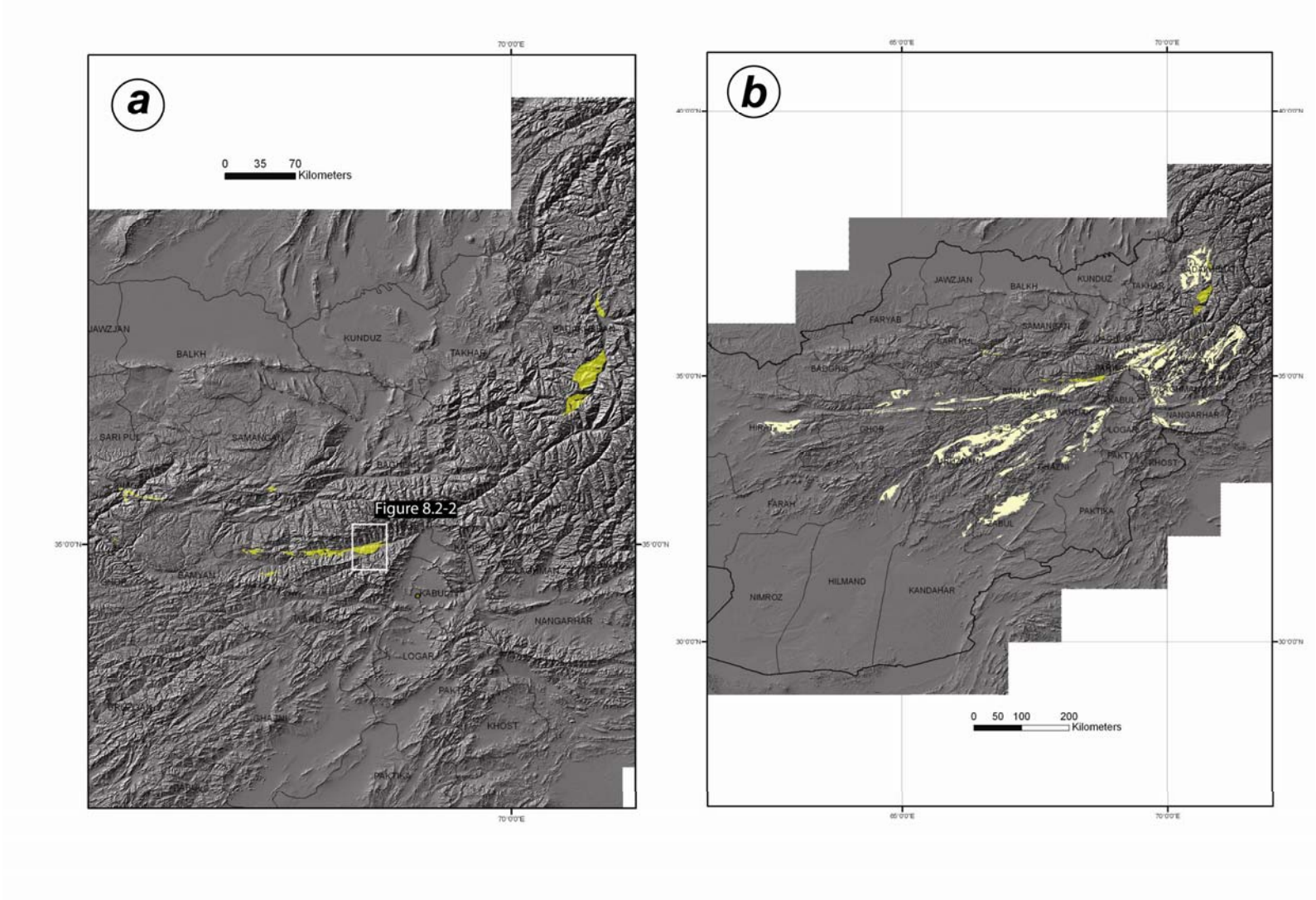

Figure 8.2-1. Maps of Phanerozoic and Proterozoic tracts for sedimentary manganese. (*a*) Map showing permissive tract sedMn01 for Lower Carboniferous-hosted manganese deposits. (*b*) Map showing total permissive tracts for sedimentary manganese. The darker yellow is the Carboniferous age tracts (sedMn01); the lighter colors are the same as the Proterozoic iron permissive tracts sedFe01 (Neoproterozoic), sedFe02 (Paleoproterozoic), and sedFe03 (Mesoproterozoic).

Figure 8.2-2. Map showing parts of permissive tract sedMn01 (yellow) that contains the Farenjal manganese and barite occurrences in Parwan Province. Tract is composed of C_1rb = Early Carboniferous rhyolite to basalt volcanic rocks and limestone, slate, sandstone conglomerate at the contact with Ossl = Ordovician sandstone, siltstone, shale, limestone and shale. Geology is from Doebrich and Wahl (2006).

8.3 Evaporite Deposits

The two major evaporite deposits addressed by the USGS-AGS assessment Team are potash (section 8.3A) and halite (section 8.3B). Halite-salt is abundant in Afghanistan, whereas Potash is not as well known (Ludington and others, 2006). A quantitative estimate was conducted for undiscovered potash resources.

8.3A Potash

Contributions by Greta J. Orris, Karen S. Bolm, and Walter J. Bawiec.

Potash, an important fertilizer mineral, may be present in the evaporate deposits in rocks that contain petroleum resources in northern Afghanistan. The term potash most commonly refers to potassium salt, KCl, but the term is also more generally used to include all forms of potassium minerals and compounds. Potash is the third most widely used fertilizer mineral and more than 95 percent of total potash consumption is used for fertilizer, with the remaining uses including such diverse products as soaps and detergents, glass and ceramics, chemical dyes, and drugs (Williams-Stroud, 1991; Harben, 2002).

8.3A.1 Descriptive deposit model

The most important deposit model for potash is potash-bearing bedded halite (Williams-Stroud, 1991); these deposits are the major source of potash in the world. Thick accumulations of chloride evaporite deposits occur in basins where evaporation exceeds the inflow of water. Traditionally it has been believed that these evaporite deposits have formed marine basins where inflow was limited by sea level changes. More recently, detailed geology on a number of deposits have shown that these deposits can form in a variety of structural and other basins, including marginal marine basins, rift basins, and closed continental basins. Some basins appear to be of continental origin. Common features include: restricted inflow, basin subsidence during evaporite deposition, a relatively arid climate, and restricted supply of clastic materials. In these systems, potash may be precipitated after halite in the areas of thickest halite or may be interbedded in a cyclical manner with halite. Two sub-types of this deposit are commonly distinguished—$MgSO_4$-rich deposits and $MgSO_4$-poor deposits. The $MgSO_4$-poor deposits are found throughout the Phanerozoic, but the $MgSO_4$-rich deposits are largely Permian, Miocene, and Quaternary (Williams-Stroud, 1991). Rocks types include gypsum-anhydrite, dolomite, and other rocks typical of evaporite sequences.

Potash-bearing bedded salt deposits are dominantly composed of salt (NaCl) with up to a few tens of percent contained K_2O. Potash is commonly present as the mineral sylvite (KCl), but other soluble potassium minerals are commonly found and may dominate in some deposits. These minerals include: carnallite, kainite, and langbeinite. Because these ore minerals are so soluble, deposits are easily destroyed by groundwater dissolution. Major evaporite basins may have potash present in one or multiple sub-basins, but the potash may be present over large areas. Deposits contain between 49 and 990 million metric tons with a mean of 265 million metric tons. Grades of potash (K_20) are between 14 and 28 wt. percent K_20 with a mean of 21 wt. percent K_20 (G. Orris, written comm., 2007).

Examples of Deposit Type: The preeminent deposits are the Middle Devonian-age deposits of the Elk Point Basin, Saskatchewan, Canada. Short descriptions of this deposit and other world-class potash-bearing bedded salt deposits may be found in Garrett (1996), and Harben and Kuzvart (1996). Major

Jurassic potash-bearing bedded halite deposits occur at Gaurdak, Karlyuk, and Okuzbulak in Turkmenistan and at Tyubegatanskoe, Khodzhaikan, and Kyzylmazar in Uzbekistan (Troitsky, 1998; Luchnikov, 1982; Kahle and Scherzberg, 2000).

Probable Age(s) of Mineralization: It is most likely that any potential potash deposits would occur in the extensive evaporites in the Jurassic of the Afghan-Tajik basin; the known deposits in neighboring Uzbekistan and Turkmenistan are of this age. Potash occurrences of Cambrian age are reported in the Salt Range Formation along Pakistan's border with Iran (Smaller Tertiary-Recent deposits are reported in Iran and while there may be some small chance for these deposits in Afghanistan, there is no report of potash in the extensive exposed Tertiary sediments and the potential for younger deposits was not considered in this assessment. Smith (1975) discussed the potential for younger K resources in Afghanistan, especially in surface and near-surface brines and playas.

Known Occurrences in Afghanistan: There are no reported potash occurrences in Afghanistan.

Exploration Guides: Evaporite basins with thick sequences of halite. Saline wells or springs may indicate salt at depth. Gypsum and anhydrite are often vertically or laterally peripheral to halite and potash. Large salt bodies produce negative gravity anomalies.

8.3A.2 Mineral Resource Tracts

A single tract permissive for the occurrence of undiscovered potash deposits was delineated in northern Afghanistan by the USGS-AGS mineral assessment team. A preliminary quantitative estimate was agreed upon, but the lack of known deposits precluded further analysis. Additional work is recommended to refine the assessment (Ludington and others, 2006).

Permissive Tract AFK-01.

Examples of Deposit Type—There are no known deposits or occurrences of potash-bearing bedded halite within Afghanistan.

Probable Age(s) of Mineralization—The Jurassic evaporites within the Afghan-Tajik Basin have the greatest potential for containing potash-bearing bedded halite deposits.

Exploration History—None for potash or halite, but there has been oil and gas exploration. While many buried potash deposits have been discovered by oil and gas exploration, some have not been recognized during this type of exploration.

Tract boundary criteria—The tract includes those parts of the Afghan-Tajik and Amu-Darya basins underlain by Jurassic salt as defined in Steinshouer and others (2006).

Needs to improve assessment—The assessment team recognized that drill hole data and more detailed geophysics would allow for better estimates of undiscovered potash.

Optimistic factors—Significant amounts of Jurassic salt underlie the Amu-Darya and Tajik basins (Ulmishek, 2004; Klett and others, 2006.) Large potash deposits exist in correlative Jurassic evaporites in neighboring Uzbekistan and Turkmenistan.

Pessimistic factors—Locally salt depth, and thus potential potash depth, may be below 3 km assessment limit; in other areas depth would likely preclude conventional mining of potash. Information available at

the time of the assessment was not adequate to locate or quantify the probable depths of potential deposits. No potash mineralization has been reported in Afghanistan.

***Quantitative Assessment*—**Estimates of undiscovered potash deposits: in tract AFK-01 are shown in table 8.3A-1

Table 8.3A-1. Probability estimates for undiscovered potash-bearing bedded halite deposits in tract AFK-01.

	Probability		
Estimator	**90 percent**	**50 percent**	**10 percent**
Consensus	0	0	1

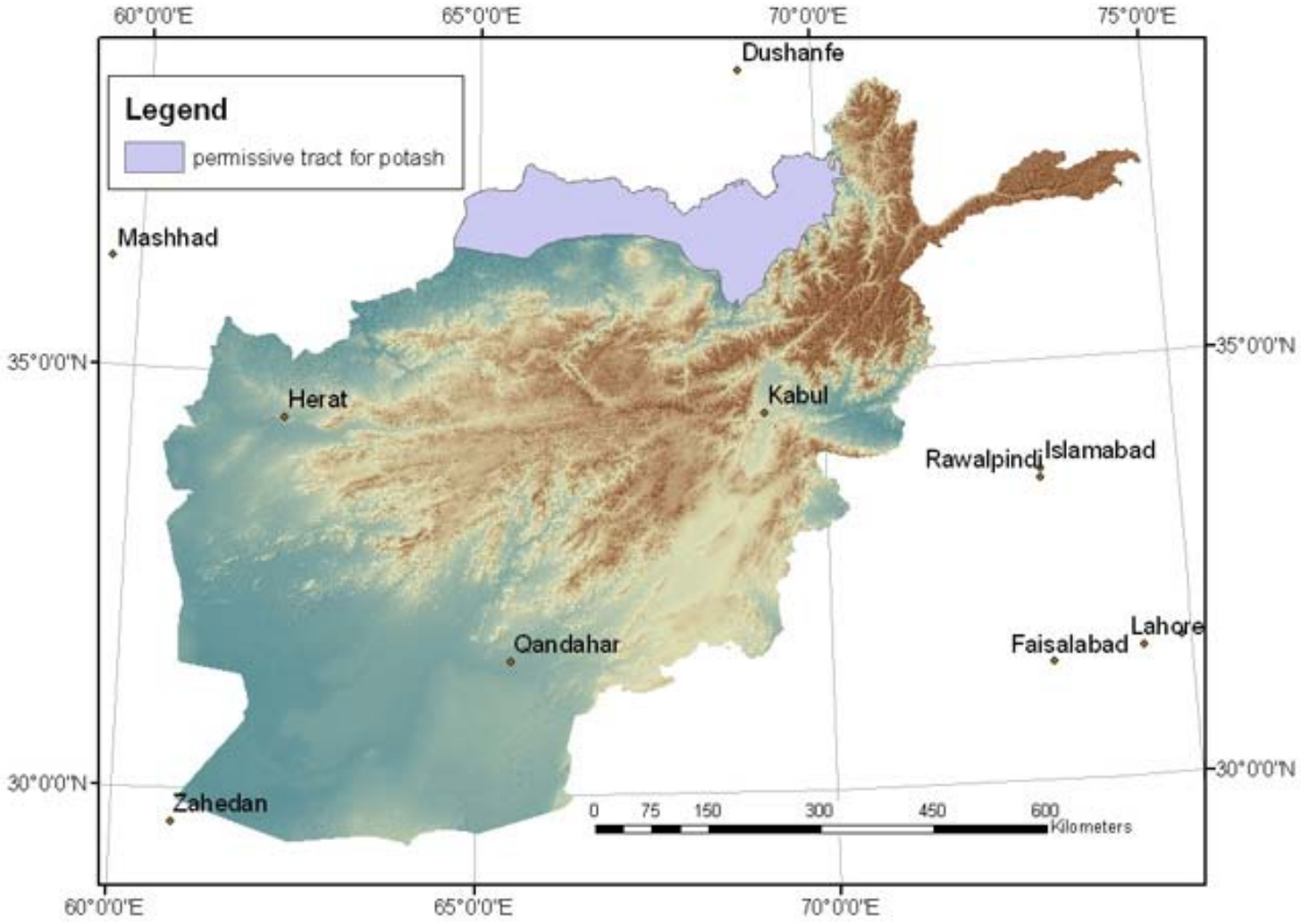

Figure 8.3A-1 Map showing tract AFK-01, the area considered permissive for the occurrence of Jurassic potash-bearing bedded salt.

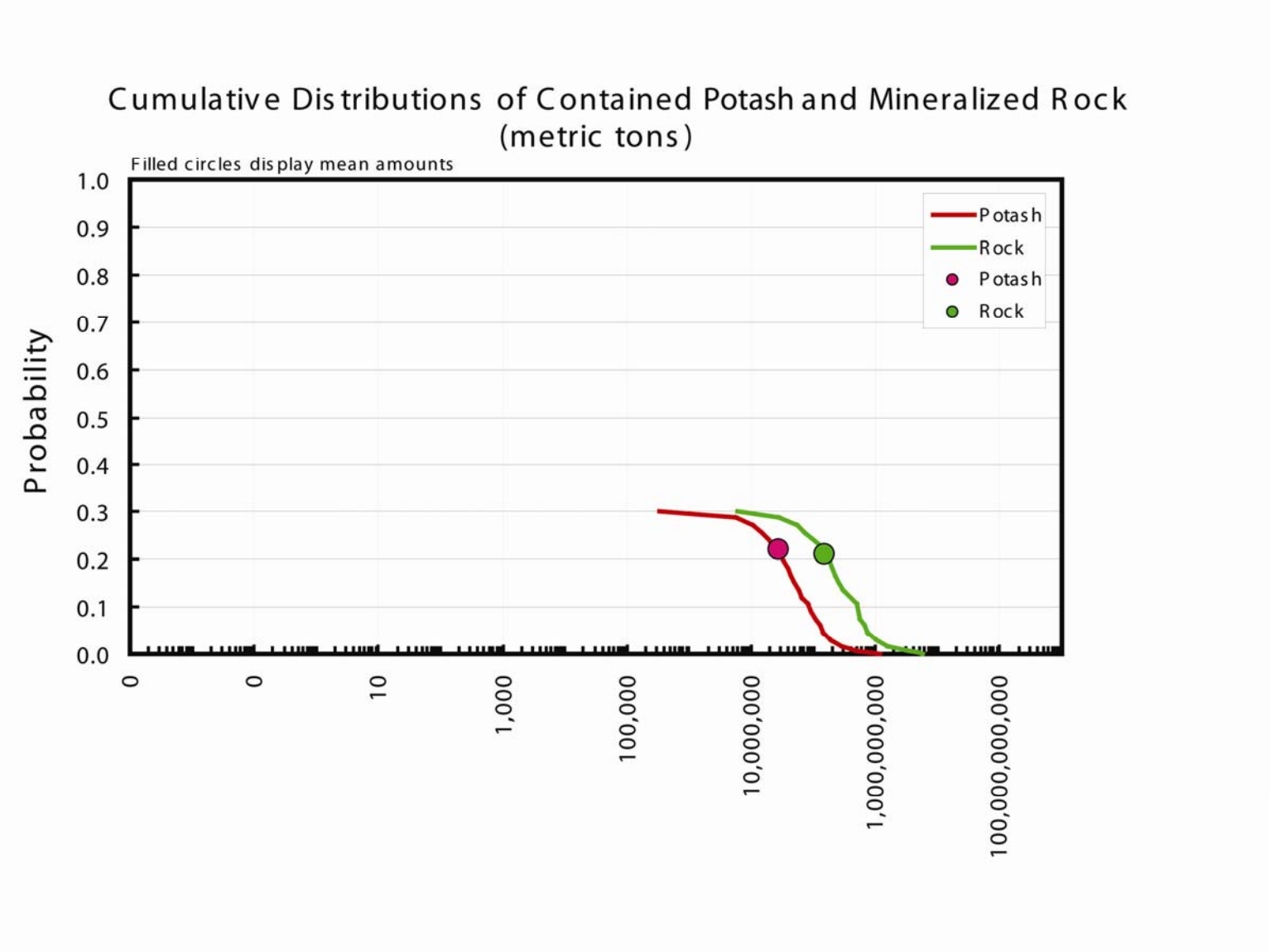

Figure 8.3A-2. Cumulative distribution for potash based on the probabilistic estimates of undiscovered deposits for tract AFK-01, the permissive tract for Jurassic evaporites of the Afghan-Tajik basin.

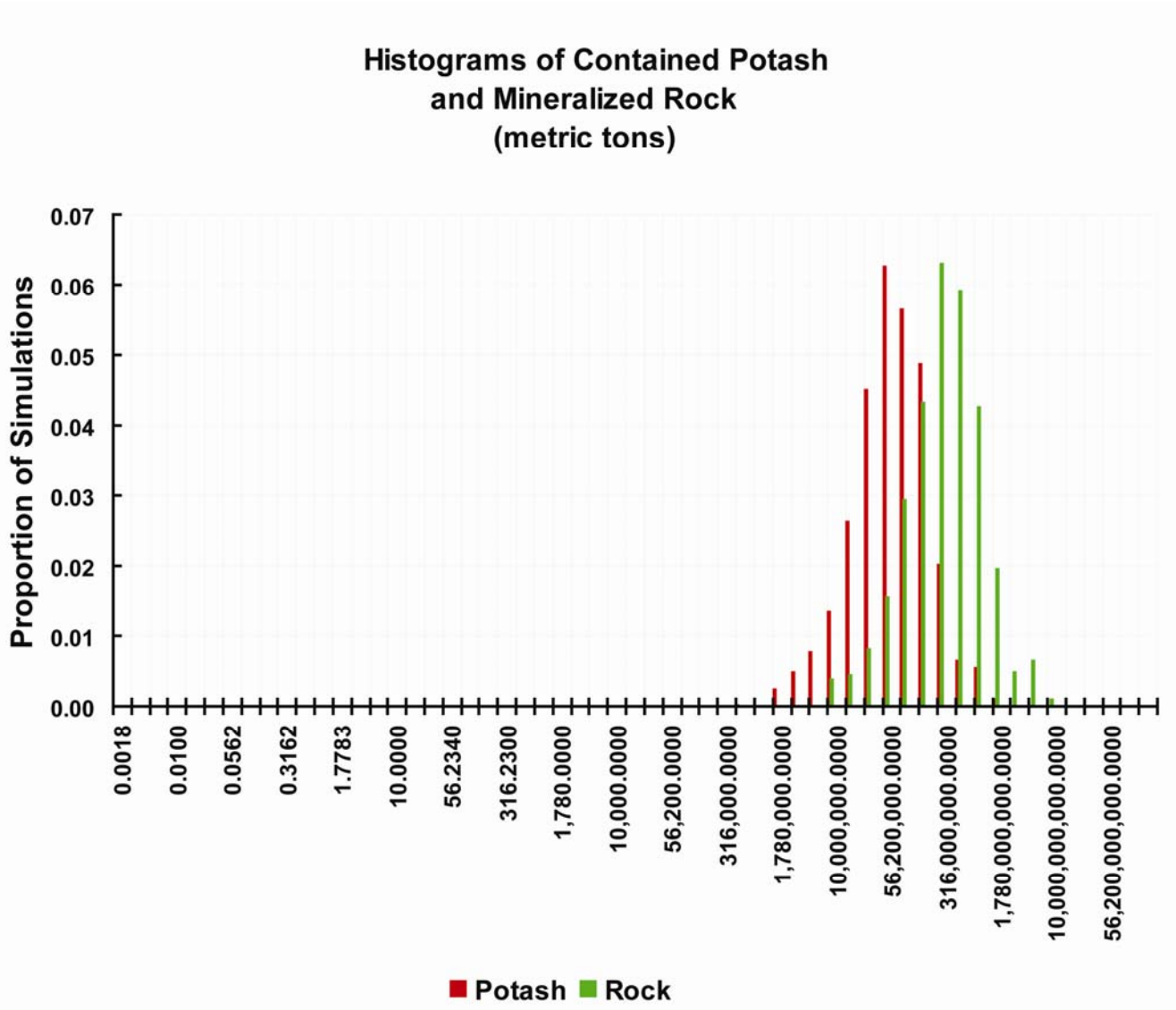

Figure 8.3A-3. Histogram of estimated potash and mineralized rock for undiscovered potash-bearing bedded salt deposits based on the probabilistic estimated for Jurassic evaporites of the Afghan-Tajik basin.

Table 8.3A-2. Table showing probabilistic distribution of estimated contained asbestos and mineralized rock for undiscovered potash-bearing bedded halite deposits for the probabilistic estimated for Jurassic evaporites of the Afghan-Tajik basin.

The tract ID is **Potash01**

There is a 90% or greater chance of 0 or more deposits.
There is a 50% or greater chance of 0 or more deposits.
There is a 10% or greater chance of 1 or more deposits.

Estimated amounts of contained metal and mineralized rock (metric tons)

quantile	Potash	Rock
0.95	0	0
0.90	0	0
0.50	0	0
0.10	85,000,000	520,000,000
0.05	140,000,000	710,000,000
mean	28,000,000	160,000,000
Probability of mean	0.22	0.21
Probability of zero	0.70	0.70

References

Abdullah, Sh., Chmyriov, V.M., Stazhilo-Alekseev, K.F., Dronov, V.I., Gannan, P.J., Rossovskiy, L.N., Kafarskiy, A.Kh., and Malyarov, E.P., 1977, Mineral resources of Afghanistan (2nd ed.): Kabul, Afghanistan, Republic of Afghanistan Geological and Mineral Survey, 419 p.

Doebrich, J.L., and Wahl, R.R., 2006, Geologic and mineral resource map of Afghanistan: U.S. Geological Survey Open–File Report 2006–1038, 1 sheet scale 1:850,000, available on line at *http://pubs.usgs.gov/of/2006/1038*/

Economic and Social Commission for Asia and the Pacific, 1995, Geology and mineral resources of Afghanistan: New York, United Nations, Atlas of Mineral Resources of the ESCAP Region, v. 12, 85 p.

Garrett, D.E., 1996, Potash- deposits, processing, properties and uses: New York, Chapman & Hall, 734 p.

Klett, T.R., Ulmishek, G.F., Wandrey, C.J., Agena, W.F., and The U.S. Geological Survey-Afghanistan Ministry of Mines and Industry Joint Oil and Gas Resource Assessment Team, 2006, Assessment of Undiscovered Technically Recoverable Conventional Petroleum Resources of Northern Afghanistan: U.S. Geological Survey Open-File Report OF06–1253.

Harben, P.W., 2002, Potassium minerals and compounds, *in* The industrial minerals handbook; A guide to markets, specifications & prices, 4th edition: Worcester Park, UK, Industrial Minerals Information, p. 264–272.

Kahle, Klaus, and Scherzberg, Heinz, 2000, New potassium-projects as a source for sodium chloride products with a high purity, *in* Geertman, R.M., ed., 8th World Salt Symposium, Volume 1: New York, Elsevier, p. 583–588.

Luchnikov, V.S., 1982, Upper Jurassic halogen deposits of southeast Central Asia: Petroleum Geology, v. 20, no. 7, p. 296–298.

Ludington, Steve, Orris, G.J., Bolm, K.S., Peters, S.G., and the U.S. Geological Survey-Afghanistan Ministry of Mines and Industry Joint Mineral Resource Assessment Team, 2007, Preliminary Mineral Resource Assessment of Selected Mineral Deposit Types in Afghanistan: U.S. Geological Survey Open–File Report 2007–1005, 44 p., available on line at *http://pubs.usgs.gov/of/2007/1005/.*

Smith, G.I., 1975, Potash and other evaporite resources of Afghanistan: U.S. Geological Survey Open-File Report 75–89, 63 p.

Steinshouer, D.W., Klett, T.R., Ulmishek, G.F., Wandrey, C.J., Ronald R. Wahl, R.R., Hill, R.J., Pribil, Michael, Pawlewicz, M.J., King, J.D., Agena, W.F., Taylor, D.J., Amirzada, Abdulla, Selab, A.M., Mutteh, Abdul-Salam, Haidari, G.N. and Wardak, M.G., 2006, Petroleum Resource Potential GIS of Northern Afghanistan: U.S. Geological Survey Open-File Report 2006–1179, 1 disk.

Troitsky, V., Petrov, I., and Grishaev, S., 1998, Industrial minerals of the CIS: Worcester Park, Surrey, England, Industrial Minerals Information Ltd., 135 p.

Ulmishek, G.F., 2004, Petroleum Geology and Resources of the Amu-Darya Basin, Turkmenistan, Uzbekistan, Afghanistan, and Iran: U.S. Geological Survey Bulletin 2201–H, 38 p.

Williams-Stroud, S., 1991, Descriptive model of potash-bearing bedded salt, *in* Orris, G.J., and Bliss, J.D., eds., Some industrial mineral deposit models; descriptive deposit models: Open-File Report OF91-11A, U.S. Geological Survey, p. 26–28.

8.3B Halite

Contributions by Greta J. Orris and Karen S. Bolm

Salt (NaCl) is not only an essential ingredient for life, but is an essential feedstock of sodium and chlorine compounds for the chemical industry (Harben and Kuzvart, 1996). Sodium chloride is found in nature in brines, including seawater, and as common salt. Salt was an object of early barter trade and documented uses and mining of salt extend back more than 5000 years.

Salt occurs in almost every geological period and is widely distributed throughout the world. Salt is produced from several types of deposits: (1) large bedded deposits of marine, transitional, or continental origin; (2) salt domes originating from thick deeply buried bedded salt deposits; (3) seawater; (4) lacustrine brines; (5) playa salts and brines; 6) groundwater brines (Harben and Kuzvart, 1996). Afghanistan is known to have bedded salt deposits, salt dome deposits, and playa deposits (Ludington and others, 2006).

8.3B.1 Descriptive deposit models

The three types of salt deposits known in Afghanistan are bedded salt deposits, related salt dome deposits, and young playa salts and brines (Lefond, 1969; Smith, 1975; Abdullah and others, 1977; Luchnikov, 1982).

Bedded Salt. The most important deposit model for potash is bedded salt (Raup, 1991a; Harben and Kuzvart, 1996; Feldman, 2006). Thick accumulations of chloride evaporite deposits occur in basins where evaporation exceeds the inflow of water. Traditionally it has been believed that these evaporite deposits have formed in marine basins where inflow was limited by sea level changes. More recently, detailed geologic studies of a number of deposits have shown that these deposits can form in a variety of structural and other basins, including marginal marine basins, rift basins, and closed continental basins. Some basins appear to be of continental origin; in these cases, evaporating interior seas become saline as result of the solutes that were carried into the basin from the leaching and flushing of rocks within the drainage basin (Feldman, 2006). Common features include: restricted inflow relative to evaporation, basin subsidence during evaporite deposition, a relatively arid climate, and restricted supply of clastic materials.

Salt Domes. Salt has a low density and will flow in a plastic manner when subjected to enough compressive stress, which can come from the weight of overlying sediments or from a variety of tectonic factors (Raup, 1991b; Harben and Kuzvart, 1996; Feldman, 2006). When this happens, salt will flow into area of decreased pressure, commonly vertically through the overlying sediments; this process forms salt domes and related features. Salt domes most commonly originate from thick bedded salt deposits.

Playa Salt and Brines. Playas are basically dry or nearly dry lakebeds or the floor of a desert basin. In these deposits, salts may form surface crusts that may be up to several meters thick or form efflorescences in the surface and peripheral sediments. Salt may also be concentrated in shallow surficial brines. Alternatively, there may be no brines at the surface, but below a surface crust, there may be one or more layers of brine- saturated sediments. Smith (1975) discussed the potential for younger K resources in Afghanistan, especially in surface and near-surface brines and playas.

Examples of Deposit Type: Salt is found in large amounts in many major bedded salt deposits are mined in Uzbekistan and Tajikistan (Troitsky and others, 1998; Luchnikov, 1982). In Tajikistan, the salt is reported to be 900 m thick between the Vaksh and Pyandzh Rivers (Luchnikov, 1982); more generally,

Luchnikov reports that the Jurassic salt is thickest in a belt that extends along the present course of the Amu-Dar'ya River and then northeast into Tajikistan.

Probable Age(s) of Mineralization: It is known that there is buried Jurassic bedded salt in the Afghan-Tajik and Amu Darya Basins; the known deposits in neighboring Uzbekistan and Turkmenistan are of this age. Salt domes are known to be linked to the Jurassic bedded salt deposits and some are at or near the surface in that part of northern Afghanistan.

Known Occurrences in Afghanistan: There is well-documented Jurassic halite at depth within the Amu-Darya and Afghan-Tajik basins. Zharkov (1984) reports that evaporites of questionable age, including rock salt, may be present in western and central Afghanistan between Rakha, Pakistan and Kerman, Iran; this salt has been reported as Devonian and Neogene in age. This area of Afghanistan is covered largely by Quaternary and Tertiary sediments and no subsurface information has been located by the assessors. A report on the Kunduz River Basin (Riedmann and Beekma, 2005) mentions that the Namak Ab River in Takhar Province cuts through a large salt deposit believed to be of Cretaceous age because it occurs with Cretaceous limestone. High purity salt was mined from diapiers at Taqca Khana and Kalafgan in Takhar Province (Smith, 1975) which are considered to be Jurassic; however, the diapiers are enclosed by Cretaceous sediments. For this reason, the salt reported by Riedmann and Beekma is probably also Jurassic. Abdullah and others (1977) report Jurassic salt at the Chal-I and Chal-II deposits also in Takhar Province.

The remaining salt deposits in Afghanistan, for which there is any data, appear to be Holocene playa brines and salt.

Exploration Guides: Evaporite basins with thick sequences of halite. Saline wells or springs may indicate salt at depth. Gypsum and anhydrite are often vertically or laterally peripheral to halite and potash. Large salt bodies produce negative gravity anomalies.

8.3B.2 Mineral Resource Tracts

Tract AFBS-01. This tract is identical to that delineated for potash-bearing bedded salt. The Jurassic salt is known to occur at depth, but it is not clear how much of the salt is shallow enough to be economic.

Examples of Deposit Type: Within the tract, Jurassic salt is known to occur at depths of up to 3 km and salt domes originating from these deposits have reached the surface in the northeastern part of the tract.

Probable Age(s) of Mineralization: The buried deposits within the Afghan-Tajik and Amu-Darya Basins and the salt domes in the same region are Jurassic.

Exploration History: None for halite, but there has been oil and gas exploration (Klett and others, 2006; Ulmishek, 2004).

Tract boundary criteria: The tract was determined by the parts of the Afghan-Tajik and Amu-Darya basins in Afghanistan that are underlain by Jurassic salt as defined in Steinshouer and others (2006). The southern boundary of the tract is based on the chloride facies boundary from Steinshouer and others (2006). Generalized stratigraphic sections indicated that most of the salt is at or less than the 3 km depth limit for this deposit type (Steinshouer and others, 2006; Klett and others, 2006; Ulmishek, 2004).

Needs to improve assessment: The assessment team recognized that drill hole data and more detailed geophysics would allow for better estimates of buried salt.

Optimistic factors: Significant amounts of Jurassic salt underlie the Amu-Darya and Tajik basins (Ulmishek, 2004; Klett and others, 2006.)

Pessimistic factors: Locally salt depth may be below the 2 km assessment limit and it is unlikely that the bedded deposits could be mined using conventional methods. Information available at the time of the assessment was not adequate to locate or quantify the probable depths of potential deposits.

Quantitative Assessment. No estimates were made, since Jurassic salt occurs at depth under the entire tract and no grade and tonnage model is applicable.

References

Abdullah, Sh., Chmyriov, V.M., Stazhilo-Alekseev, K.F., Dronov, V.I., Gannan, P.J., Rossovskiy, L.N., Kafarskiy, A.Kh., and Malyarov, E.P., 1977, Mineral resources of Afghanistan (2nd ed.): Kabul, Afghanistan, Republic of Afghanistan Geological and Mineral Survey, 419 p.

Economic and Social Commission for Asia and the Pacific, 1995, Geology and mineral resources of Afghanistan: New York, United Nations, Atlas of Mineral Resources of the ESCAP Region, v. 12, 85 p.

Feldman, S.R., 2006, Salt, *in* Kogel, J.E., Trivedi, N.C., Barker, J.M., and Krukowski, S.T., eds., Industrial minerals and rocks, 7th edition: Littleton, Colo., Society for Mining, Metallurgy, and Exploration, Inc., p. 793–813.

Harben, P.W., 2002, Potassium minerals and compounds, *in* The industrial minerals handybook; A guide to markets, specifications and prices, 4th edition: Worcester Park, UK, Industrial Minerals Information, p. 264–272.

Kahle, Klaus, and Scherzberg, Heinz, 2000, New potassium-projects as a source for sodium chloride products with a high purity, *in* Geertman, R.M., ed., 8th World Salt Symposium, Volume 1: New York, Elsevier, p. 583-588.

Klett, T.R., Ulmishek, G.F., Wandrey, C.J., Agena, W.F., and The U.S. Geological Survey-Afghanistan Ministry of Mines and Industry Joint Oil and Gas Resource Assessment Team, 2006, Assessment of Undiscovered Technically Recoverable Conventional Petroleum Resources of Northern Afghanistan: U.S. Geological Survey Open-File Report OF06–1253.

Lefond, S.J., 1969, Handbook of world salt resources: New York, Plenum Press, 384 p.

Luchnikov, V.S., 1982, Upper Jurassic halogen deposits of southeast Central Asia: Petroleum Geology, v. 20, no. 7, p. 296–298.

Ludington, Steve, Orris, G.J., Bolm, K.S., Peters, S.G., and the U.S. Geological Survey-Afghanistan Ministry of Mines and Industry Joint Mineral Resource Assessment Team, 2007, Preliminary Mineral Resource Assessment of Selected Mineral Deposit Types in Afghanistan: U.S. Geological Survey Open–File Report 2007–1005, 44 p., available on line at *http://pubs.usgs.gov/of/2007/1005/*

Raup, O.B., 1991a, Descriptive model of bedded salt, *in* Orris, G.J., and Bliss, J.D., eds., Some industrial mineral deposit models; descriptive deposit models: Open-File Report OF91-11A, U.S. Geological Survey, p. 29–30.

Raup, O.B., 1991b, Descriptive model of salt domes; Deposit subtype: diapiric salt structures, *in* Orris, G.J., and Bliss, J.D., eds., Some industrial mineral deposit models; descriptive deposit models: Open-File Report OF91-11A, U.S. Geological Survey, p. 31–33.

Riedmann, Frank, and Beekma, Jelle, 2005, Implementing the Kunduz River Basin authority, a joint presentation by KRBP and DWHH/GAA: Kabul Water Conference 02.08—03.08. 2005, unpublished presentation, 9 p.

Smith, G.I., 1975, Potash and other evaporite resources of Afghanistan: U.S. Geological Survey Open-File Report 75–89, 63 p.

Steinshouer, D.W., Klett, T.R., Ulmishek, G.F., Wandrey, C.J., Ronald R. Wahl, R.R., Hill, R.J., Pribil, Michael, Pawlewicz, M.J., King, J.D., Agena, W.F., Taylor, D.J., Amirzada, Abdulla, Selab, A.M., Mutteh, Abdul-Salam, Haidari, G.N. and Wardak, M.G., 2006, Petroleum Resource Potential GIS of Northern Afghanistan: U.S. Geological Survey Open-File Report 2006–1179.

Troitsky, V., Petrov, I., and Grishaev, S., 1998, Industrial minerals of the CIS: Worcester Park, Surrey, England, Industrial Minerals Information Ltd., 135 p.

Ulmishek, G.F., 2004, Petroleum Geology and Resources of the Amu-Darya Basin, Turkmenistan, Uzbekistan, Afghanistan, and Iran: U.S. Geological Survey Bulletin 2201-H, 38 p.

Zharkov, M.A., 1984 (1974), Paleozoic salt bearing formations of the world: New York, Springer-Verlag, 427 p.

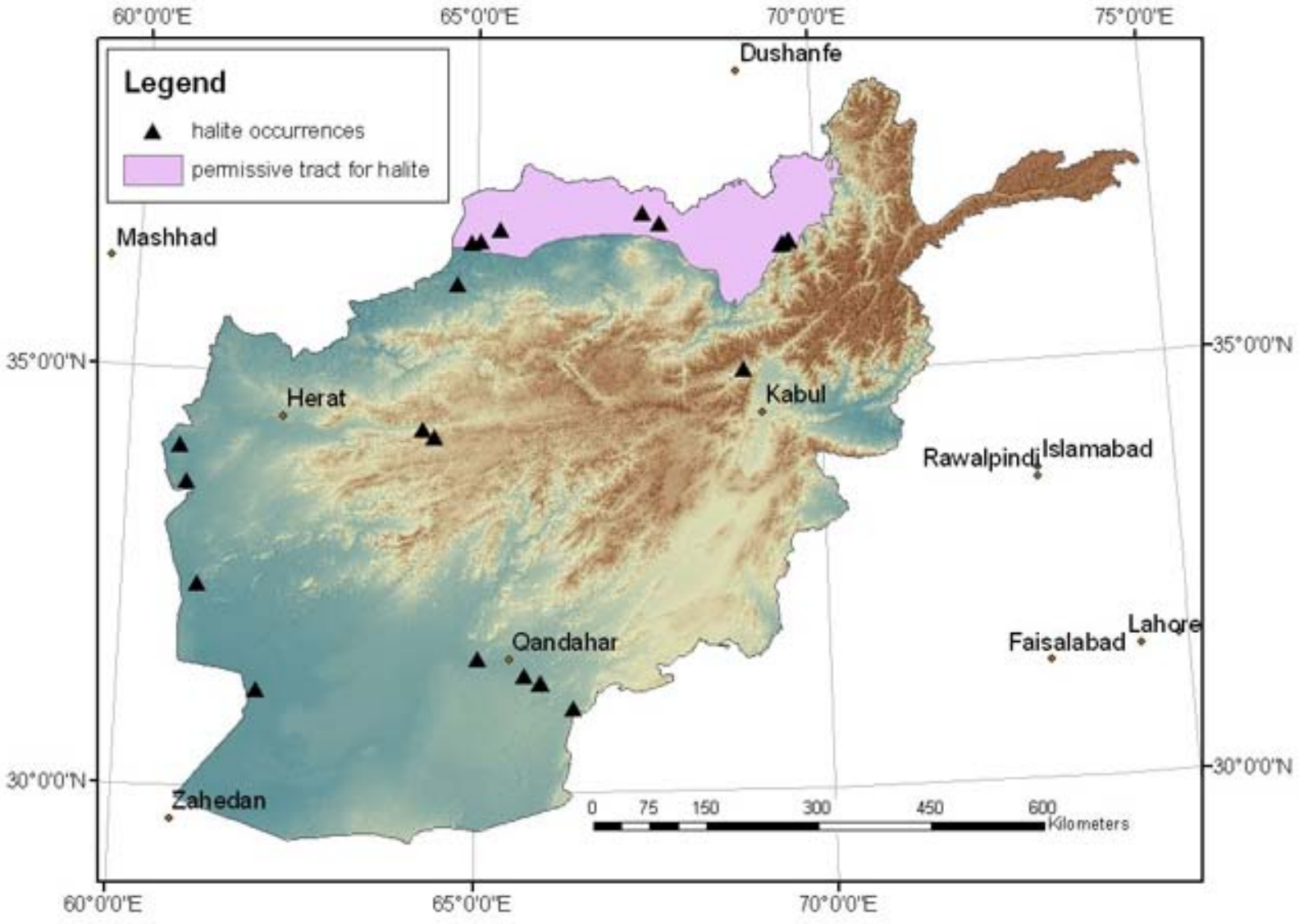

Figure 8.3B-1. Map showing tract AFBS-01, the area considered permissive for the occurrence of Jurassic bedded salt. Most of the halite occurrences outside of the tract are in very young rocks and are of limited size.

8.4 Sedimentary phosphorite

Contributions by Stephen G. Peters and Greta J. Orris.

Phosphate that is hosted in sedimentary rocks is a common deposit type and a number of sedimentary sequences in Afghanistan are permissive for the occurrence of undiscovered phosphorite deposits. Few phosphorite occurrences are known in Afghanistan. Phosphorite is present within volcanic rocks in the radioactive Khanneshin area in Helmand Province (section 3.0). There is one known phosphorite occurrence contained within sedimentary rocks in Herat Province (Abdullah and others, 1977).

8.4.1 Descriptions of phosphorite deposit models

The two deposit model types that may be applicable for future assessment of undiscovered phosphorite deposits in Afghanistan are the upwelling-type and warm current type phosphate deposits as described below.

Upwelling-type phosphate deposits (model 34c, Mosier, 1986a) are phosphorite sediments from a major stratigraphic unit within a sequence of marine sediments in upwelling areas in basins with good connection to the open sea (Slansky, 1980); Sheldon, 1964). They are with phosphorite, marl, shale, chert, limestone, dolomite, and volcanic materials of Precambrian through Miocene age. The depositional environment is marked by areas that were highly productive in plankton. Deposition occurs mostly in warm latitudes, mostly between the 40th parallels. Tectonic setting is intra-plate shelf, platform, miogeosynclines, and eugeosynclines. Associated deposit types are sedimentary Mn. Mineralogy consists of apatite + fluorapatite + dolomite + calcite + quartz + clays (montmorillonite or illite) ± halite ± gypsum ± iron oxides ± siderite ± pyrite ± carnotite. Ore textures are pellets, nodules, phosphatized shell and bone material. Deposits form in basins, or parts of basins, favorable for the accumulation of organic-rich sediments and for their evolution into phosphorite. Individual beds may be one meter thick or more and may extend over hundreds of square kilometers. Weathering products are limonite and goethite. Geochemical signatures are elevated concentrations of P, N, F, C, and U. The deposits commonly are anomalously radioactive (Krauss and others, 1984). Mean tonnage for upwelling phosphorite deposits are 330 million metric tons and mean grades of phosphate ($P_2 0_5$) are 25 percent $P_2 0_5$ (Mosier, 1986b).

Warm-current type phosphate deposits (model 34d, Mosier 1986c) contain phosphorites that are formed in warm currents along the eastern coasts of continent. They consist of phosphatic limestone or sandstone. (Cathcart and Gulbrandsen, 1973; Sheldon, 1964). The geological environment consists of phosphatic limestone and sandstone as well as chert and diatomaceous material. Age range of the deposits is Early Cretaceous through Pliocene. Depositional environment is basins of structural lows that lie along the flanks of rising domes or at the mouths of rivers and estuaries. Deposition occurs in warm paleo latitudes mostly between the 40th parallels. Deposits are formed by dynamic upwelling or by the cool countercurrent that were derived from warm density currents. Tectonic Setting is the continental shelf and the deposits may be with eugeosynclinal rocks. Mineralogy consists of fluorapatite + quartz + dolomite + montmorillonite + kaolinite + calcite ± wavellite ± crandallite ± illite ± clinoptilolite ± palygorskite ± smectite ± cellophane. Texture of the deposits is phosphatic pellets and fossil fragments with a carbonate matrix. Ore controls are stratigraphic phosphatic horizons within embayments and estuarine environments in proximity to the open sea. Basins on flanks of structural highs (domes, arches, anticlines) also are important controls for phosphate deposition. Weathering usually generates goethite. Geochemical signature is P, C, U, N, F. The deposits are anomalously radioactive.

Mean tonnages for warm-current type deposits is about 400 million metric tons and mean grades are 24 percent P_20_5 (Mosier, 1986d).

8.4.2 Known sedimentary phosphorite occurrences

The known sedimentary phosphorite occurrence is Kotal-i-Sebzak, in northeastern Herat Province. Phosphorite mineralization lies at the base of an Upper Cretaceous clay formation (within map unit K_1ssc of Doebrich and Wahl, 2006) with interbedded sandstone and limestone (fig. 8.4-1). The interval is a 0.3 to 1.1 m thick phosphorus bed with irregular 0.5 to 5 to 6 cm across phosphorite nodules that are cemented by calcareous-phosphate and grade 6.2 to 9.7 wt. percent phosphorus pentoxide. The USGS-AGS assessment team agreed that a permissive tract for sedimentary phosphorite deposits should include map unit K_1ssc. However, a tract was delineated in this preliminary assessment because additional research was necessary to identify if additional phosphate-bearing sedimentary units were present in the country. Due to lack of information about the Kotal-i-Sebzak occurrence, the deposit model could not be identified by the team and therefore no assessment was attempted pending further investigation.

References

Abdullah, Sh., Chmyriov, V.M., Stazhilo-Alekseev, K.F., Dronov, V.I., Gannan, P.J., Rossovskiy, L.N., Kafarskiy, A.Kh., and Malyarov, E.P., 1977, Mineral resources of Afghanistan 2nd ed, Kabul, Afghanistan, Republic of Afghanistan Geological and Mineral Survey, 419 p.

Cathcart, J. B., and Gulbrandsen, R. A., 1973, Phosphate deposits, *in* Brobst, D. A., and Pratt, W. P., eds., United States mineral resources: U.S. Geological Survey Professional Paper 820, p. 515–525.

Doebrich, J.L., and Wahl, R.R., 2006, Geologic and mineral resource map of Afghanistan: U.S. Geological Survey Open–File Report 2006–1038, 1 sheet scale 1:850,000, available on line at *http://pubs.usgs.gov/of/2006/1038/*.

Krauss, U.H., Saam, H.G., and Schmidt, H.W., 1984, International strategic minerals inventory: Summary report—Phosphate: U.S. Geological Survey Circular 930-C, 41 p.

Mikhailov, K.Ya., 1967, Report on geological surveying and prospecting for coal at scale 1:200,000 (sheets 222–C, 502–D, 503–B; part of sheets 221–F, 222–D, 222–F, 502–C, 502–F, 503–C, 503–D, 503–E, 504), Department of Geological and Mineral Survey, Kabul, scale 1:200,000, unpub. data.

Mosier, D.L., 1986a, Descriptive model of upwelling type phosphate deposits, *in* Cox, D.P., and singer, D.A., eds., Mineral Deposit Models: U.S. Geological Survey Bulletin 1693, p 234.

Mosier, D.L., 1986b, Grade and tonnage model of upwelling type phosphate deposits, *in* Cox, D.P., and singer, D.A., eds., Mineral Deposit Models: U.S. Geological Survey Bulletin 1693, p 234.

Mosier, D.L., 1986c, Descriptive model of warm-current type phosphate deposits, in Cox, D.P., and singer, D.A., eds., Mineral Deposit Models: U.S. Geological Survey Bulletin 1693, p 237.

Mosier, D.L., 1986d, Grade and tonnage model warm-current type phosphate deposits, in Cox, D.P., and singer, D.A., eds., Mineral Deposit Models: U.S. Geological Survey Bulletin 1693, p 237.

Orris, G.J., and Bliss, J.D., 2002, Mines and Mineral Occurrences of Afghanistan, U.S. Geological Survey Open–File Report 2002–110, 95 p,, available on line at *http://geopubs.wr.usgs.gov/open–file/of02–110/*.

Sheldon, R. P., 1964, Paleolatitudinal and paleogeographic distribution of phosphorite: U.S. Geological Survey Professional Paper 50 l–C, p. C106–C113.

Slansky, Maurice, 1980, Ancient upwelling models—Upper Cretaceous and Eocene phosphorite deposits around west Africa, *in* Sheldon, R. P., and Burnett, W. C., eds., Fertilizer mineral potential in Asia and the Pacific: Honolulu, East-West Resource Systems Institute, Proceedings of the Fertilizer Raw Materials Resources Workshop, August 20-24, 1979, p. 145–158.

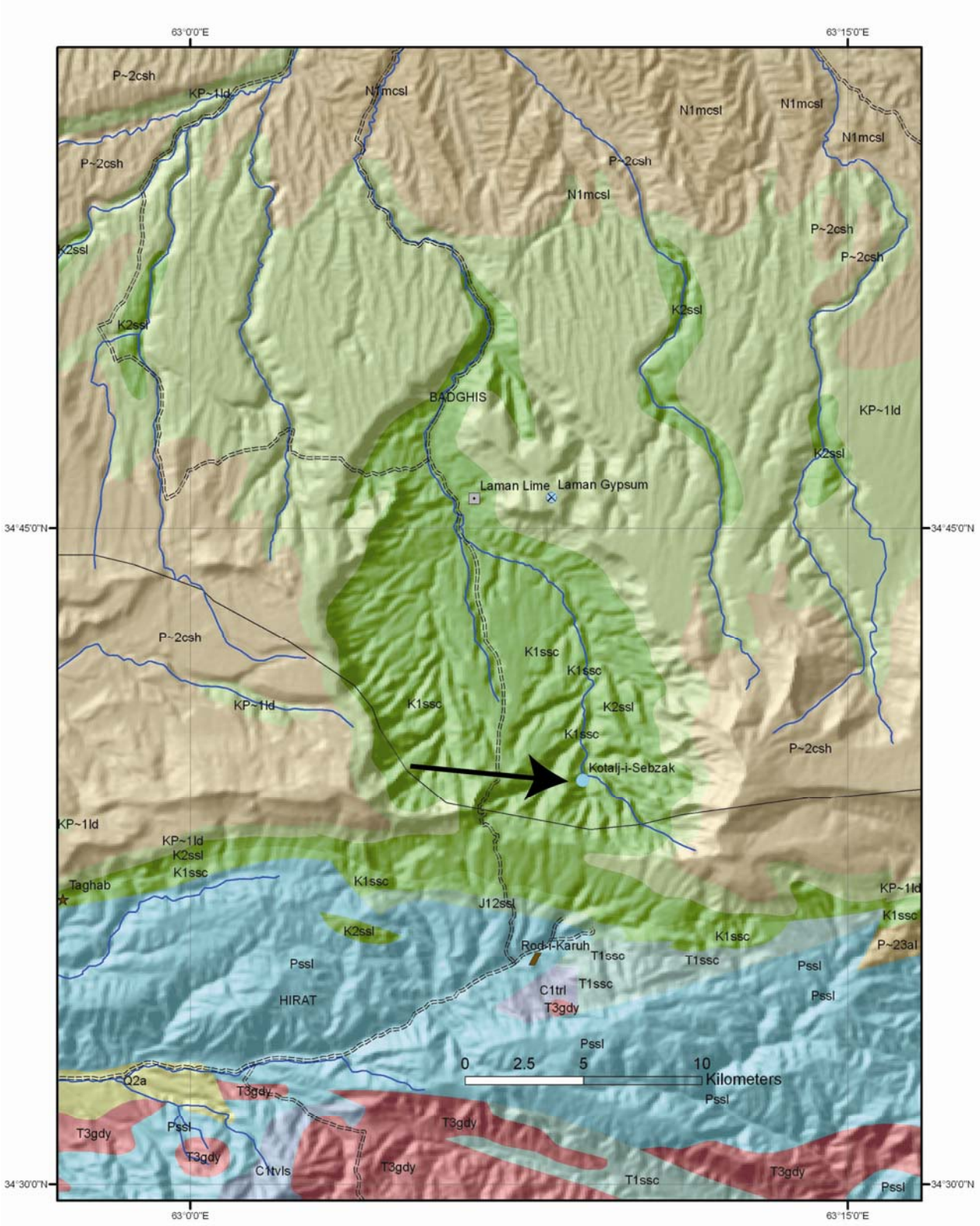

Figure 8.4-1. Geologic map showing location of the Kotal-i-Sebzak sedimentary phosphate occurrence (light blue dot, arrow) on the Herat-Badghis Province boundary within Cretaceous phosphate-bearing clay layers. Geology and symbol legend from Doebrich and Wahl, 2006).

8.5 Celestite

Contributions by Greta J. Orris, Stephen G. Peters and Karen S. Bolm.

Celestite deposits are known in northern Afghanistan in Baghlan and Kunduz Province and two deposits were estimated by Russian workers to contain together over 1million metric tons of Celestite ore. It is probable that large celestite deposits, similar to those in Pakistan and Iran, occur in Afghanistan. Targeted exploration would probably reveal additional deposits. Celestite ($SrSO_4$) is currently the dominant, if not the sole commercial source of strontium. Over 75 percent of the production of celestite is used in the production of radiation-absorbent glass for television, computer, sonar, and other screens (Harben, 2002). Half of the world's production of just over 300,000 metric tons/yr is sourced from Mexico; most of the remaining production is from Spain (Harben and Kuzvart, 1996).

8.5.1 Description of celestite deposit model

Sedimentary celestite deposits are the main source of celestite production. The known deposits in Afghanistan and Iran contain characteristics similar to the bedded celestite type (model 35a.1, Orris, 1992). Sedimentary celestite deposits can form in a variety of ways including primary precipitation and through diagenetic and alteration processes. The strontium to form these deposits is variously believed to be sourced from marine-derived brines, from fluids resulting from the conversion of aragonite to calcite or gypsum to anhydrite, from waters formed by dolomitization of limestone, from dissolution of subaerially-exposed gypsum, and from basinal waters that have leached Sr from nearby rocks (Evans, 1999). Celestite commonly is proximal to evaporate deposits, as well as limestone and dolomite. Mineralization is in the form of concretions, seams, or impregnations (Harben and Kuzvart, 1996). Compared to sedimentary barite deposits, celestite deposits are small with a median tonnage of 830,000 metric tons (fig. 8.5-1) and a median grade of 80 vol. percent $SrSO_4$ (fig. 8.5-2) (Orris, 1992).

Examples of Deposit Type—The preeminent deposits are the Early Cretaceous deposits of Coahuila, Mexico, where the celestite deposits are found around the periphery of the Coahuila Platform (Rodriguez Garza and McAnulty, 1996). The Montevive mine in Spain has been a major producer. There is also a celestite deposit in the Dasht-E-Kavir desert of Iran; this deposit occurs in the lower part of the Oligocene Qum (Qom) formation and is exposed in a northwest-trending ridge system. At the Nakhjir deposit, a 2–to 4–m-thick seam of celestite is mined by open-pit; over one million metric tons of celestite are reported to be present at the nearby Talheh deposit (Harbena and Kuzvart, 1996). Small amounts of celestite production have also been reported in Pakistan. No geologic information was available on these deposits.

Probable Age(s) of Mineralization—The two celestite deposits known in Afghanistan are reported to be Paleogene in age (Abdullah and others, 1977). Since the known deposits in Iran are also Paleogene, specifically Oligocene, in age, it is believed that any undiscovered deposits will also be found in sediments of that age.

Known Occurrences in Afghanistan—Abdullah and others (1977) report two celestite deposits in Afghanistan, Kunduz and Tangi-Murch. At the Kunduz (Kartaw) deposit, the celestite forms a bed 1,400 m along strike that extends 10 to 14 m down dip and is 0.9 to 1.5 (average 0.9) m thick. Speculative resources of one million metric tons of white to bluish crystalline celestite were estimated. At Tangi-Murch in Baghlan Province, Kazak and others (1965) are cited as reporting celestite beds within bituminous limestone (Abdullah and others, 1977). The four celestite bodies are reported to contain speculative resources of 0.085 million metric tons of ore containing 53.96 vol. percent celestite. The

Tangi-Murch deposit is present in the Paleogene bituminous limestones of the Bukharsk and Suzuksk units.

Tract boundary criteria: A permissive tract was delineated using the digital geologic map of Afghanistan (Doebrich and Wahl, 2006). The tract area consists of those map units that have evaporite deposits identified as a major or dominant component. Evaporite-bearing rocks of all ages were combined in this tract because we lacked information to develop criteria for differing probabilities of occurrence in rocks of different ages. Gypsum-anhydrite-bearing sediments of Late Cretaceous to Paleogene age were selected and then buffered five (5) km outward because of the uncertainty of map unit boundaries due to near-horizontal stratigraphy (figs. 8.5-3). Units in which limestone is a minor component in this area could be considered to have lower potential. Additional areas of interest were noted proximal to the known occurrences (fig. 8.5-4a and b)

Exploration Guides—Almost no information is available on exploration for sedimentary celestite deposits. In some cases, exploring near other known celestite deposits, or more generally near evaporite deposits might be useful. Hand specimens of celestite are easily identified by their high density. It is likely that in Afghanistan, additional undiscovered celestite deposits would be discovered in Paleogene sedimentary units.

Quantitative Assessment: No estimates were made, because of lack of information from the known occurrences to adequately match the grade and tonnage model.

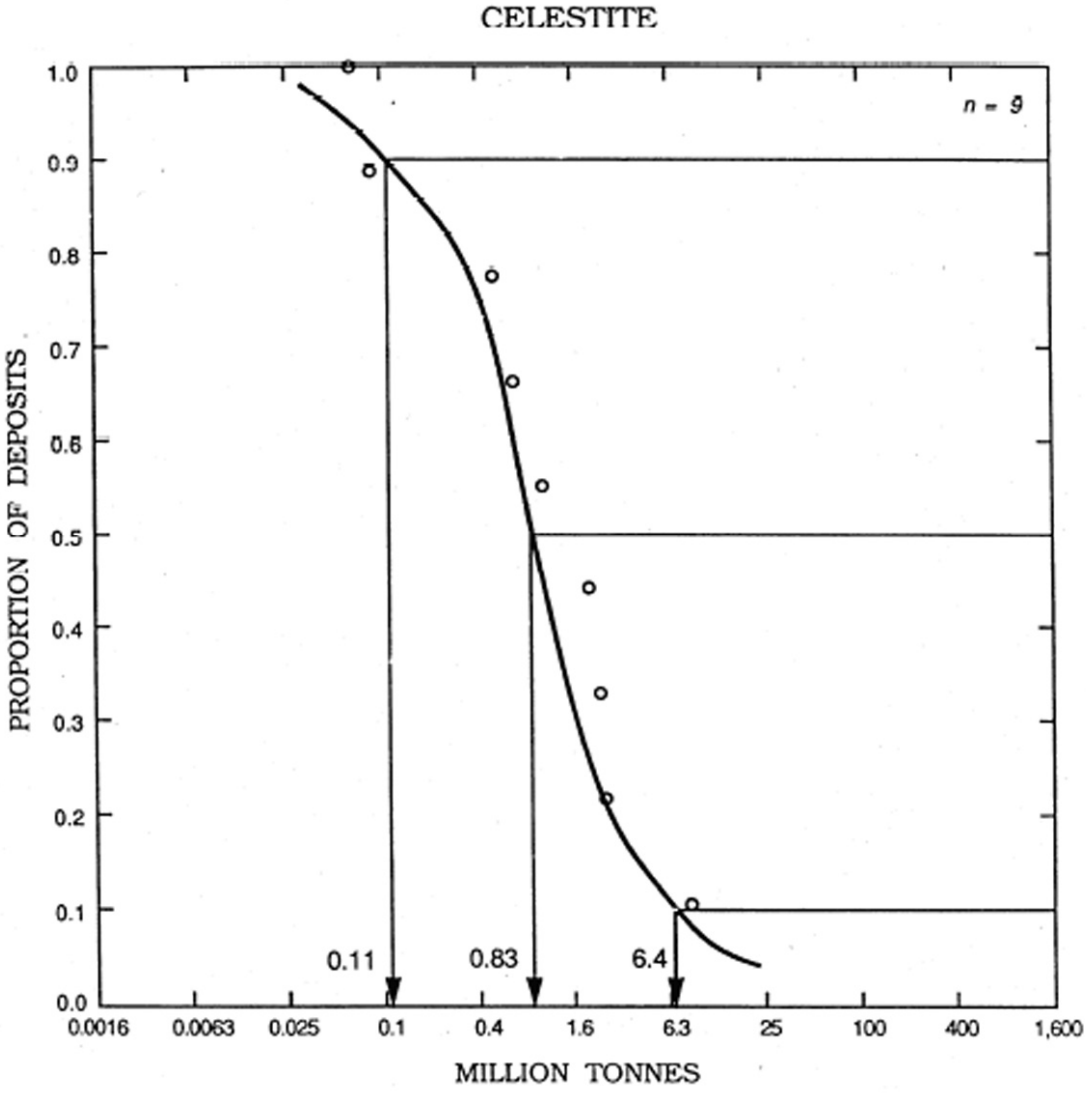

Figure 8.5-1. Cumulative distribution of sedimentary celestite tonnages for well-explored deposits (Orris, 1992).

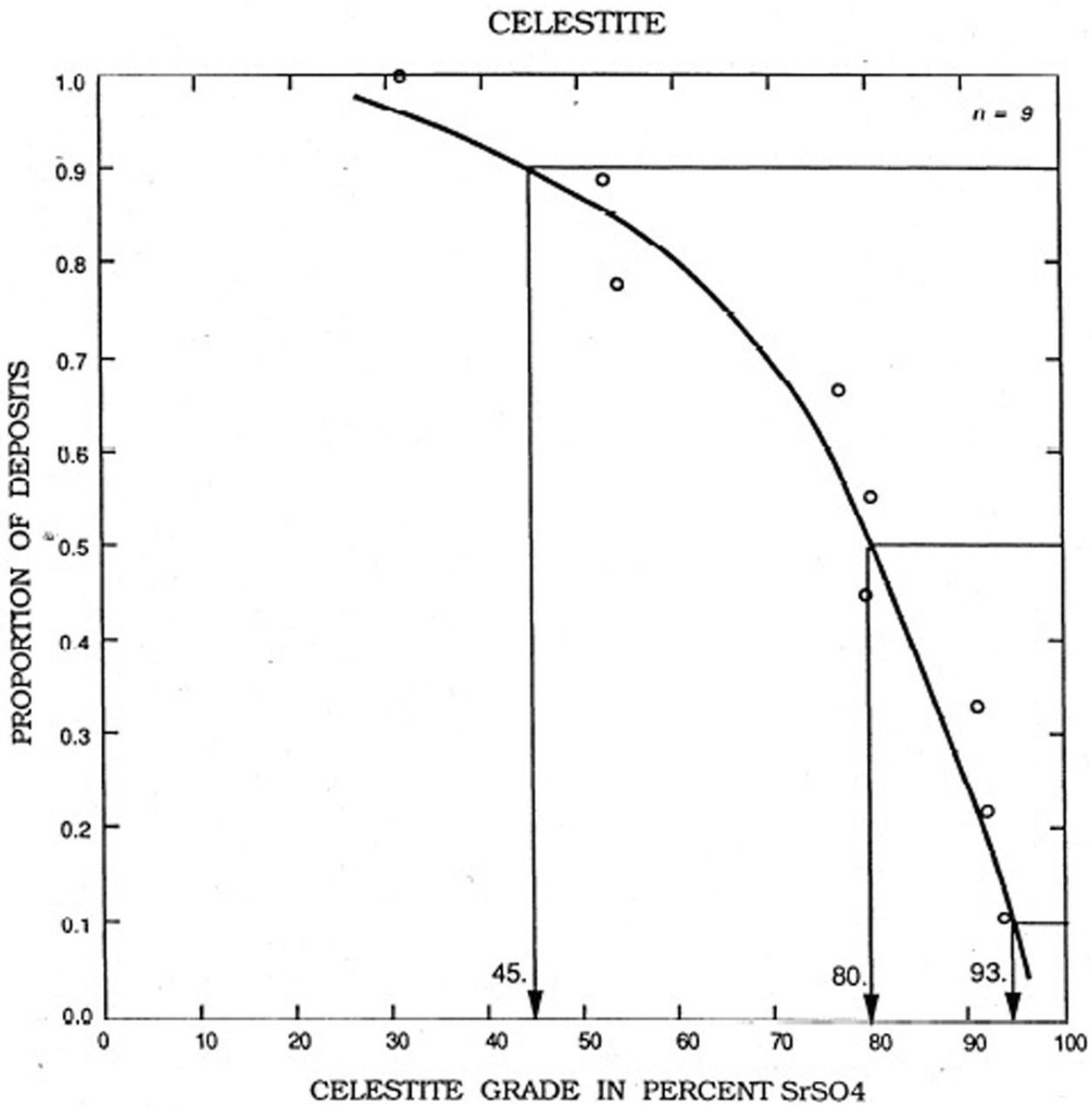

Figure 8.5-2. Cumulative distribution of sedimentary celestite deposits grades (Orris, 1992).

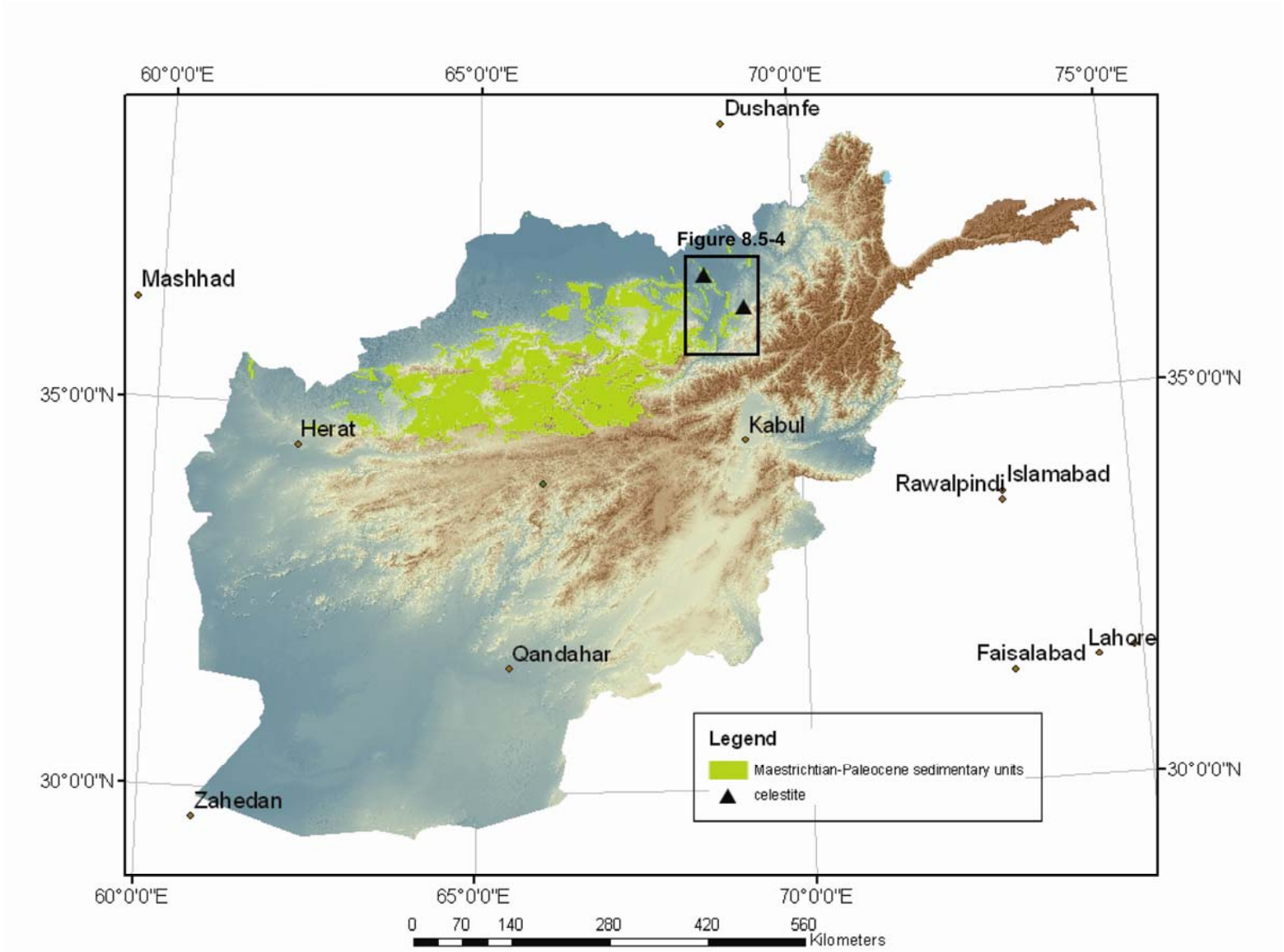

Figure 8.5-3. Permissive tract for the occurrences of undiscovered celestite deposits based on distribution of Maestrichtian-Paleocene sedimentary rocks. Inset shows area of two known celestite occurrences.

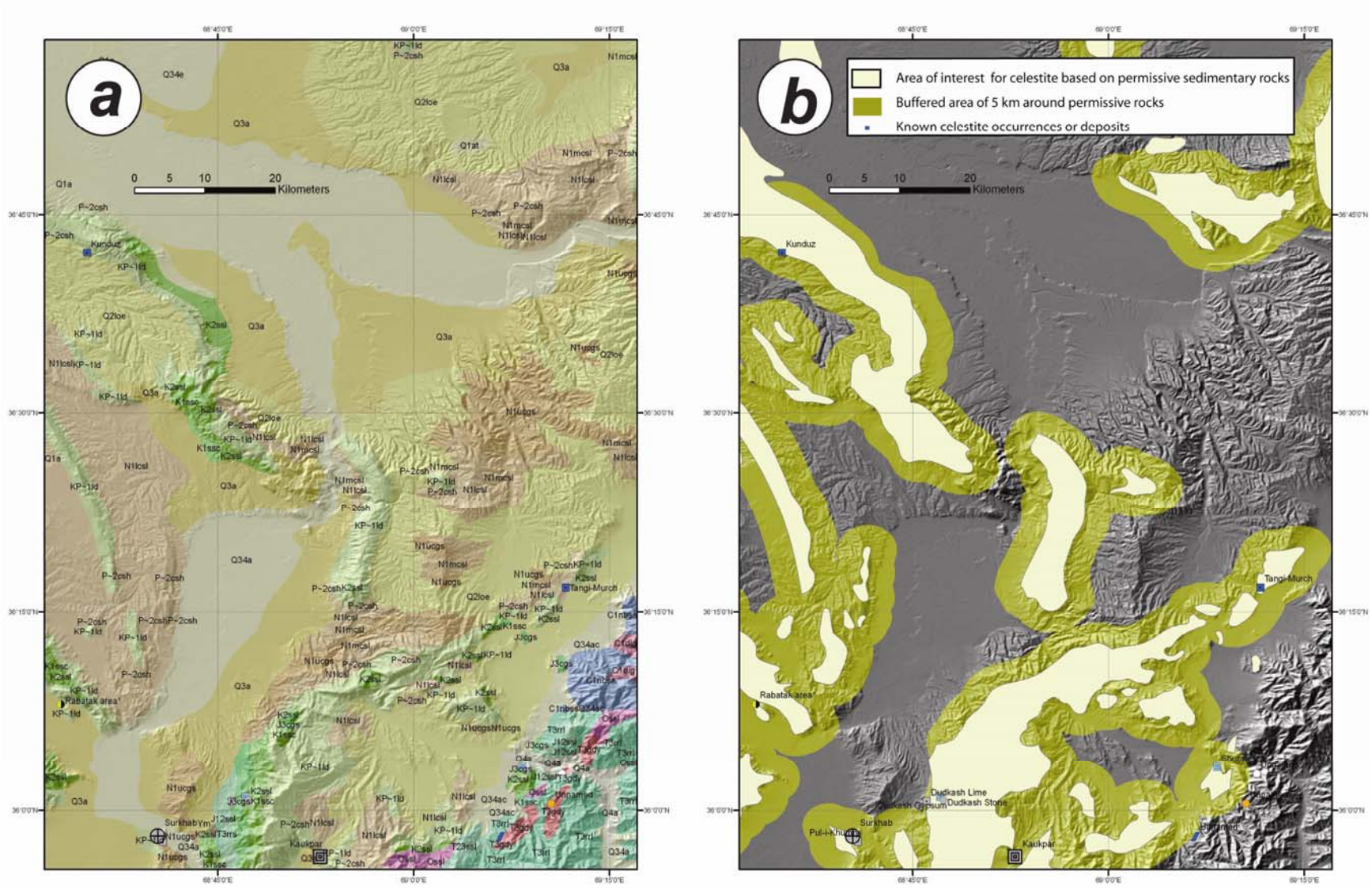

Figure 8.5-4. Map showing location of known celestite deposits Tangi-Murch in Baghlan province, and Kunduz in Kunduz Province northern Afghanistan. (*a*) Geologic map from Doebrich and Wahl, 2006). (*b*) Area of interest and 5 km buffer. Mineral occurrence data from Orris and Bliss (2002).

References

Abdullah, S., Chmyriov, V.M., Stazhilo–Alekseyev, K.F., Dronov, V.I., Gannan, P.J., Rossovskiy, L.N., Kafarskiy, A.Kh., and Malyarov, E.P., 1977, Mineral resources of Afghanistan (2d ed.): Kabul, Afghanistan, Republic of Afghanistan Geological and Mineral Survey, 419 p.

Doebrich, J.L., and Wahl, R.R., 2006, Geologic and mineral resource map of Afghanistan: U.S. Geological Survey Open–File Report 2006–1038, 1 sheet scale 1:850,000, available on line at *http://pubs.usgs.gov/of/2006/1038/*.

Evans, John, 1999, Evaporites- Their evolution and economics: Malden, Maine, Blackwell Science Ltd., p. 138–140.

Harben, P.W., 2002, Celestite and strontium compounds, *in* The Industrial Minerals Handbook; A guide to markets, specifications & prices, 4th ed.: Worcester Park, UK, Industrial Minerals Information, p. 94–98.

Harben, P.W., and Kuzvart, Milos, 1996, Celestite, *in* Industrial minerals: A global geology: London, Industrial Minerals Information Ltd., p. 91–97.

Kazak, Yu. M., Lapke, F.F., Galstukhin, E.A., and Koretskiy, M.S., 1965, Report on the geological exploration at the Farenjal barite deposit in 1963–64 and prospecting–exploration investigations at the Tangi–Murch celestite deposit in 19 V. 1–3: Kabul, Department of Geological and Mineral Survey, unpub. data.

Orris, G.J., 1992, Preliminary grade and tonnage model of bedded celestite, *in* Orris, G.J., and Bliss, J.D., eds., 1992, Industrial mineral deposit models: grade and tonnage models: U.S. Geological Survey Open–File Report 92–437.

Orris, G.J., and Bliss, J.D., 2002, Mines and Mineral Occurrences of Afghanistan, U.S. Geological Survey Open–File Report 2002–110, 95 p, available on line at *http://geopubs.wr.usgs.gov/open–file/of02–110/*.

Rodriguez Garza, A., and McAnulty, W.N., Jr., 1996, Overview of celestite deposits in south-central Coahuila, Mexico—geology and exploitation, *in* Austin, G.S., Hoffman, G.K., Barker, J.M., Zidek, J., and Gilson, N., eds., Proceedings, 31st Forum on the Geology of Industrial Minerals- The Borderland Forum: New Mexico Bureau of Mines & Mineral Resources Bulletin 154, p. 27–32.

8.6 Barite (including bedded and vein barite)

Contributions by Stephen G. Peters, Greta J. Orris, and Stephen D. Ludington.

Barite is present in a number of layered and cross cutting deposits in central Afghanistan, many of which are spatially related to lead and zinc deposits. Amounts of barite are probably sufficient to support local industry and exploitation of oil and gas.

8.6.1 Bedded Barite and deposit models

Bedded barite Deposits (model 31b, Orris, 1986) or stratiform barite deposits consist of stratiform deposits of barite interbedded with dark-colored cherty and calcareous sedimentary rocks. They are present in generally dark-colored chert, shale, mudstone, limestone or dolostone and also in quartzite, argillite, and greenstone. Deposits range in age from Proterozoic to Paleozoic. The depositional environment is epicratonic marine basins or embayments (often with smaller local restricted basins). The tectonic setting of the deposits is in hinge zones controlled by syn-sedimentary faults. The deposits are spatially proximal to many sedimentary exhalative Zn–Pb deposits. Mean tonnage for bedded barite deposits is 1.24 million metric tons and the mean grade is 52.7 vol. percent barite. Barite vein deposits contain a mean tonnage of 110,000 metric tons and a mean grade of 60 percent barite (Orris, 1986,1992).

Mineralogy consists of barite ± minor witherite ± minor pyrite, galena, or sphalerite. Barite typically contains several percent organic matter plus some H_2S in fluid inclusions. Ore textures are stratiform, commonly lensoid to poddy with ore laminated to massive and with layers of barite nodules or rosettes. Barite may exhibit primary sedimentary features. Small country rock inclusions may show partial replacement by barite. Alteration is typified by secondary barite veining and weak to moderate sericitization may also be present. Weathering is indistinct, generally resembling limestone or dolostone. Occasionally weathered-out rosettes or nodules are present. A geochemical signature consists of elevated Ba and, where peripheral to sediment-hosted Zn–Pb, may have lateral (Cu)–Pb–Zn–Ba zoning or regional manganese haloes. Organic C content is usually high.

Many of the barite occurrences and deposits in Afghanistan are cross cutting and are clearly vein-type deposits. The spatial proximity of many of the deposits with the Heart fault and with lead and zinc deposits in the central part of the country suggest that many of the deposits are epigenetic and may post date the stratigraphic sequences that they are hosted in.

8.6.2 Description of barite deposits and occurrences

A zone in central Afghanistan that lies along and adjacent to the Herat fault was identified by the USGS-AGS assessment team as being a likely place for the occurrence of epigenetic barite deposits and nearby lead and zinc deposits (fig. 8.6-1). Two main clusters of deposits are present along the zone, the Herat area of vein and bedded barite occurrences in the west and the Farenjal area northwest of Kabul (fig. 8.6-1). In addition the Kushakak bedded barite deposit lies in Ghor Province in the central part of the zone, barite deposits are located nearby to the Haji Gak iron deposit, and small celestite deposits are present in the northeast part of the country (fig. 8.6-1).

There are about six (6) barite occurrences in the Herat area, which also is underlain by a 70 km long 20 to 30 km wide northwest-trending geochemical halo anomaly along a northern strand of the Herat fault (fig. 8.6-2). The largest prospect is the Sangilyan occurrence which covers an area of over 3 km^2 and is hosted

in Eocene to Oligocene volcanic and sedimentary rocks and contains three (3) mineralized zones. Each of the zones is up to 2,500 m long and 200 to 700 m wide and these are characterized by 24 major and numerous minor fracture-filled barite veins that are 70 to 1,000 m long and 0.4 to 5.7 m thick. A number different barite types are present including: (1) monomineralic, coarse-crystalline barite that is 0.5 to 5.5 m thick and grades 80 to 98.6 wt. percent barite, (2) fine-grained barite that is present along chilled contacts between the enclosing veins and host rock that are 0.1 to 0.7 m thick and grade 75 to 94 wt. percent barite, (3) coarse grained mixtures of barite and calcite, (4) barite with fault breccia, and (5) disseminated barite. Vertical zoning is present in some of the monometallic coarse-crystalline barite veins where the surface 50 to 100 m grades downward to coarse-grained barite and calcite and then to calcareous barite grading 10 to 60 wt. percent barite. The barite veins are usually monomineralic and also may contain witherite, galena, sparse disseminated chalcopyrite and pyrite as well as small quartz crystals, calcite, malachite and limonite. Resources calculated for the deposit are 1,493,000 metric tons barite and the mine was active in 1977 (Abdullah and others, 1977 sourcing a work by Iorov and others in 1973).

Additional occurrences in the Herat area are the Gardani-Burida prospect hosted in terrigenous Paleogene sedimentary rocks that contains five (5) milky-white to pink coarse- to fine-grained, lenticular barite-bearing bodies that are 5 to 20 m long and 0.2 to 0.6 m thick (Abdullah and others, 1977 sourcing a work by Iorov and others in 1973). The Gulron occurrence lies within a 30– to 700–m-long and 0.15– to 0.7–m-thick fault zone that cuts Eocene sedimentary rocks. The occurrence contains eight (8) barite veins with transparent Iceland spar crystals that are 10 by 20 cm in size and 15 barite-calcite veins and two (2) calcite veins. The barite veins assay 80 to 95.5 wt. percent barite and the barite-calcite veins grade 12 to 26 wt. percent barite (Abdullah and others, 1977 sourcing a work by Iorov and others in 1973). The Zandadshon prospect lies along the Herat fault zone in Proterozoic, Cambrian and Middle to Upper Jurassic rocks and is 20 to 90 m long and 0.05 to 1.60 wt. percent barite.

The Ferenjal barite area in Ghor Province contains about six (6) barite occurrences that are hosted in Ordovician sedimentary rocks. The main Farenjal barite deposit lies in Ordovician brecciated limestone and contains barite-bearing bodies with lead and zinc disseminated mineralization over an area that contains 16 fine-grained barite lenses that are 10 to 70 m long and 1 to 9 m wide and grade 83.66 wt. percent barite. The proximal lead and zinc mineralization is with the barite in the brecciated limestone and is 500 m long and 100 m down dip and 10 to 20 m thick and up to 20 to 40 m thick. There are ancient workings in the area and the speculative resources are 150 to 0.2 million metric tons barite and 25,000 to 30,000 metric tons combined lead and zinc. (Kazak and others, 1965; Kasanov and others, 1967).

Additional occurrences in the Ferenjal area are the Northern Farenjal occurrence also hosted in Ordovician massive and bedded limestone and are composed of a 200–m-long barite vein that is 2 m thick and grades about 97 wt. percent barite. The Tanghi-Lohi occurrence is hosted in Lower Quaternary brecciated rocks and contains six (6) fragmental barite-bearing zones over an area of 305 $km^{2.}$ The additional unnamed occurrences are located in Ordovician brecciated limestones.

References

Kazak, Yu. M., Lapke, F.F., Galstukhin, E.A., and Koretskiy, M.S., 1965, Report on the geological exploration at the Farenjal barite deposit in 1963–64 and prospecting–exploration investigations at the Tangi–Murch celestite deposit in 19 V. 1–3, Department of Geological and Mineral Survey, Kabul, unpub. data.

Khasanov, R.M., Plotnikov, G.I., Bayazitov, R., Sayapin, V.I., and Trifonov, A., 1967, Report on revised estimation investigations of mineral deposits and occurrences of copper, lead, zinc and gold in 1965–V. I–II, Department of Geological and Mineral Survey, Kabul, unpub. data.

Orris, G.J., 1992, Preliminary grade and tonnage model of barite veins (27e), *in* Orris, G.J., and Bliss, J.D., Industrial minerals deposits models; grade and tonnage models: U.S. Geological Survey Open–File Report 92–437, p. 32, available on line at *http://pubs.er.usgs.gov/usgspubs/ofr/ofr92437*.
Orris, G.J., 1986a, Descriptive model of bedded barite, Descriptive model of bedded barite, *in* Cox, D.P., and Singer, D.A., eds., Mineral deposit models: U.S. Geological Survey Bulletin 1693, p. 216.

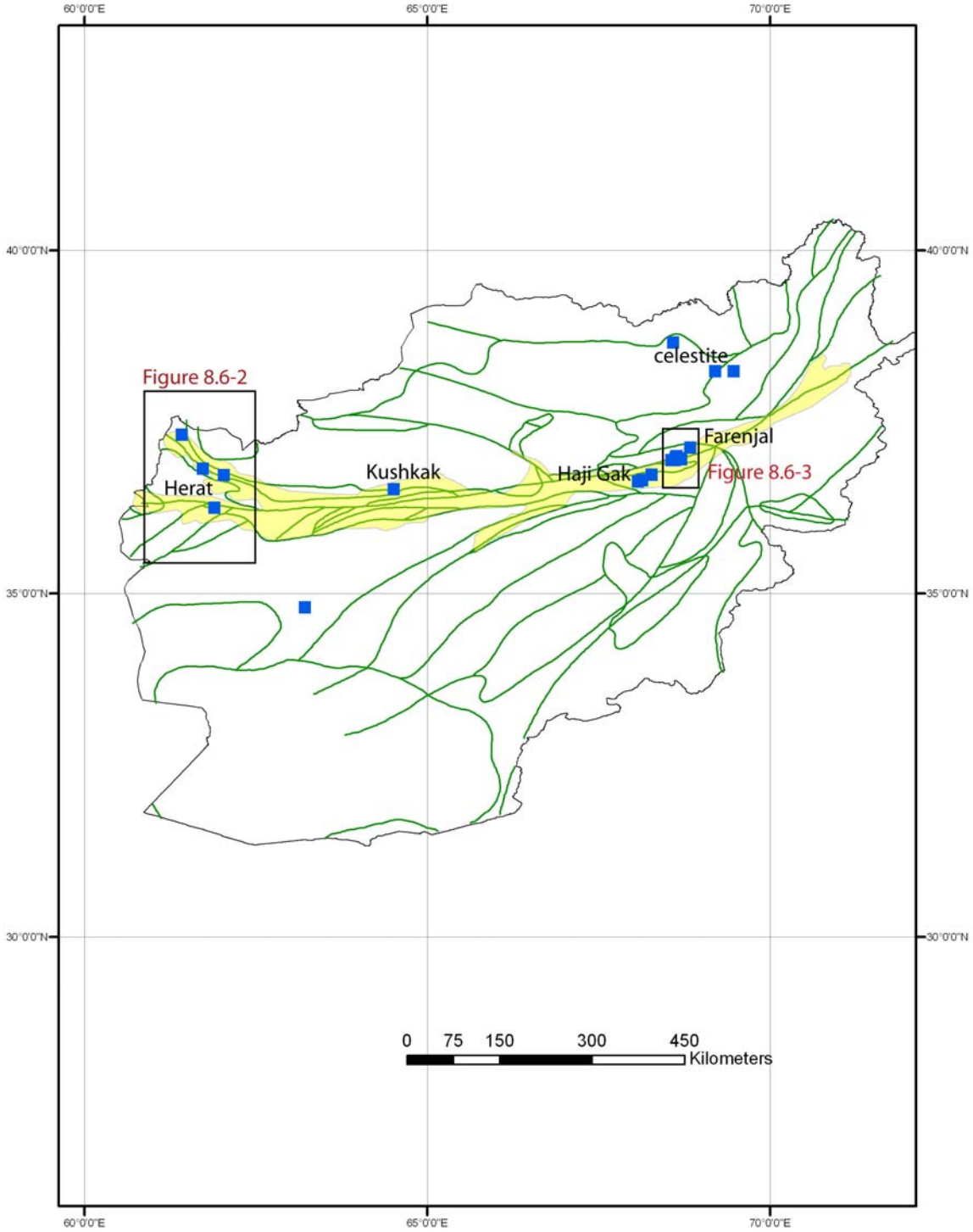

Figure 8.6-1. Map showing permissive tract for the location of undiscovered epigenetic (and stratabound) barite and lead and zinc deposits in Afghanistan. Insets show clusters of deposits in the Herat and Farenjal areas.

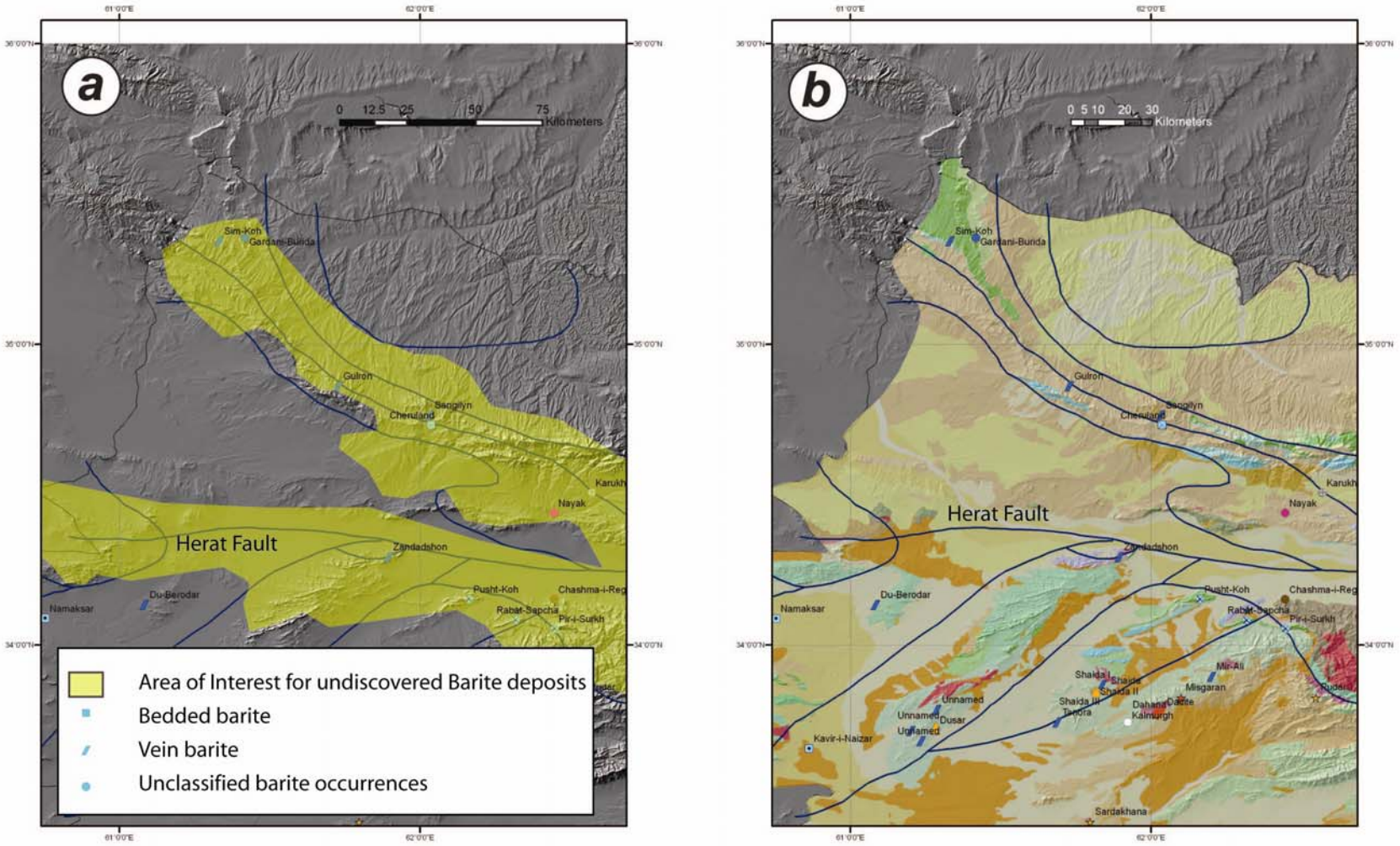

Figure 8.6-2. Maps showing location of barite occurrences and permissive tract for undiscovered barite deposits in the Herat area, Western Afghanistan. (*a*) Location of the main deposits along the Herat fault within the outline of the tract. The northwestern-trending tract is underlain by Tertiary sedimentary and volcanic rocks and is interpreted to be a tectonized zone along splays of the Herat fault. (*b*) Geologic map and occurrence symbols of the Herat barite area from Doebrich and Wahl (2006). Blue lines are major faults.

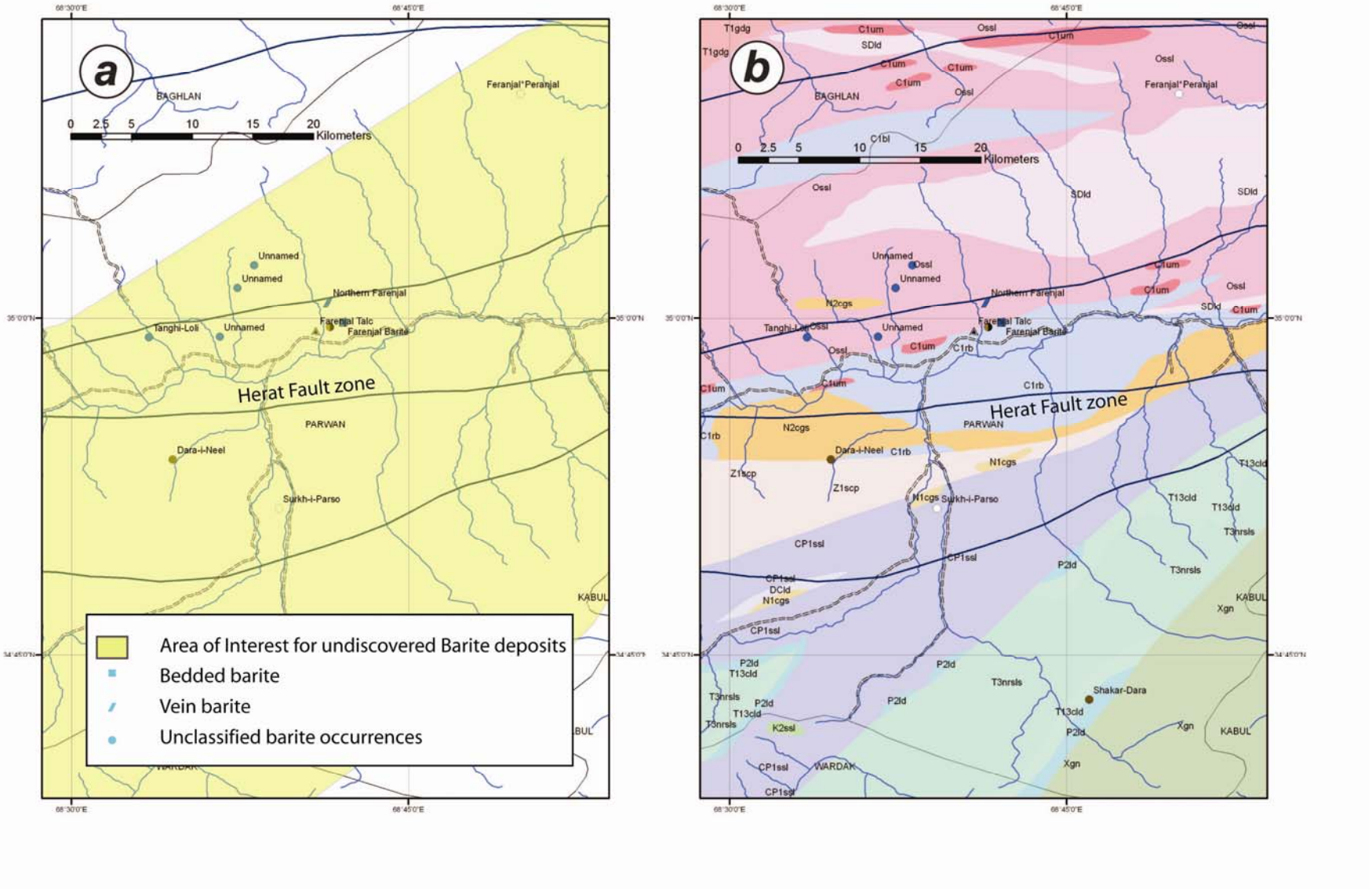

Figure 8.6-3. Maps showing location of barite occurrences in the Farenjal barite area along the Herat fault zone in Parwan Province. See figure 8.6-1 for location. (*a*) Main occurrences (arrow shows Farenjal occurrence) and part of permissive tract for undiscovered barite deposits. (*b*) Geologic map showing host rocks for the barite occurrences. Ossl = Ordovician sandstone, limestone, siltstone, shale, and chert, C_1rb = Early Carboniferous felsic and mafic volcanic rocks including limestone, shale, sandstone, and conglomerate.

8.7 Native Sulfur

Contributions by Stephen G. Peters, Greta J. Orris. and James D. Bliss.

Significant sulfur deposits are present in sedimentary rocks of the Afghan-Tajik Basin and other areas in northern Afghanistan. Resource estimates from two occurrences total about 450,000 metric tons of sulfur and were calculated by Russian workers (Abdullah and others, 1977). Most deposits formed from microbial breakdown of organic fuel deposits but also from processes with hot-spring deposits. Sulfur is used for sulfuric acid and the production of phosphate fertilizers, leaching metal ores, chemicals, synthetic materials, pulp and paper products, and explosives. Native sulfur is used for agricultural chemicals, petroleum, and coal products.

Descriptive deposit models for native sulfur

Three deposit models may be applicable to the sulfur deposits of Afghanistan, the stratabound sulfur, salt dome sulfur, and fumarolic sulfur models. In addition, sulfur may be a recoverable byproduct of oil and gas production. Deposits of the stratabound and fumarolic models are known to occur. While no salt dome sulfur deposits are known, this deposit type may be present in the domes of Jurassic salt in the Afghan-Tajik Basin.

Stratabound sulfur (Long, 1992a) is also referred to as bedded or stratiform sulfur. There are typically no byproducts of sulfur production for deposits of this type. The deposits are composed of native sulfur filling pores and replacing the matrix of anhydrite-gypsum-bearing stratigraphic units. Sulfur is produced by sulfate-reducing anaerobic bacteria feeding on hydrocarbons trapped in the host strata, typically thick anhydrite-gypsum and hydrocarbon-bearing strata (Harben and Kuzvart, 1996).

Stratabound sulfur deposits are found in evaporite basins and evaporite-bearing reef complexes specifically with gypsum and anhydrite-bearing facies. Known deposits are hosted by evaporites of Paleozoic to Recent age, but the mineralization may be much younger than the host rock (Long, 1992a). In these deposits, native sulfur occurs in evaporite sequences that may include biogenic limestone and older, or correlative, hydrocarbon-bearing strata, as well as the required sulfate facies. Gangue mineralogy includes calcite, anhydrite and sometimes hydrated gypsum; lesser quantities of barite, celestite, and various metal sulfide minerals may be present.

Formation of stratabound sulfur deposits requires a stratigraphic or structural trap, structural features that allow hydrodynamic interaction between the sulfates and hydrocarbons, and an overlying barrier to contain he reactions and preserve the deposit (Barker and others, 1979). Most deposits exhibit strong structural controls that vary from basin to basin. Commonly, deposits develop at the edges of evaporite basins within or adjacent to structures that concentrate hydrocarbons and (or) channel water (Harben and Kuzvart, 1996). Some occur along structurally controlled solution collapse structures and grabens, whereas others are present along solution collapse structures within uplifted blocks. Other deposits are stratigraphically controlled, such as within evaporite-bearing carbonate reef complexes or up dip pinch outs of evaporite deposits (Long, 1992a).

Native sulfur forms from sulfate reduction by bacteria that occurs within 900 m of the surface and requires considerable quantities of hydrocarbons, about 0.3 to 0.6 m^3 of oil per tonne of sulfur produced (Long, 1992a). Bacterial reduction of sulfate yields H_2S gas, which must be trapped and oxidized to native sulfur to produce an economic deposit. The H_2S gas may migrate higher into the host rock, where it may be trapped by impermeable clay layers and oxidized by ground or sea water. Alternatively the H_2S may be

oxidized during hydration of anhydrite to gypsum along an oxidizing-reducing fluid interface within the host rock. The H_2S may also be converted into polysulfides, and then reduced by $C0_2$ during bacterial reduction of anhydrite.

Stratabound sulfur orebodies are up to 26 km long containing zones of up to 120 m thick with 20 wt. percent sulfur or better. The deposits weather to a distinctive sulfur-bearing soil known as “sour dirt”. The geochemical signature consists of H_2S gas that may be detected in the outcrops of biogenic limestone or may issue from faults or fractures in overlying strata. Sulfur-bearing ground waters may leach potassium from feldspars, precipitate silica, carbonate, gypsum, and uranium. Leakage of biogenic carbon dioxide may result in precipitation of calcite with isotopically light carbon in near-surface rocks and soils. Range of contained sulfur in most stratabound deposits is between less than to up to 500 million metric tons (Long, 1992a).

Examples of Deposits—Major stratabound sulfur deposits include the Culberson deposit in Texas (Wallace and Crawford, 1992), the Tarnobrzeg deposit in Poland (Niec, 1992), and the Mishraq deposit in Iraq, the largest stratabound sulfur deposit in the world (Ober, 2006; Barker and others, 1979). Associated deposit types are bedded gypsum and biogenic limestone.

Exploration Guides—Exploration criteria for stratabound sulfur deposits include: Hydrocarbon-bearing evaporite basins with thick anhydrite (-gypsum) sequences, especially near the peripheries of the basins. The anhydrite with large deposits may have a measurable negative gravity anomaly. Other geophysical techniques might be useful depending on the mineralization (such as magnetite or sulfides) and the geologic history of the deposit. H_2S may be detectable by smell in outcropping limestone or along faults and fractures in strata overlying deposits (Long, 1992a). The presence of “sour dirt” may indicate underlying a sulfur deposit.

Salt dome sulfur (Long 1992b) is also called cap rock sulfur and is typified by native sulfur that cements porous zones and replaces the matrix of anhydrite-gypsum-limestone cap rock in salt domes. This sulfur formed in a biogenic process similar to that which forms stratabound sulfur deposits (Ober, 2006; Harben and Kuzvart, 1996). Sulfur is produced by sulfate-reducing anaerobic bacteria feeding on hydrocarbons trapped in the salt-dome cap rock. Salt domes without hydrocarbons do not form sulfur deposits. The currently producing deposits of this type are found only in the Gulf Coast region of the USA and Mexico, although other deposits are known (Ober, 2006).

Salt dome sulfur deposits occur in hydrocarbon-bearing evaporite basins that have experienced salt diapirism. Host rocks are limestone and anyhydrite-gypsum that form or are near the cap rock of salt domes. The native sulfur may have gangue mineralogy that includes calcite, anhydrite, occasional hydrated gypsum, and possibly celestite and barite (Harben and Kuzvart, 1996).

Formation of salt domes requires a relative thick sequence of salt; 300 to 600 m of overburden is required to initiate salt movement. Anhydrite cap rock is formed by dissolution of salt by ground or sea water within 1,500 m of the surface or ocean floor. Cap rock and sulfur deposits may subsequently be buried to 4,000 m depth or more. Sulfate reduction by bacteria occurs within 750 to 900 m of the surface and requires considerable quantities of hydrocarbons, about 0.3 to 0. 6 m^3 of oil per tonne of sulfur produced (Ober, 2006; Long, 1992b). Bacterial reduction of sulfate yields H_2S gas, which must be trapped and oxidized to native sulfur to produce an economic deposit. Mechanisms of formation are then similar to those in the stratabound sulfur deposits.

Salt-dome sulfur deposits are up to 70–m-thick irregular bodies within zones of 150 m thick of sulfur-bearing sediments containing better than 20 wt. percent sulfur. Recoverable sulfur may cover an area of up

to 600 hectares and the dome may be up to 8 km in diameter. Sulfur may sometimes be found on the flanks of salt domes, to depths of as much as 1,000 m deep. Geochemical and weathering features are similar to the stratabound sulfur deposits. Tons of contained sulfur in most deposits range from less than 10 to up to 89 million metric tons (Long, 1992b).

Examples of Deposits—Two typical deposits are those of the Boling Dome in Texas (Samuelson, 1992) and the Sulphur dome in Louisiana (Kelley, 1926). Associated deposit types include salt-dome oil and gas, salt-dome salt, cap rock limestone, cap rock gypsum; polymetallic sulfide and sulfate deposits and deposits of strontium sulfide. While other deposits are known, economic producing deposits are restricted to the Gulf Coast of the USA-Mexico.

Exploration Guides—Exploration criteria for salt dome sulfur deposits include known diapirism or a buried evaporite basin containing a thick sequence of salt. Many near-surface domes have a topographic expression. Some salt and limestone may cause a relative gravity low. H_2S gas may be detectable in outcropping caprock or from dome-related structures (Long, 1992b).

Fumarolic sulfur deposits (Long, 1992c) are also referred to as volcanic sulfur deposits. They differ from the stratabound and salt-dome sulfur deposits because they are not formed by the biogenic alteration of anhydrite and hydrocarbons, but by the interaction of volcanic fluids and gases with surrounding rock. The deposits occur as surficial sublimates, open space fillings and replacements of native sulfur in the vent areas of volcanoes. They also are present as rare precipitates in volcanic lakes fed by thermal waters, as thermal spring deposits, as molten sulfur flows and as alluvial deposits (Long, 1992c).

Deposits are hot-spring mercury, hot-spring Mn where the ultimate source of heat and mineralizing fluids may be intrusions with related epithermal gold and silver, or polymetallic deposits. These deposits are typically Miocene to Recent in age. Older deposits are tend to be destroyed by erosion and (or) alteration processes. Native sulfur is deposited in porous volcaniclastic rocks and lava flows or wall rocks with felsic volcanic centers. Less porous rocks act as fluid seals. Gangue mineralogy may of iron sulfide minerals, hydrothermal clays, and gypsum. In addition, cinnabar, stibnite, barite, malanterite, and selenium arsenic sulfate minerals may be present. The mean tonnage of fumarolic sulfur deposits is about 1 million tons (Long, 1992c).

8.7.2 Description of Sulfur Occurrences and Deposits

The main stratabound and salt-dome related deposits are present in the northern part of Afghanistan in Balkh, Samanghan, Baghlan and Gugirt Provinces (fig. 8.7-1). Much of the early exploration for sulfur in the northern part of the country was conducted in the 1950s by Ahad, Botman, Husein, and Gulyam Ali Khan who are noted in Abdullah and others (1977). The Alburz (Elburz) occurrence in Balkh Province is a sulfur-rich zone over an area 450 to 500 m by 700 m in size that is strongly altered Upper Cretaceous rocks that contain native sulfur consisting of siliceous-opaline, trioplite, alum-gypsum, and siliceous-carbonated ores (fig. 8.7-2). The average grade is 40 wt. percent sulfur. Speculative reserves are 200,000 metric tons of sulfur (Sokolov and Zimin, 1975). The Astana occurrence is about 1 m thick and is hosted in Eocene rocks (Abdullah and others, 1977). The Samanghan occurrence is also in Eocene limestone and is 200 meters from a hydrogen-sulfide spring containing native sulfur. The Dasht-i-Safed occurrence lies in Upper Cretaceous to Paleocene marl and gypsum and is interbedded with sulfur-bearing celestite that is 1.0 to 1.5 m thick and grades 0.3 to 3.0 percent barium with unknown amounts of sulfur (Mikhailov and others, 1967) (fig. 8.7-3).

Several additional sulfur occurrences contain characteristics that are compatible with the fumarolic sulfur model and lie along the central parts of Afghanistan either within or proximal to the Herat fault. They

include the Gugirt, Sanglich and Doshk Sul occurrences (fig. 8.7-1). The Gugirt sulfur occurrence is hosted in Proterozoic metamorphic rocks along an east-striking fault. The mineralized area is 120 by 180 m and 12 m thick consisting of brecciated rocks cemented by yellow-grey sulfur and smaller lenses that are 1 to 3 m long and 0.5 contain pure sulfur. Assays are 20.65 to 38.9 wt. percent sulfur. The Sanglich occurrence in Badakhshan Province is hosted in Archean marble that contains sulfur-bearing beds that grade up to 80 wt. percent sulfur. Speculative resources are 250,000 metric tons sulfur (Abdullah and others, 1977).

The Doshk Sul occurrences in Ghor Province consists of a sulfurous spring that forms a small lake that is 14 by 20 m and is surrounded by unconsolidated argillaceous and carbonated rocks rich in sulfur (Dronov and others, 1971)

8.7.3 Description of Sulfur Tracts

Permissive tract—sulf01

Deposit types—Stratabound sulfur (Long, 1992a), possibly also including salt dome sulfur deposits (Long, 1992b).

Age of mineralization—Post Late-Cretaceous to Eocene.

Examples of deposit type—There are at least two (2) mineral occurrences in Afghanistan that probably belong to this deposit type. The Astana occurrence is found in Samanghan Province. At this location, sulfur forms a 1–m-thick stratiform lodes in an Eocene sedimentary rock sequence that includes limestone and sulfate minerals. The Dasht-i-Safed occurrence is in rocks mapped as Late Cretaceous to Paleocene marl and gypsum. At this site, native sulfur is found along with celestite in a bed 1.0-1.5 m thick; the sulfur is reported to occur between the marls and gypsum. The Murghab (Badghis Province) and Rabatak (Baghlan Province) occurrences also are believed to be stratabound sulfur based on the geologic units in which they are located, but there is insufficient additional detail to be sure of the classification. Lastly, the Samanghan (Shadian) deposit is of uncertain origin; while it is located in Eocene sediments, it is also only about 200 m from a hydrogen sulfide spring and may have more of a fumarolic/geothermal origin.

Exploration history—There has been no significant exploration for this deposit type also sampling and measurement of many of the occurrences has taken place.

Importance of deposits—The known occurrences appear to be relatively small, but deposits of this type can be extremely large. The largest deposit of this type, Mishraq, is found in neighboring Iraq.

Tract boundary criteria—Gypsum-anhydrite-bearing sediments of Late Cretaceous to Paleogene age were selected that were believed to contain hydrocarbons or to overlay hydrocarbon-bearing sediments. The tract was bounded on the north by the chloride facies of the underlying Jurassic rocks and to the south by the basin edge. The extent of the permissive tract may differ for stratabound and salt dome sulfur deposits. The tract for the stratabound sulfur deposits is unlikely to extend outside the southern boundaries of the oil and gas-bearing parts of Afghan-Tajik basin. Therefore, parts of the tract area in the southeastern part of Afghanistan may not be permissive. The permissive tract for salt dome sulfur would include the area underlain by Jurassic salt (Hal-K tract section 8.3) modified by the petroleum-bearing rocks. There would be overlap with the stratabound tract. Internal areas of Figures 8.7-1a and 8.7-2a have been designated as areas of interest in orange where more favorable stratigraphy is present.

Important data sources—Geologic map and mineral occurrence data bases (Abdullah and others, 1977; Orris and bliss, 2002; Doebrich and others, 2006).

Needs to improve assessment—The assessors believed that more detailed information on the sulfur occurrences and, in general, more detailed geologic and geophysical data would help to refine the tract boundaries and the estimates.

Optimistic factors—Sulfate- and hydrocarbon-bearing sediments; presence of sulfur occurrences of this deposit type; presence in Iraq of a large deposit of this type.

Pessimistic factors—The occurrences all appear to be small and of limited extent.

Quantitative assessment—Stratabound Sulfur deposits, Afghanistan. Were estimated using the model of Long (1992). Salt dome and fumarolic sulfur deposits were not estimated in this preliminary assessment. The mean expected number of undiscovered stratabound sulfur deposits resulting from the estimated number of deposits its 2.2, which results in a mean value of 6 million metric tons sulfur and tabulated below.

Estimated number of deposits (1/22/07)

Level of estimate	Number of deposit
90% chance of at least	0
50% chance of at least	1
10% chance of at least	6

Probability assignment for Monte Carlo Simulation (MCS)

Number of deposits	Probability of selection during MCS
0	.30
1	.24
2	.08
3	.08
4	.08
5	.08
6	.14

Summary of the amount of sulfur (in million tons) in undiscovered stratabound sulfur deposits in Afghanistan

[p (mean)—probability of mean; p(0)—probability of zero or no stratabound sulfur resources]

90% of at least	50% of at least	10% of at least	Mean (10^6 t)	p(mean)	P(0)
0.0	6.0	500.	6.0	0.5	0.3

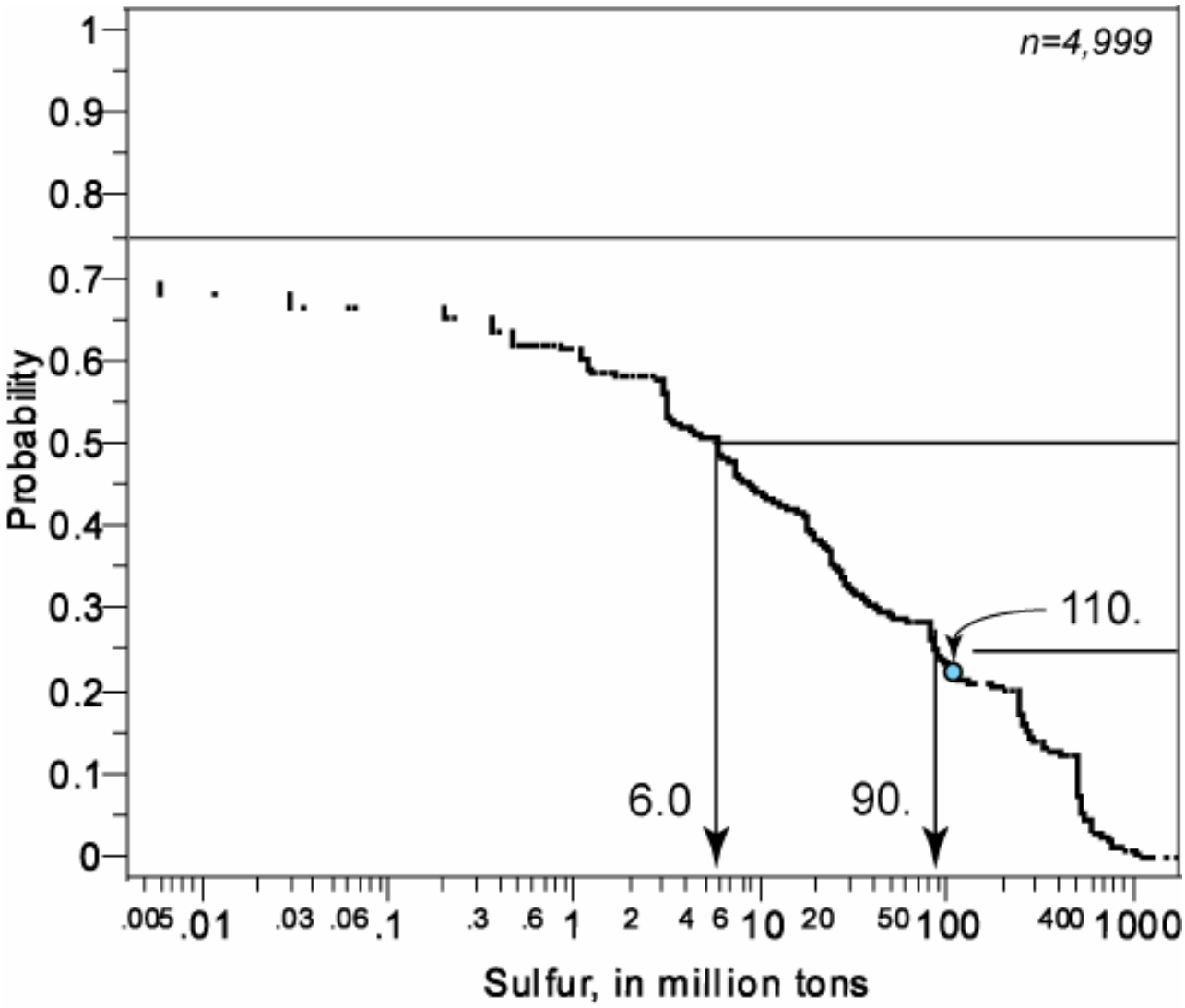

Figure 8.7-1. Output of Monte Carlo simulation for sulfur resources in stratabound sulfur deposits of Afghanistan. Values of the 75th, 50th, and 25th percentiles are given along the bottom axis when available. Blue point on curve is for the average amount of resources (110 million t) for those iterations not zero and has a probability of 0.23.

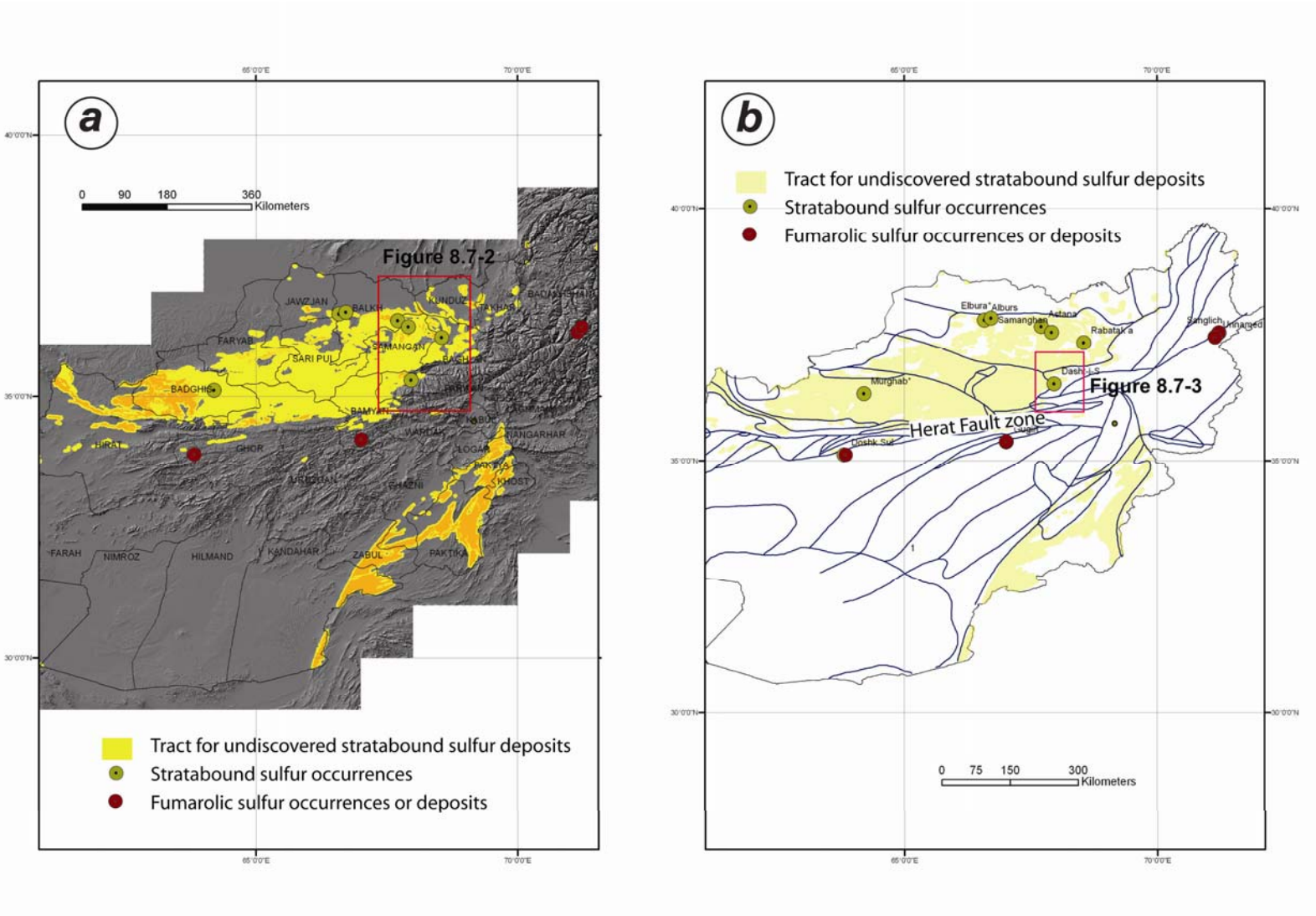

Figure 8.7-2. Maps showing location of sulfur occurrences and deposits in Afghanistan. (*a*) Permissive tract (yellow) and areas of interest (orange) in Eocene sedimentary and volcanic rocks for stratabound and salt-dome related deposits including location of known occurrences, as well as location of fumarolic sulfur occurrences. (*b*) Map showing faults (blue lines) and location of fumarolic sulfur locations proximal to the Herat Fault and its major strands. Note that the Alburz sulfur deposit may also be fumarolic because it contains opal.

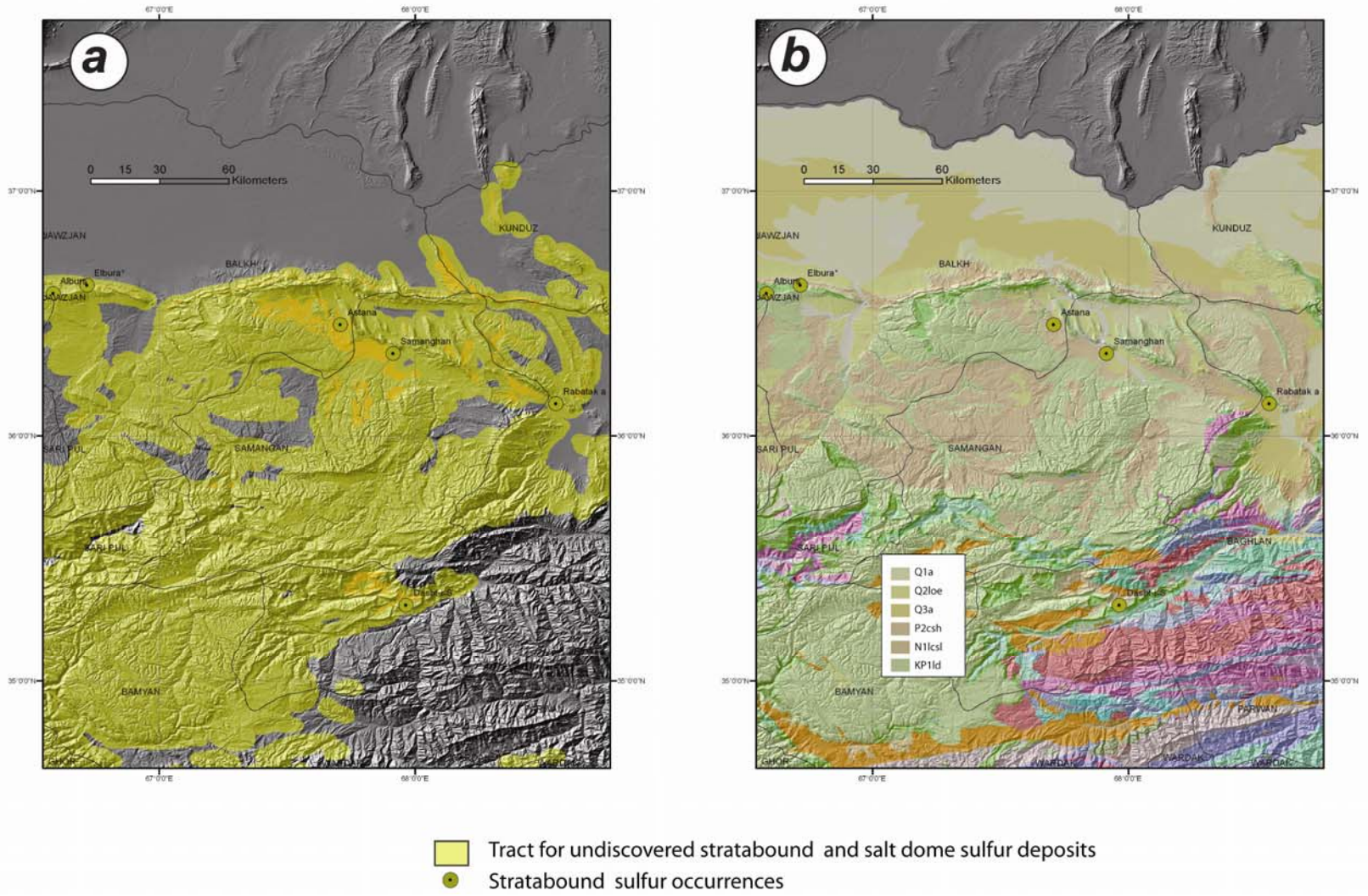

Figure 8.7-3. Maps showing details of the northern stratabound occurrences (Alburz area) of sulfur in Afghanistan. (a) Map showing permissive tract (yellow) and areas of interest (orange). (*b*) Geologic map of area in (a) Q1a = Early Pleistocene sediments including gravel, sand siltstone, limestone, gypsum and volcanic rocks, $Q2_1oe$ = Middle Pleistocene detrital sediments including gravel, sand, clay, travertine and basalt, Q_3a = Late Pleistocene detrital sediments, P_2csh = Eocene clay, shale, siltstone, sandstone, limestone, marl, gypsum and conglomerate, N_1lcsl = Early Miocene red clay, siltstone, sandstone, conglomerate, and limestone, KP_1ld = Late Cretaceous to Paleocene limestone, marl, dolomite, sandstone, clay, siltstone, gypsum and conglomerate.

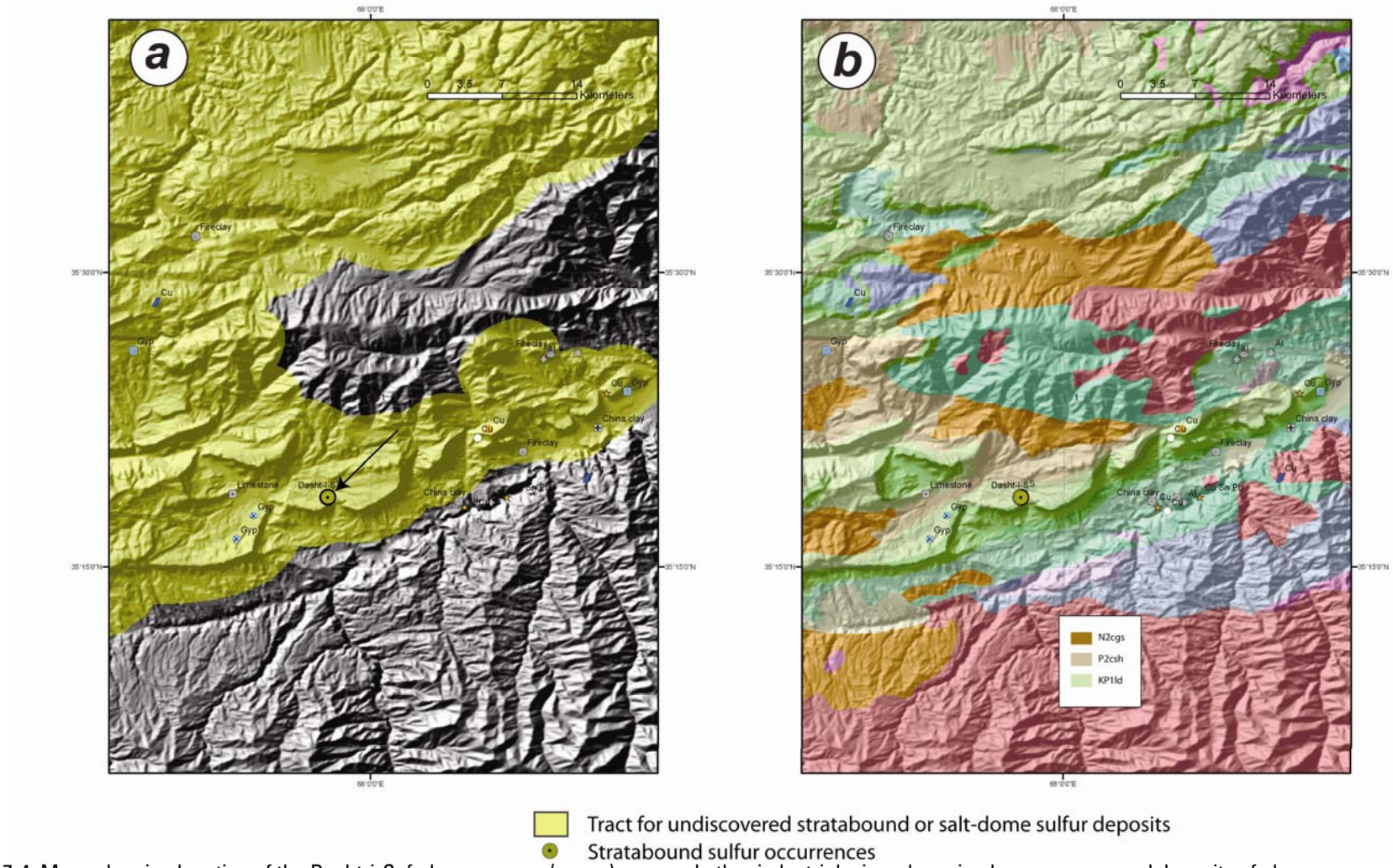

Figure 8.7-4. Maps showing location of the Dasht-i-Safed occurrence (arrow) area and other industrial mineral proximal occurrences and deposits of clay, gypsum and base metals. (a) Map showing part of tract for undiscovered stratabound sulfur deposits in the Dasht-i-Safed area. (b) Geologic map (Doebrich and Wahl, 2006) of the Dasht-i-Safed area showing important host or stratigraphic units. P_2csh = Eocene clay, shale, siltstone, sandstone, limestone, marl, gypsum and conglomerate, N_1lcsl = Early Miocene red clay, siltstone, sandstone, conglomerate, and limestone, KP_1ld = Late Cretaceous to Paleocene limestone, marl, dolomite, sandstone, clay, siltstone, gypsum and conglomerate.

References

Abdullah, Sh., Chmyriov, V.M., Stazhilo-Alekseev, K.F., Dronov, V.I., Gannan, P.J., Rossovskiy, L.N., Kafarskiy, A.Kh., and Malyarov, E.P., 1977, Mineral resources of Afghanistan, 2nd ed, Kabul, Afghanistan, Republic of Afghanistan Geological and Mineral Survey, 419 p.

Barker, J. M., 1983, Sulfur, *in* Lefond, S.J., ed., Industrial minerals and rocks, 5th ed., v. 2: American Institute of Mining, Metallurgical and petroleum Engineers, New York, p. 1,235–1,274.

Barker, J.M., Cochran, D.E., and Semrad, R., 1979, Economic geology of the Mishraq native sulfur deposit, Northern Iraq: Economic Geology, v. 74, p. 484–495.

Doebrich, J.L., and Wahl, R.R., 2006, Geologic and mineral resource map of Afghanistan: U.S. Geological Survey Open–File Report 2006–1038, 1 sheet scale 1:850,000, available on line at *http://pubs.usgs.gov/of/2006/1038/*.

Dronov, V.I., Kalimulin, S.M., and Sborshchikov, I.M., 1972, The geology and minerals of North Afghanistan, Department of Geological and Mineral Survey, Kabul, unpub. data.

Harben, P.W., and Kuzvart, Milos, 1996, Sulfur, *in* Industrial minerals: A global geology: London, Industrial Minerals Information Ltd., p. 396-406.

Kelley, P.K., 1926, The Sulphur salt dome, Louisiana, *in* Moore, R.C. ed., Geology of salt dome oil fields: American Association of Petroleum Geologists, Tulsa, Oklahoma, p. 452–469.

Long, K.R., 1992a, Descriptive model of stratabound sulfur and contained sulfur model for stratabound sulfur and contained-sulfur model of stratabound sulfur: U.S. Geological Survey Open–File Report 92–0000705, 9 p.

Long, K.R., 1992b, Descriptive model of salt-dome sulfur and contained-sulfur model for salt dome sulfur: U.S. Geological survey Open–File Report 92-0000-403, 8 p.

Long, K.R., 1992c, Descriptive model of fumarolic sulfur and contained sulfur model for fumarolic sulfur, *in* Orris, G.J., and Bliss, J.D., eds., Some industrial mineral deposit models: descriptive deposit models: U.S. Geological Survey Open–File Report 92–000091-11A, p. 13–15.

Mikhalov, K.Ya, Kolchanov V.P., Kulakov V.V., Pashkov B.R., Androsov M.A., and Chalyan M.A., 1967, 1967, Report on geological surveying and prospecting for coal at scale 1:200000 (sheets 222–C, 502–D, 503–B; part of sheets 221–F, 222–D, 222–F, 502–C, 502–F, 503–C, 503–D, 503–E, 504),): Kabul, Department of Geological and Mineral Survey, Kabul, scale 1:200,000, unpub. data.

Niec, M., 1992, native sulfur deposits in Poland, *in* Wessel, G.R., and Wimberly, B.H., ed., native sulfur, developments in geology and exploration: Society for Mining, Metallurgy, and Exploration, Littleton, Colorado, p. 23–50.

Ober, Joyce, 2006, Sulfur, *in* Kogel, J.E., Trivedi, N.C., Barker, J.M., and Krukowski, S.T., eds., Industrial minerals and rocks, 7th ed., Society for Mining, Metallurgy, and Exploration, Ltd., Littleton, Colorado, p. 935–970.

Orris, G.J., and Bliss, J.D., 2002, Mines and Mineral Occurrences of Afghanistan, U.S. Geological Survey Open–File Report 2002–110, 95 p, available on line at *http://geopubs.wr.usgs.gov/open–file/of02–110/*.

Samuelson, S.F., 1992, Anatomy of an elephant: Boling Dome, *in* Wessel, G.R., and Wimberly, B.H., eds., Native sulfur, developments in geology and explorations: Littleton, Colorado, Society for Mining, Metallurgy, and Exploration, Ltd., Littleton, Colorado, p. 59–71.

Sokolov, A.S., and Zimin, V.N., 1975, The Elburz sulphur deposit in northern Afghanistan: USSR, State Chemical Minerals Research Institute, USSR, 137 p., unpub. data.

Wallace, C.S.A., and Crawford, J.E., 1992, Geology of the Culberson ore body, *in* Wessel, G.R., Wimberly, B.H., ed., native sulfur, developments in geology and exploration: Society for Mining, Metallurgy, and Exploration, Littleton, Colorado, p. 91–105.

8.8 Gypsum

Contributions by Greta J. Orris, Karen S. Bolm, and Stephen D. Ludington.

There are abundant, widely dispersed potential sources of gypsum that would be sufficient for any industry that might develop around it. Gypsum ($CaSO_4$ $2H_2O$) is a versatile mineral, although its predominant use has been as a construction material (Sharpe and Cork, 2006). Gypsum has probably been mined since Egyptian times. Today, gypsum is used for wallboard (the largest use), Portland cement, fertilizer, soil amendments, filler, as well as plaster and other uses (Harben and Kuzvart, 1996). Gypsum deposits are distributed through much of the world, but as a low unit value commodity, development of deposits can be sensitive to proximity to market area, transportation and fuel/utility costs, and the availability of water for processing (Sharpe and Cork, 2006).

Anhydrite ($CaSO_4$) is the anhydrous form of gypsum. Both minerals may form as primary minerals, but they are easily converted from one to the other (Sharpe and Cork, 2006).

8.8.1 Descriptive deposit models

Gypsum and anhydrite are usually deposited in evaporitic sedimentary environments, peripheral to halite and bittern deposition if present. Gypsum deposits of both marine and continental origin are present in Afghanistan.

Bedded Gypsum. An important deposit model associated with bedded gypsum is potash (Raup, 1991; Harben and Kuzvart, 1996). Bedded gypsum deposits occur in large-scale basin and in sabkhas or salt flats.

8.8.2 Gypsum Tract Description

Permissive tract—AFGy-01 (Preliminary)

Participants: Greta Orris, Jim Bliss, Steve Ludington, Karen Bolm (GIS)

Deposit types—Gypsum

Probable Age of Mineralization—Late Cretaceous to Paleocene, Eocene, Neogene. It is known that there is buried Jurassic bedded salt in the Afghan-Tajik and Amu Darya Basins; the known deposits in neighboring Uzbekistan and Turkmenistan are of this age. Salt domes are known to be with the Jurassic bedded salt deposits and some are at or near the surface in that part of northern Afghanistan (Ludington and others, 2006).

Examples of deposit type—Known surface exposures of Late Jurassic, Late Cretaceous to Paleocene, and, less commonly, Neogene deposits. Examples: Late Jurassic Dudkash deposit in Baghlan; Late Cretaceous to Pliocene Sary-Asya deposit in Samangan Province; Neogene Surkh-Rod deposit in Nangarhar Province. Gypsum is found throughout the world. The Silurian Salina Formation contains gypsum deposits that occur in the Michigan and Appalachian basins of New York, Pennsylvania, West Virginia, Ohio, and Michigan. Gypsum is a major evaporite in the Paris Basin, France. Gypsum of probable Jurassic age is known at Gaurdak in Turkmenistan.

Exploration history—Largely unknown, although the Russians and Afghans conducted geologic surveys in the 1960's and early 1970's that made note of some of these deposits.

Exploration Guides: Evaporite basins with thick sequences of halite. Saline wells or springs may indicate salt and gypsum at depth. Gypsum and anhydrite are often vertically or laterally peripheral to halite. Large salt bodies produce negative gravity geophysical anomalies.

Why is tract being delineated—This deposit type is spatially proximal to other evaporite deposits. Gypsum is a key component of wallboard, a cost-effective building material, and has additional uses in cement and agriculture. Gypsum demand increases with an expanding national GDP. Most of the currently active gypsum quarries are mined on a small scale and the utilization of the mined material is not specified in the literature. Larger-scale exploitation uses standard open-pit methods.

How is tract delineated—The main tract was delineated using outcrops of sedimentary units where gypsum was listed as a major or dominant component (fig. 8.8-1). Although it is likely that gypsum-bearing rocks of different ages have different potential, we combined all ages of rocks due to an equal lack of distinguishing geologic information other than age. Areas of less promise consist of geologic units in which limestone is listed as a minor component (area in bright blue on figure 8.8-2). Eocene and younger deposits may be of terrigenous origin.

Importance of deposits—Gypsum is a key component in the manufacture of wallboard, a cost-effective building material, and there are additional uses in cement and agriculture. Most currently active gypsum quarries are mined on a small scale and the specific utilization of the mined material is not known. Larger operations would use standard open-pit mining methods. The demand for gypsum normally increases with an increasing national gross domestic product (GDP). Oil and gas assessment data; known salt occurrences; geologic map compilation (Doebrich and Wahl, 2006).

Tract boundary criteria—The tract was delineated using the digital geologic map of Afghanistan (Doebrich and others, 2006). The tract consists of those map units that have gypsum identified as a major or dominant component. Gypsum-bearing rocks of all ages are combined in this tract because we lack information to develop criteria for differing probabilities of occurrence in rocks of different ages. Units in which limestone is a minor component could be considered to have lower potential.

Important data sources—Geologic map, mineral deposit database, data from oil and gas assessment.

Needs to improve assessment—Information about consistency of chemical and physical properties of gypsum within known deposits would be particularly helpful, along with confirmation of the age and mode of occurrence of different gypsum deposits. All these would require site visits.

Optimistic factors—Some of the deposits are many thousands of meters long and 5 to >30 m thick. The few reported grades range from 89 to >99 vol. percent gypsum. Tracts are large in area and would readily host large deposits if present.

Pessimistic factors—Very little data have been reported on gypsum quality; there is no information available on the consistency of the gypsum in terms of chemical or physical characteristics across the outcrop areas of gypsum of any given age.

Quantitative assessment—Available information is not sufficient to allow a quantitative assessment (Ludington and others, 2006).

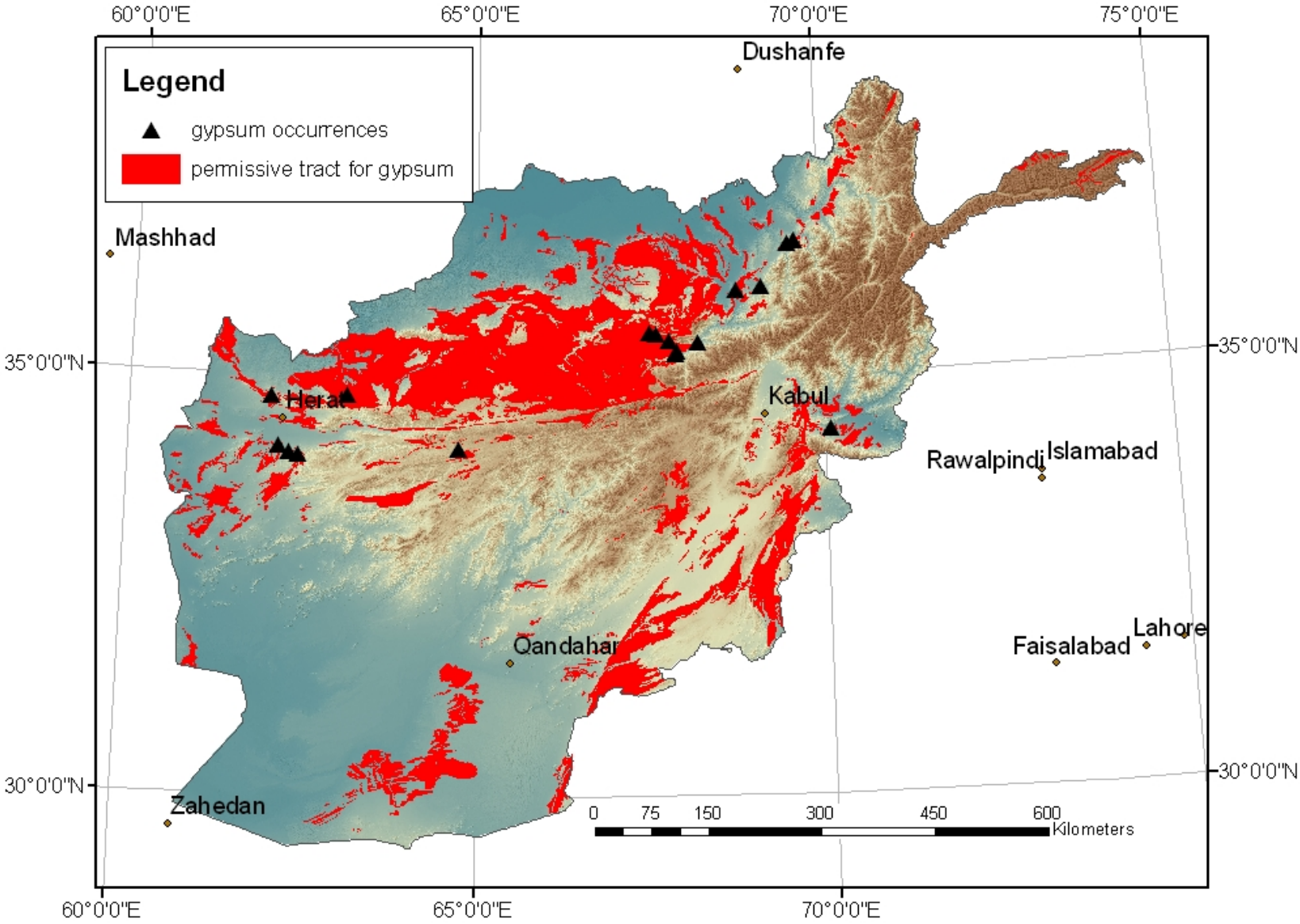

Figure 8.8-1. Tract AFGy-01, the area considered permissive for the occurrence of gypsum.

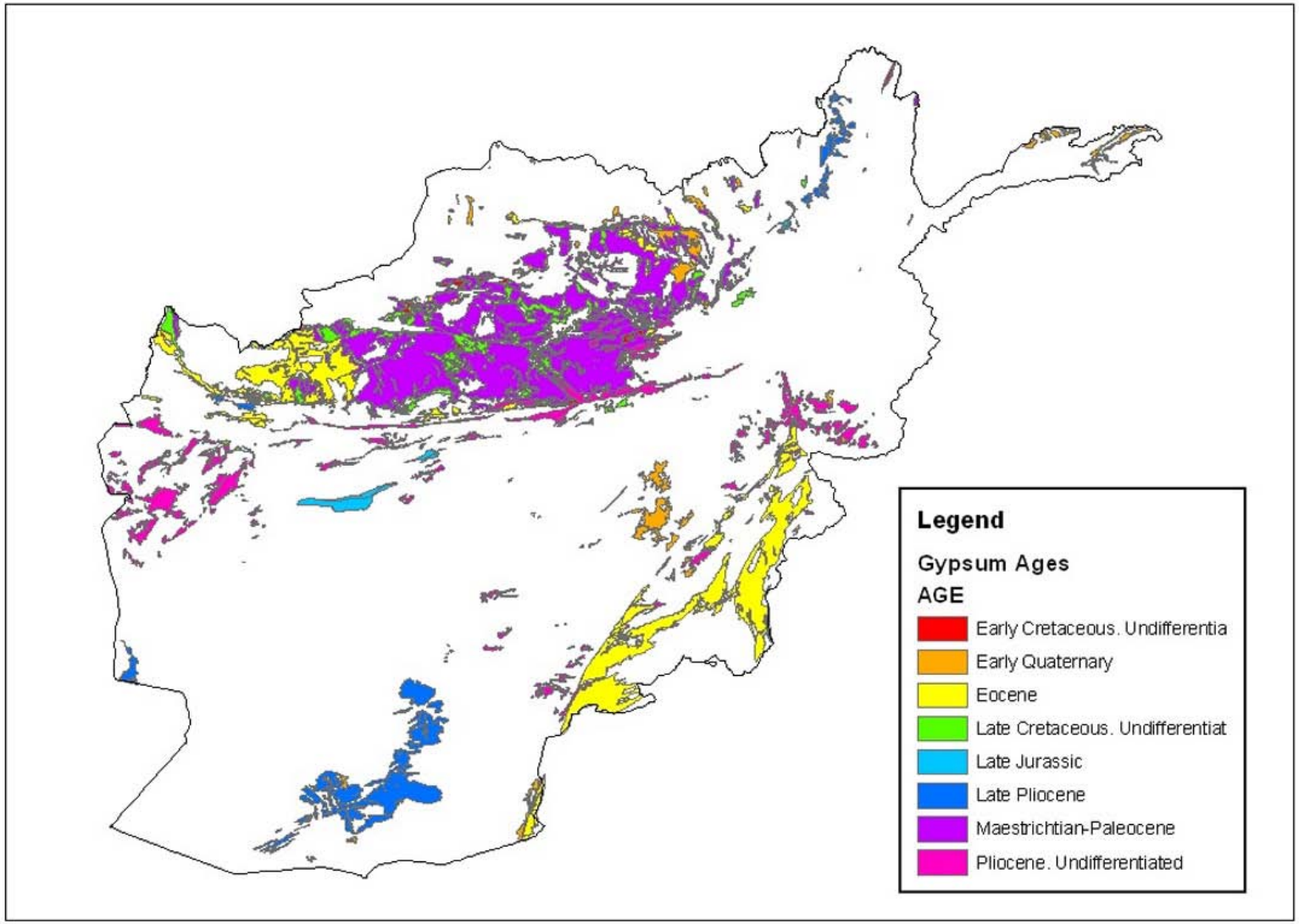

Figure 8.8-2. Map showing age of gypsum-bearing rocks in Afghanistan.

References

Harben, P.W., 2002, Potassium minerals and compounds, *in* The Industrial Minerals Handbook; A guide to markets, specifications & prices, 4th edition: Worcester Park, UK, Industrial Minerals Information, p. 264–272.

Kahle, Klaus, and Scherzberg, Heinz, 2000, New potassium-projects as a source for sodium chloride products with a high purity, *in* Geertman, R.M., ed., 8th World Salt Symposium, Volume 1: New York, Elsevier, p. 583–588.

Luchnikov, V.S., 1982, Upper Jurassic halogen deposits of southeast Central Asia: Petroleum Geology, v. 20, no. 7, p. 296–298.

Ludington, Steve, Orris, G.J., Bolm, K.S., Peters, S.G., and the U.S. Geological Survey-Afghanistan Ministry of Mines and Industry Joint Mineral Resource Assessment Team, 2007, Preliminary Mineral Resource Assessment of Selected Mineral Deposit Types in Afghanistan: U.S. Geological Survey Open–File Report 2007–1005, 44 p, available on line at *http://pubs.usgs.gov/of/2007/1005/*.

Raup, O.B., 1991, Descriptive model of bedded gypsum; Deposit subtype: Marine evaporite gypsum (Model 35a.5), *in* Orris, G.J., and Bliss, J.D., 1991, Some industrial mineral deposit models: descriptive deposit models: U.S. Geological Survey Open-File Report, p. 34–35.

Sharpe, Roger, and Cork, Greg, 2006, Gypsum and anhydrite, *in* Kogel, J.E., Trivedi, N.C., Barker, J.M., and Krukowski, S.T., eds., Industrial minerals & rocks, 7th edition: Littleton, Colo., Society for Mining, Metallurgy, and Exploration, Inc., p.519–540.

Smith, G.I., 1975, Potash and other evaporite resources of Afghanistan: U.S. Geological Survey Open-File Report 75–89, 63 p.

Ulmishek, G.F., 2004, Petroleum Geology and Resources of the Amu-Darya Basin, Turkmenistan, Uzbekistan, Afghanistan, and Iran: U.S. Geological Survey Bulletin 2201–H, 38 p.

Zharkov, M.A., 1984 (1974), Paleozoic salt bearing formations of the world: New York, Springer-Verlag, 427 p.

8.9 Borates

Contributions by David M. Sutphin and Greta J. Orris.

Afghanistan contains two potential sources of boron, lacustrine deposits, and skarn deposits. Borate minerals have been known and used since at least the 5th century when Byzantine artisans used Turkish borax in pottery glazes and as fluxes for precious metal (Barker, 1990). Since the 1880s, deposits of the southwestern United States have dominated the world market; however, the largest known borate reserves were discovered about 1950 in Turkey (Barker, 1990). In nature, boron always occurs combined with other elements. Its compounds are important in manufacturing applications, for example, the glass-forming properties of borate minerals and refined chemicals account for one-half U.S. consumption of these products, specifically in the manufacture of specialty glasses such as Pyrex, frits, and insulation-grade and textile-grade glass fibers (Lyday, 1985).

At least 200 known borate-bearing minerals exist (Garrett, 1998), but only seven are commercially important (Barker, 1990; Jensen and Bateman, 1981). The top borate minerals are borax (+ kernite, tincalconite which are other hydration levels), colemanite, ulexite, and datolite. Other minerals that have some commercial importance are sassolite, inyoite, priceite, probertite, szaibelyite, inderite, pinnoite, hydroboracite, ludwigite, boracite; each of these minerals is or has been mined on a commercial scale.

Elements similar in character, which may be found with boron, include lithium, tantalum, cesium, beryllium, uranium, and thorium (Ostroschenko, 1967). Borates often are produced with other commodities such as potash, soda ash, salt cake, and nahcolite in lacustrine or brine deposits (Barker, 1990). Celestite, as well as orpiment and realgar—two arsenic-bearing minerals—are common in borate deposits. Boron is widespread in nature but usually is present only in trace amounts in ore from which it cannot economically be recovered. Large-scale borate accumulation on continents is restricted to evaporite sediments formed in the arid parts of the volcanic-tectonic belts of western North and South America, the eastern Mediterranean, or Asia. Marine accumulations are generally small. (Walker, 1963, 1975; Shaw and Burgry, 1966;

8.9.1 Geology of Borate Deposits

Kistler and Smith (1983) reviewed the world's borate producing regions and reserves. Barker and Lefond (1985) compiled 18 papers on borate geology, exploration, mining, processing, and end uses. Barker (1990) gives a brief overview of borate exploration. Harben and Bates (1984) summarized the world borate situation.

Barker (1990) discussed the formation of borate deposit types and their characteristics. Commercial borate deposits form in five main ways: (1) by precipitation from brines in lakes, (2) as crusts or crystals in mud within playas, (3) by direct precipitation near springs (warm or hot) or fumaroles, (4) by evaporation of marine water, and (5) by crystallization at or near granitic contacts or in veins. Deposits formed by precipitation in permanent shallow lakes are large and produce most of the world's borates. Other types of occurrences are relatively small and most are generally uneconomic. In Afghanistan, three main potential sources of boron have been identified: lacustrine deposits, pegmatites. At one iron skarn occurrence, boron is cited as possible minor commodity. Boron is not mentioned as a possible commodity (major or minor) in the iron skarn deposit model (Cox, 1986; Mosier and Menzie, 1986). Obolenskiy and others (2003) present a model for boron skarn deposits, but those deposits are not further discussed here. Lacustrine deposits and pegmatite permissive areas are discussed below.

Lacustrine borate deposits

Lacustrine borate deposits form in shallow lakes that often have a proximal or distal hot spring as a boron source (Barker, 1990). An existing borate-bearing deposit or bedrock may be a secondary source. An arid climate helps produce supersaturation. Occasional outflow from the basin removes impurities, such as competing ions. Subsequent diagenesis, remobilization, folding, faulting, and erosion normally alter and complicate borate mineralogy and distribution in the primary deposits. Borate lakes are relatively uncommon, but several are known in the western United States, Tibet, and South America. Orris (1992; 1997) developed methodologies for assessing boron in Quaternary salar and lacustrine settings.

Lacustrine borate permissive area

Deposit type—Lacustrine borate

Age of mineralization—Jurassic to Recent

Examples of deposit type— None in Afghanistan; Kramer, Searles Lake, and Boron in the United States; borate lakes in South America.

Exploration history—Unknown

Tract boundary criteria—Rocks were selected on the basis of their having gypsum, barite, or evaporates in their descriptions. Rock units containing one or more evaporate-type mineral deposits in figure 8.9-2 were also included. A 1–km-wide buffer was used around the formation boundaries. There must be contemporaneous volcanism within the drainage basins for the formation of borates. Smith (1975) suggested that the Cenozoic basins below the Hindu Kush might be good areas to contain undiscovered borate deposits. A preliminary separate permissive tract for boron in pegmatites was also considered by the USGS-AGS assessment team and is portrayed in Figure 8.2-3.

Important data sources—Doebrich and Wahl (2006), Orris and Bliss (2002), Abdullah and others (1977).

Needs to improve assessment—Detailed geologic mapping and detail geochemical survey with the specific goal of exploring for evaporate mineralization.

Optimistic factors—Afghanistan has evaporate deposits ranging from Jurassic to Recent in age. Future exploration in these areas may identify borate mineralization. Recent to Tertiary saline lake deposits would be likely targets for exploration. Prospecting for boron minerals begins with the identification of sedimentary basins that were at one time favorable for the accumulation of borate-rich water (Smith and others, 1973).

Pessimistic factors—The mineral deposit database (Orris and bliss, 2003) does not list boron or borate as a major commodity; only an iron skarn cites boron as a minor commodity.

Quantitative assessment—No estimate of the numbers of undiscovered lacustrine borate deposits was attempted, but the areas outlined above are the most probable in Afghanistan to yield such deposits.

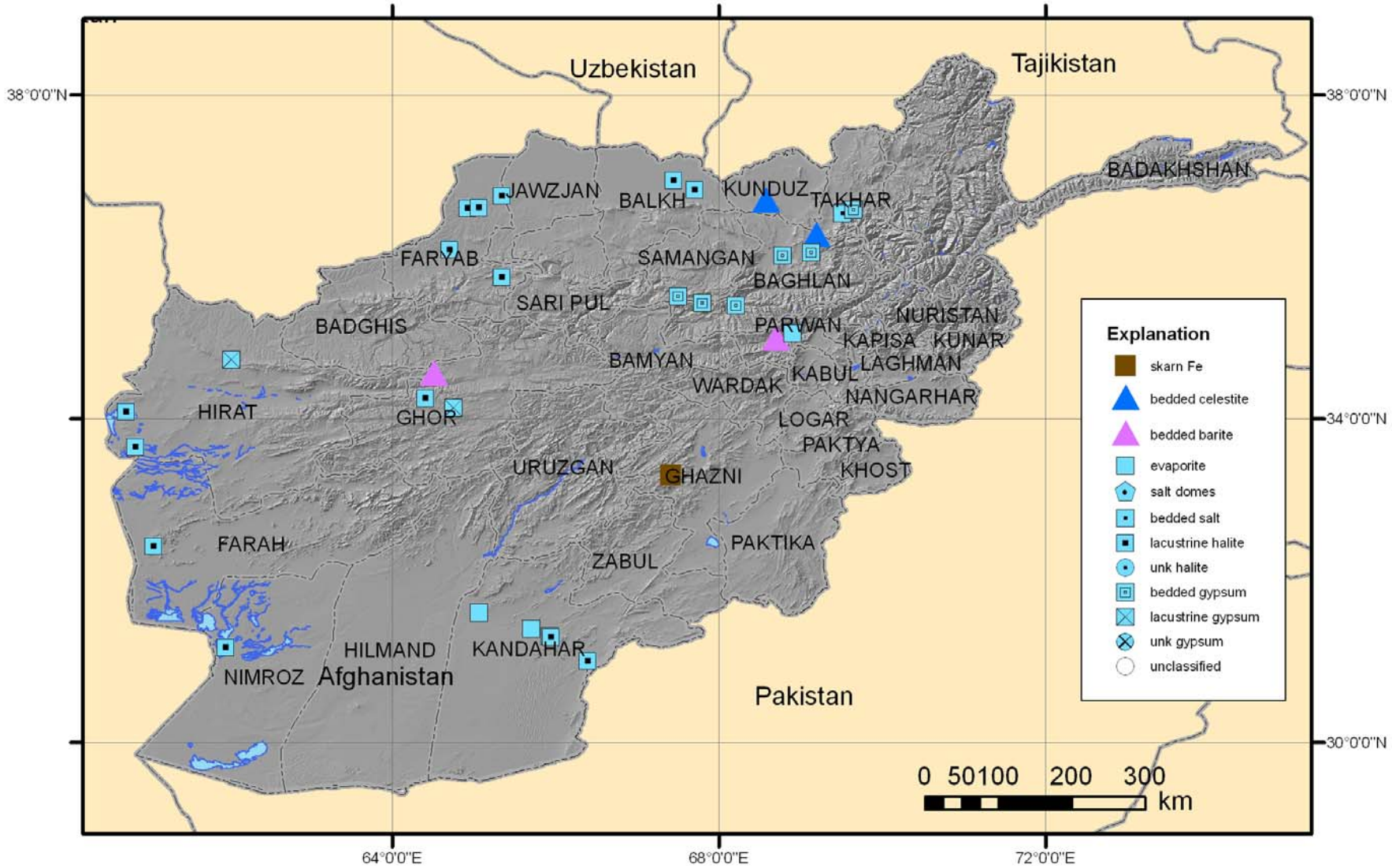

Figure 8.9-1. Locations of mineral deposit types having bedded minerals, such as barite, celestite, gypsum, and halite, which may give clues to borate mineralization in Afghanistan. The one iron skarn on the map lists boron as a secondary commodity. Dark blue lines are drainages into playas (light blue).

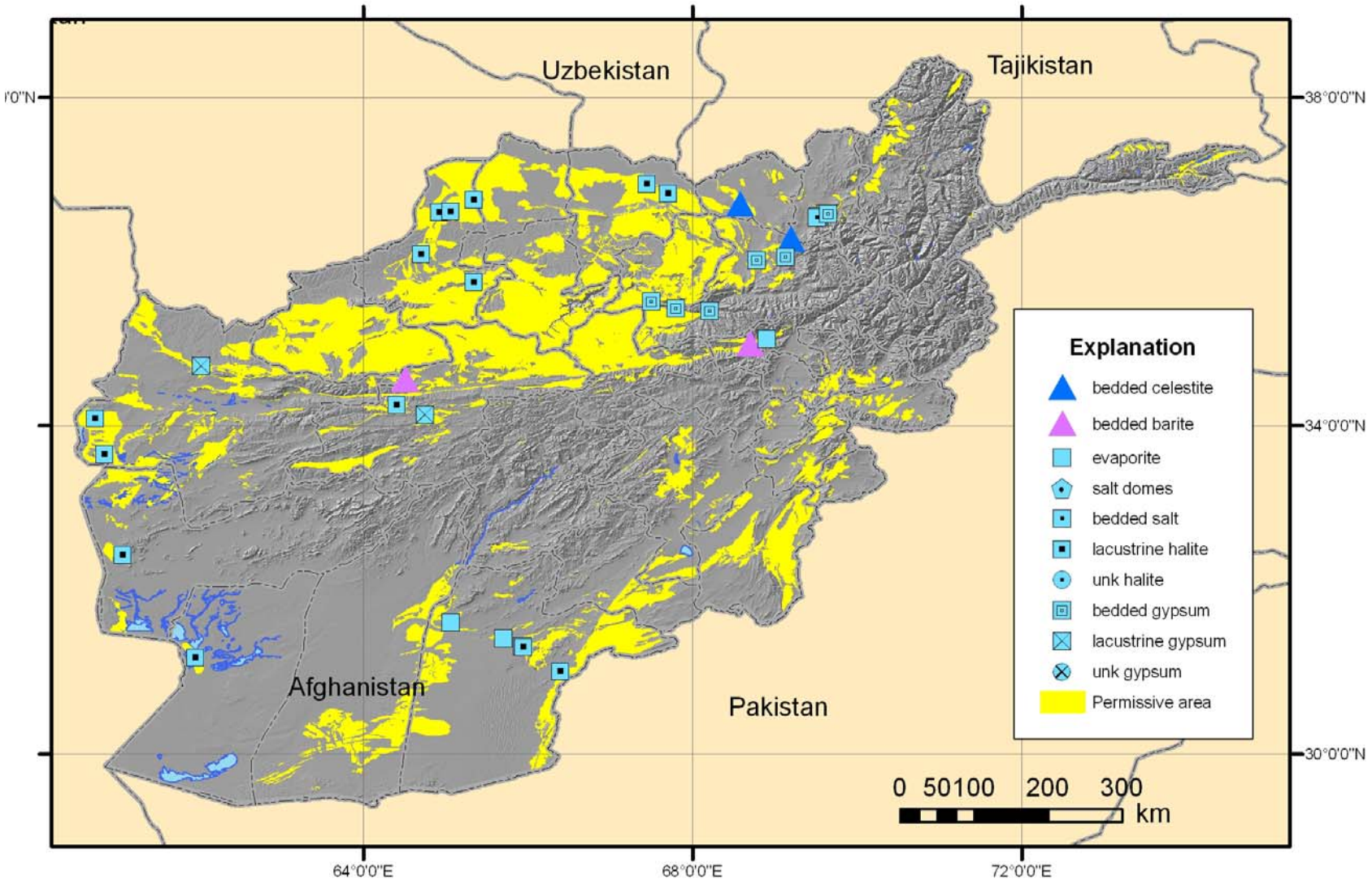

Figure 8.9-2. Permissive tract for the occurrence of undiscovered lacustrine borate deposits. Dark blue lines are water drainages into playas (light blue).

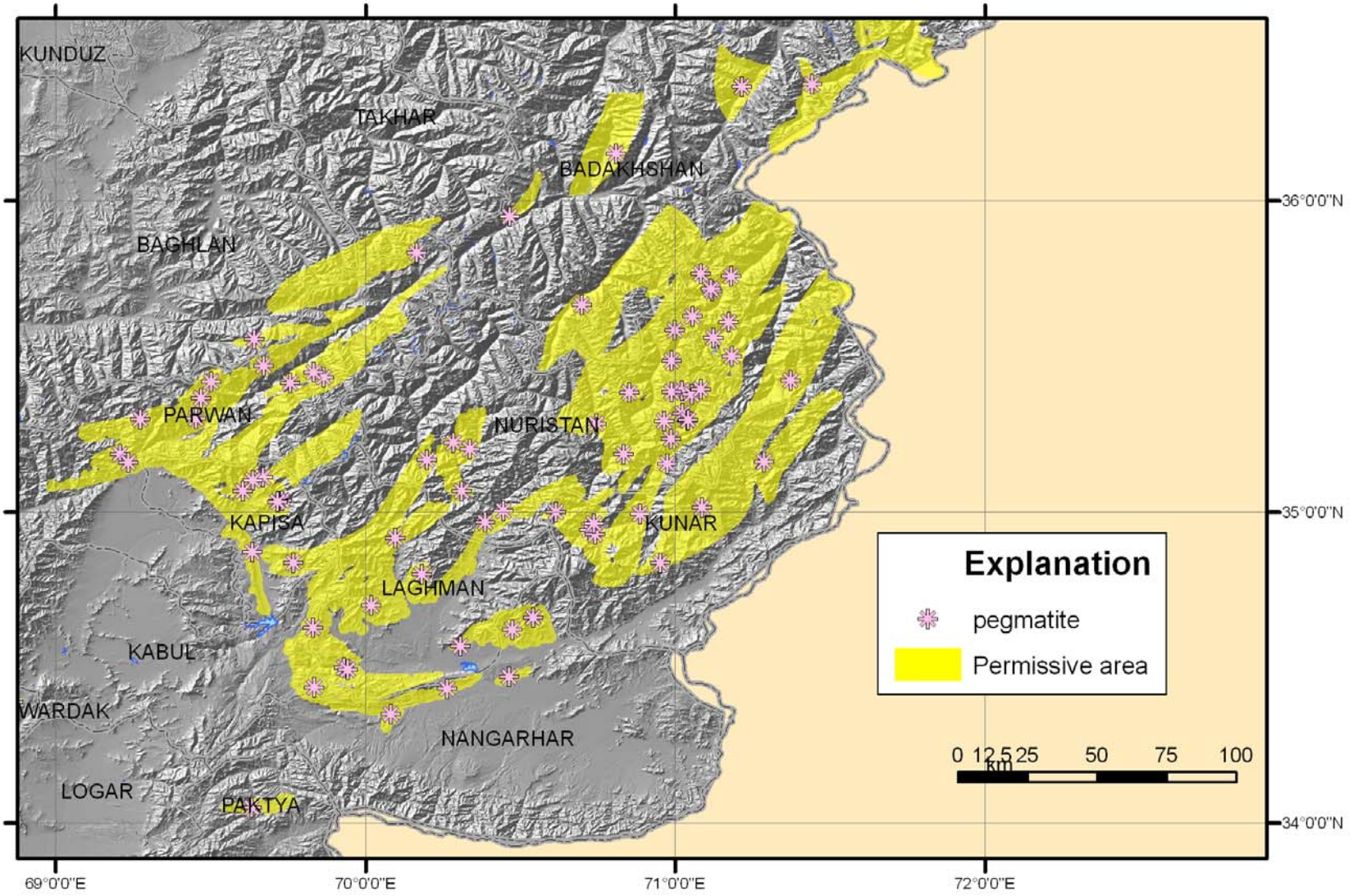

Figure 8.9-3. Part of the permissive area for boron-bearing pegmatites veins in eastern Afghanistan.

References

Abdullah, Sh., Chmyriov, V.M., Stazhilo-Alekseev, K.F., Dronov, V.I., Gannan, P.J., Rossovskiy, L.N., Kafarskiy, A.Kh., and Malyarov, E.P., 1977, Mineral resources of Afghanistan, 2nd ed.: Kabul, Afghanistan, Republic of Afghanistan Geological and Mineral Survey, 419 p.

Barker , J.M., 1990, Borate exploration, *in* Olson, R.H., Bentzen, E.H., III, and Presley, G.C., eds., Surface Mining, 2d ed.: Society for Mining, Metallurgy, and Exploration, online books, available on line at *http://books.smenet.org/Surf_Min_2nd Ed/sm-ch02-sc10-ss03-bod.cfm* (6 Feb 2007).

Barker, J.M., and Lefond, S.J., eds., 1985, Borates—Economic geology and production, AIME, New York, 274 p.

Cox, D.P., 1986, Descriptive model of Fe skarn deposits, *in* Cox, D.P., and Singer, D.A., eds., Mineral Deposit Models: U.S. Geological Survey Bulletin 1693, p. 94, available online at *http://pubs.usgs.gov/bul/b1693/html/bullfrms.htm/*.

Doebrich, J.L., and Wahl, R.R., 2006, Geologic and mineral location map of Afghanistan: U.S. Geological Survey Open-file Report, scale 1:850000.

Garrett, D.E., 1998, Borates- Handbook of deposits, processing, properties, and uses: New York, Academic Press, 483 p.

Harben, P.W., and Bates, R.L. 1984, Geology of the Nonmetallics: Metal Bulletin, New York, 392 p.

Jensen, M.L., and Bateman, A.M., eds., 1981, Economic mineral deposits: John Wiley and Sons, Inc., 3d revised edition, 604 p.

Kirkham, R.V., 1984, Evaporites and brines, *in* Eckstrand, R.O., Canadian Mineral Deposits Types—A Geological Synopsis: Geological Survey of Canada, Economic Geology Report 36, p. 13–15.

Kistler, R.B., and Smith, W.C., 1983, Boron and Borates, *in* Lefond, S.J., ed., Industrial Minerals and Rocks, 5th ed.: AIME, New York, p. 533–560.

Lakin, H.W., Hunt, C.B., Davidson, D.F., and Oda, U., 1963, Variation in minor element content of desert varnish: U.S. Geological Survey Professional Paper 475–B, p. B28–B31.

Lyday, P.A., 1985, Boron, Minerals Yearbook, U.S. Bureau of Mines, preprint, 12 p.

Mosier, D.L., and Menzie, W.D., III, 1986, Grade and tonnage model of Fe skarn deposits, *in* Cox, D.P., and Singer, D.A., eds., Mineral Deposit Models: U.S. Geological Survey Bulletin 1693, available online at *http://pubs.usgs.gov/bul/b1693/html/bullfrms.htm/*.

Obolenskiy, A.A., Rodionov, S.M., Ariunbileg, Sodov, Dejidmaa, Gunchin, Distanov, E.G., Dorjgotov, Dangindorjiin , Gerel, Ochir, Duk Hwan Hwang, Fengyue Sun, Gotovsuren, Ayurzana, Letunov, S.N., Xujun, Li, Nokleberg, W.J., Ogasawara, Masatsugu, Seminsky, Z.V., Smeloy, A.P., Sotnikoy, V.I., Spiridonov, A.A., Zorina, L.V. , and Hongquan, Yan, 2003, Boron (datolite) skarn: Mineral deposit models for Northeast Asia: U.S. Geological Survey Open–File Report 03-203, 44 p. Available online at *http://geopubs.wr.usgs.gov/open-file/of03-203/MINMOD/NE_Asia_Min_Dep_Models.pdf*.

Oftedal, I., 1964, On the occurrences and distribution of boron in pegmatite: Norsk Geol Tidsakr, v. 44, p. 217–225.

Orris, G.J., 1992, Preliminary descriptive model of lacustrine borates, *in* Industrial Mineral Deposit Models—Descriptive models for three lacustrine deposit types: U.S. Geological Survey Open-File Report 92-593, p. 2-6.Orris, G.J., 1997, Two methodologies for assessing boron in Quaternary salar and lacustrine settings: Tucson, Arizona, University of Arizona, unpublished Ph.D dissertation, 281 p.

Orris, G.J., and Bliss, J.D., compilers, 2002, Mines and Mineral Occurrences of Afghanistan: U.S. Geological Survey Open-File Report 02–110, 95 p. available on line at *http://geopubs.wr.usgs.gov/open-file/of02-110/*.

Ostroschenko, V.D., 1967, Geochemistry of boron and cesium in the volcanic rocks of western Tien-Shan: Geochemistry, p. 800–806.

Reynolds, R.C., 1965, The concentration of boron in Precambrian seas: Geochimica et Cosmochimica Acta, v. 29, no. 1, p. 1–16.
Shaw, D.M., and Bugry, R., 1966, A review of boron sedimentary geochemistry in relation to new analyses of some North American shales: Canadian Journal of Earth Science, v. 3, p. 49–63.
Smith, G.I., 1975, Potash and other evaporite resources of Afghanistan: U.S. Geological Survey Open-File Report 75–89, 63 p.
Smith, G.I., Jones, C.L., Culbertson, W.C., Ericksen, G.E., and Dyni, J.R., 1973, Evaporites and brines, *in* Brobst, D.A., and Pratt, W.P., United States Mineral Resources: U.S. Geological Survey, Professional 820, p. 197–216.
Walker, C.T., 1963, Size fractionation applied to geochemical studies of boron in sedimentary rocks: Journal of Sedimentary Petrology, v. 33, no. 3, p. 694–702.
Walker, C.T., 1975, Geochemistry of Boron: Dowden, Hutchinson, and Ross, Inc., Stroudsburgh, 414 p.